A NUMERICAL STUDY ON BEAM STABILTY IN ECCENTRICALLY BRACED FRAMES

A THESIS SUBMITTED TO
THE GRADUATE SCHOOL OF NATURAL AND APPLIED SCIENCES
OF
MIDDLE EAST TECHNICAL UNIVERSITY

BY

GÜL YİĞİTSOY

IN PARTIAL FULFILLMENT OF THE REQUIREMENTS
FOR
THE DEGREE OF THE MASTER OF SCIENCE
IN
CIVIL ENGINEERING

SEPTEMBER 2010

Approval of the thesis:

A NUMERICAL STUDY ON BEAM STABILITY IN ECCENTRICALLY BRACED FRAMES

submitted by **GÜL YİĞİTSOY** in partial fulfillment of the requirements for the degree of **Master of Science in Civil Engineering Department, Middle East Technical University** by,

Prof. Dr. Canan Özgen _____
Dean, Graduate School of **Natural and Applied Sciences**

Prof. Dr. Güney Özcebe _____
Head of Department, **Civil Engineering**

Assoc. Prof. Dr. Cem Topkaya _____
Supervisor, **Civil Engineering Dept., METU**

Examining Committee Members:

Assoc. Prof. Dr. Ahmet Yakut _____
Civil Engineering Dept., METU

Assoc. Prof. Dr. Cem Topkaya _____
Civil Engineering Dept., METU

Asst. Prof. Dr. Afşin Sarıtaş _____
Civil Engineering Dept., METU

Asst. Prof. Dr. Yalın Arıcı _____
Civil Engineering Dept., METU

Volkan Aydoğan, M.Sc. _____
Civil Engineer, PROMA

Date: 02.09.2010

I hereby declare that all information in this document has been obtained and presented in accordance with academic rules and ethical conduct. I also declare that, as required by these rules and conduct, I have fully cited and referenced all material and results that are not original to this work.

Name, Last name : Gül Yiğitsoy

Signature :

ABSTRACT

A NUMERICAL STUDY ON BEAM STABILITY IN ECCENTRICALLY BRACED FRAMES

Yiğitsoy, Gül
M.Sc., Department of Civil Engineering
Supervisor: Assoc. Prof. Dr. Cem Topkaya

September 2010, 102 pages

A two-phase research program was undertaken numerically to assess the behavior of the beam outside of the link that is designed for overstrength of the link in eccentrically braced frames (EBFs). In the first phase, software was developed to conduct a statistical analysis of the typical cases designed according to the AISC Seismic Provisions for Structural Steel Buildings. In this analysis, it was noticed that most of the statistically analyzed cases do not satisfy the code requirement provided for overstrength factor. Furthermore, the analyses results revealed that troublesome designs are highly influenced by normalized link length and slenderness of the beam. In this phase, redistribution of forces between beam and brace after the yielding of beam was also studied and it was observed that the forces not carried by the yielded beam are taken by the brace. In second phase, a total of 91 problematic designs were analyzed on finite element program to investigate the effective parameters on the overstrength issue, and overall and local stability of the beam outside of the links. According to analysis results, it was observed that unbraced beam length and flange slenderness are responsible for the stability of the system. Based on these results, the boundary values were suggested to prevent lateral torsional buckling of the beam and local buckling of the brace connection panel separately. Moreover, the overstrength factor specified by code was found conservative for the intermediate and long links although it is fit for the short links.

Keywords: Eccentrically Braced Frames, Finite Element, Overstrength

ÖZ

DIŞMERKEZ ÇELİK ÇAPRAZLI ÇERÇEVE SİSTEMLERİNDE
KİRİŞ STABİLİTESİNİN NÜMERİK İNCELENMESİ

Yiğitsoy, Gül
Yüksek Lisans, İnşaat Mühendisliği Bölümü
Tez Yöneticisi: Doç. Dr. Cem Topkaya

Eylül 2010,102 sayfa

Dışmerkez çelik çaprazlı çerçeve sistemlerinde (EBFs) bağ kirişinde oluşan dayanım fazlalığına göre tasarlanan bağ kirişi dışında kalan kirişin davranışını değerlendirmek için numerik olarak iki fazlı araştırma programı yürütülmüştür. İlk fazda, AISC Çelik Yapılar için Sismik Şartname'ye göre tasarlanmış tipik durumların istatistiksel analizini yürütmek için bilgisayar yazılımı geliştirilmiştir. Bu analizde, istatistiksel olarak analiz edilmiş durumların birçoğunun şartnamede verilmiş dayanım fazlalılığı faktör şartını sağlamadığı görülmüştür. Bunun yanında, analiz sonuçları problemli tasarımların normalize edilmiş bağ kirişi uzunluğu ve kirişin narinliği tarafından yüksek derecede etkilendiğini göstermiştir. Bu fazda, kirişin akmasından sonra kiriş ve çapraz arasındaki yük dağılımı da incelenmiş ve akmış kiriş tarafından taşınamayan yüklerin çapraz tarafından taşındığı görülmüştür. İkinci fazda, toplam 91 problemli tasarım, dayanım fazlalılığı sorunu ve bağ kiriş dışında kalan kirişin genel ve yerel stabilitesi üzerinde etkin olan parametreleri araştırmak için sonlu elemanlar programında analiz edilmiştir. Analiz sonuçlarına göre mesnetlenmemiş kiriş uzunluğunun ve tabla narinliğinin sistemin stabilitesinden sorumlu olduğu gözlemlenmiştir. Bu sonuçlara göre, kirişte yanal burulmayı ve çapraz bağlantı panelinde yerel burulmaları önlemek için ayrı ayrı sınır değerleri önerilmiştir. Ayrıca, şartnamede belirtilen dayanım fazlalığı faktörü kısa bağ kirişleri için uygun olduğu halde, orta uzunluklu ve uzun bağ kirişleri için konservatif bulunmuştur.

Anahtar Kelimler: Dışmerkez Çelik Çaprazlı Çerçevler, Sonlu Eleman, Dayanım Fazlalığı

To My Family

ACKNOWLEDGMENTS

The author is grateful to her advisor, Assoc. Prof. Dr. Cem Topkaya for his invaluable guidance, assistance, support and insight throughout the research and is grateful for the opportunity to work with him.

Special thanks go to Dr. Taichiro Okazaki for his guidance and suggestions throughout this study.

Scientific and Technological Research Council of Turkey (TÜBİTAK – 105M242), which is supporter of this study, is gratefully acknowledged.

The author also thanks to all of her friends for their support and kind friendship.

Finally, the author wishes to express her gratitude to her family; her sister Başak Yiğitsoy, her mother Sakine Yiğitsoy and her father Abbas Yiğitsoy for their everlasting love and encouragement.

TABLE OF CONTENTS

LIST OF TABLES

TABLES

LIST OF FIGURES

FIGURES

CHAPTER 1

INTRODUCTION

1.1 Description of Eccentrically Braced Frames (EBFs)

Eccentrically braced frames (EBFs) are lateral force resisting systems providing good inelastic capacity for steel structures under large cyclic loading. Because EBFs possess high elastic stiffness in addition to significant energy dissipation and high degree of ductility at inelastic range, it can be thought as a hybrid system between moment resisting frames (MRFs) and concentrically braced frames (CBFs). The main characteristic of EBFs is that the eccentric connection of brace with beam causes a weak, small beam segment named as a *link.* The other components of EBFs are columns, braces and beam outside of the link. Several different configurations are possible for EBFs as shown in Figure 1.1.

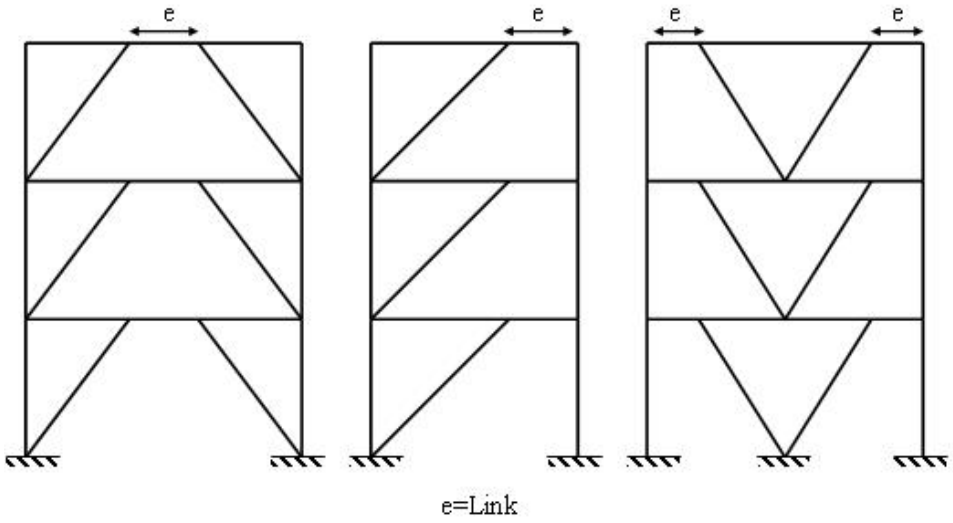

Figure 1.1: Examples of Eccentrically Braced Frames

Inelastic activity and energy dissipation of EBFs takes places primarily in the link. EBFs are designed so that the link yields while all other components show elastic behavior under large seismic loading. Therefore, the beam outside of the link, the brace and the column are sufficiently proportioned against the forces created by fully yielded and strain hardened link. Energy is dissipated through stable inelastic deformation of the link. The degree of inelastic behavior of the link is measured by its inelastic rotation capacity. The rotation angle of the link is calculated as shown in Figure 1.2.

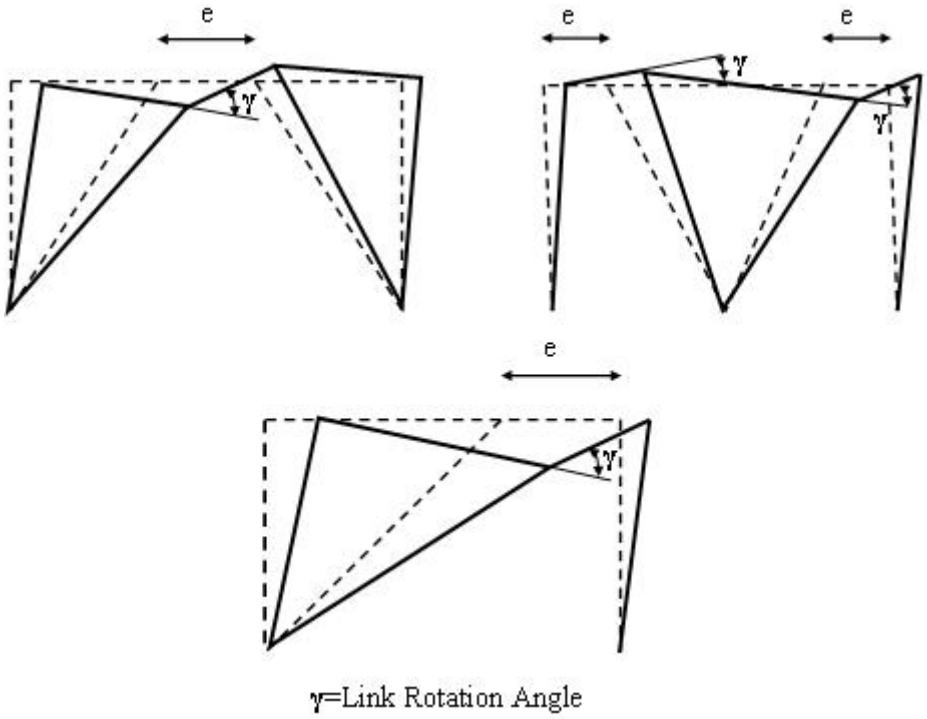

Figure 1.2: Link Rotation Angle

The link length (e) is the major determining factor on the yield mechanism of links. Usually the normalized link length $e/(M_p/V_p)$ is used to classify link types, where V_p is the plastic shear capacity and M_p is the plastic moment capacity of the link. For $e \leq 1.6\ M_p/V_p$, shear forces control the yielding, so such type of links are called as *shear yielding links*. For $e \geq 2.6 M_p/V_p$, the link is subjected to high bending moment at the end of links and it yields

before the link reaches to its plastic shear capacity. These links are named as *flexure yielding link*. For intermediate lengths, $1.6M_p/V_p<e<2.6M_p/V_p$, the link yields both due to shear force and bending moment ,and links in this interval are defined as *combined shear and flexural yielding link.*

EBFs give chance to restrict all inelastic deformation to only one component. In addition to its structural advantages; EBFs enable wide openings for architectural purposes as shown in Figure 1.3.

Figure 1.3: Application of EBF

1.2 Design of EBFs According to the AISC Seismic Provisions for Structural Steel Buildings (2005) and Relevant Research on Code Development

The AISC Seismic Provisions for Structural Steel Buildings (2005) hereafter referred as the AISC Seismic Provisions provide guidance on the design of EBF systems. There are rules presented in Eurocode 8 and Turkish Seismic Specification; however, these rules are essentially the same as those presented in the AISC Seismic Specification. In this section the AISC Seismic Specification provisions covered in this thesis are reviewed in the light of the past research studies that lead to these rules.

First research studies on EBFs date back to early 1970's. Since then extensive research studies were carried out. Engelhardt and Popov (1989a), Engelhardt, Kasai and Popov (1987), Engelhardt and Popov (1988), and Bruneau, Uang, and Whittaker (1997) provide summary of earlier studies, overview of general behavior of EBFs and design recommendations. These researchers also present significant observations obtained from past researches conducted to that date and the problems that can be encountered during design of EBFs. Moreover design examples for EBFs are available based on Uniform Building Code by Becker and Ishler (1996) and AISC Seismic Design Manual (2006).

The main element of EBFs, the link, should be properly designed to show stable ductile behavior under large shear forces. In addition to the link length (e) and the link type, the web stiffener spacing and width to thickness ratios of the link section determine the inelastic capacity.

1.2.1 Link Length and Shear Strength of the Link

As explained in the introduction section, the link length is the primary factor in determining the yield mechanism. Theoretically, the limit link length which determines the yielding mechanism can be derived from equilibrium. When the link length is less than $2M_p/V_p$ ($e<2M_p/V_p$), the link yields due to shear forces and when the link length is greater than $2M_p/V_p$ ($e>2M_p/V_p$), the link yields due to formation of plastic hinges at the link ends. Actual conditions differ from the theoretical calculations because of the interaction between shear and flexural yielding. In general, due to strain hardening there is always an interaction

between shear and flexural yielding especially for normalized link lengths ($e/(M_p/V_p)$) close to 2. The experimental investigation performed by Kasai and Popov (1986a) on 7 specimens under monotonic and cyclic loading showed that strain hardening causes interaction of shear and moment. These researchers suggested that the link length should be limited to $1.6M_p/V_p$ to make sure that the behavior is dominated by shear yielding of the link.

According to AISC Seismic Provision (2005), the nominal shear strength of the link (V_n) is calculated as;

$$V_n = \text{lesser of} \quad (\ V_p \ \text{or} \ 2\frac{M_p}{e}) \tag{1.1}$$

However, the axial force developed on the link influences the nominal shear strength. Unless the required axial strength is greater than 15 percent of the nominal axial yield strength, the effect of axial load on the link can be neglected.

1.2.2 Link Section

The proper width to thickness ratios for flange and web of the link section are required to secure the link against local buckling and fracture. In earlier editions of the AISC Seismic Provisions the same flange slenderness limit designated for special moment frames was accepted for EBFs. Therefore, link's flange width to thickness ratio for EBFs was restricted to seismically compact section limit of $0.3(E/F_y)^{1/2}$. Arce, Engelhardt, Okazaki and Ryu (2005) performed an experimental study to determine whether the current limit can be increased to the compact section limit of $0.38(E/F_y)^{1/2}$. In this study the authors conducted 23 tests from 5 different wide flange shapes having various flange slenderness under different loading protocols. Engelhardt and Okazaki (2007) also made additional experiments using the same test setup mentioned above for completeness of the research. Based on the findings of these experimental researches, the authors reported that width to thickness ratio for short links ($e \leq 1.6M_p/V_p$) can be increased to $0.38(E/F_y)^{1/2}$ but the limit, $0.3\ (E/F_y)^{1/2}$, should be maintained for longer link lengths. AISC Seismic Provision (2005) adopted this relaxation and shear yielding link only have to satisfy the compact section limit.

1.2.3 Link Rotation Capacity

The plastic rotation capacity of the link depends on its length in other words its yield mechanism. Most of the earlier researches on shear yielding links showed that the plastic rotation capacity of the shear link can be as high as 0.1 radians. To determine long link behavior, Popov and Engelhard (1989b) conducted a comprehensive study on long links. These researchers tested 14 specimen having link lengths varying between $1.2M_p/V_p$ *to* $3.6M_p/V_p$ under cyclic loading. According to test results, the plastic rotation capacity was recommended to be 0.08 radians for short links ($e \leq 1.6M_p/V_p$), 0.02 radians for very long links ($e \geq 3M_p/V_p$). In addition, linear interpolation between the rotation limits stated above was recommended for the intermediate link length region. Nonetheless Popov and Engelhardt (1989b) emphasized that the plastic rotation limits suggested for the links $e > 1.6M_p/V_p$ can be appropriate for the cases except the link directly connected to column.

According to the AISC Seismic Specification (2005), the following inelastic rotation limits are recommended for different link lengths without restriction on the configuration of the link;

$$0.08\,\text{radians} \quad \text{for} \quad e \leq 1.6\frac{M_p}{V_p} \tag{1.2}$$

$$0.02\,\text{radians} \quad \text{for} \quad e \geq 2.6\frac{M_p}{V_p} \tag{1.3}$$

$$\text{Linear interpolation between } 0.02 \text{ and } 0.08 \text{ radians for } 1.6\frac{M_p}{V_p} < e < 2.6\frac{M_p}{V_p} \tag{1.4}$$

1.2.4 Link Stiffeners and Lateral Bracing of the Link

Link stiffeners are needed to prevent web shear buckling of the link. Kasai and Popov (1986b) proposed a rule for stiffener spacing for shear yielding links based on analytical and experimental results. They used the experimental results of 30 shear yielding links tested up to that date and combined the results with the plastic plate buckling theory to develop stiffener spacing criteria for shear yielding links.

Popov and Engelhardt (1989b; 1992) also observed that the dominant force causing instability on EBFs with long links is not shear but flexure resulting in lateral torsional buckling of the beam and local flange buckling. The results of this investigation revealed that the stiffeners located only at ends of the link are adequate for flexural yielding links.

In the current code, AISC Seismic Specification (2005), the rules mentioned above with small changes are provided for link stiffener spacing as follows; The intermediate link stiffeners are required for the links $e \leq 1.6M_p/V_p$ such that maximum stiffener spacing for a link rotation angle of 0.08 radian is $(30t_w\text{-}d/5)$ and maximum stiffener spacing for a link rotation angle of 0.02 radian is $(52t_w\text{-}d/5)$ where t_w is the thickness of the link web and d is the depth of the link section. For the link rotation angle between 0.02 radian and 0.08 radian, the stiffener spacing is calculated by linear interpolation. For the links $2.6M_p/V_p < e \leq 5M_p/V_p$, intermediate stiffeners placed at $1.5b_f$ from ends of the link are needed, where b_f is the flange width of link. For intermediate lengths, $1.6M_p/V_p < e \leq 2.6M_p/V_p$, stiffeners shall satisfy both the requirements for the short links $e \leq 1.6M_p/V_p$ and for the long links $e > 2.6M_p/V_p$. No intermediate web stiffeners are required for links $e > 5M_p/V_p$. Intermediate stiffeners can be one sided if the depth of the link section is less than 635mm (25inch) otherwise code requires that the intermediate stiffeners are placed on both sides of the web. AISC Seismic Specification (2005) only permits full depth intermediate web stiffeners.

According to AISC Seismic Specification (2005), in addition to intermediate web stiffeners, the braced ends of the link shall be stiffened by full depth web stiffeners placed both sides of the link web.

AISC Seismic Specification (2005) also specifies that the lateral restraint shall be located at top and bottom flanges at the ends of the link to prevent the out-of plane movement of the link.

1.2.5 Design of the Brace and the Beam Outside of the Link

The brace and the beam outside of the link are exposed to high bending moments and axial forces due to the fully yielded and strain hardened link. Therefore, these components of

EBFs must be designed as beam-columns to have enough capacity to carry combined axial and flexural forces generated by the link.

The major factor affecting the magnitude of the axial forces developed on the brace and beam outside of the link are the angle between the beam and the brace, and the ultimate shear force at the link. The commentary to the AISC Seismic Provisions (2005) suggests that at least a 40 degree angle between the brace and beam will be helpful to prevent development of high axial load on beam outside of the link. After the link yields, the ultimate shear force developed on the link is directly influenced by its overstrength. The overstrength can be due to two sources. The first one is attributable to material overstrength where the actual yield strength is greater than the nominal yield strength. The second one is due to strain hardening of the link where the link develops excess strength due to cyclic hardening. Historically the two were combined and a single overstrength value which includes both the material overstrength and the overstrength due to strain hardening was proposed by researchers. Engelhardt and Popov (1988) suggested an overstrength factor of 1.5 based on past researches performed on shear yielding links. In another research, Engelhardt, and Popov (1989b) observed that the proposed overtrength value, 1.5, seems very high for intermediate link lengths. Arce, Engelhardt, Okazaki and Ryu (2005) also studied the overstrength factor to check the validity of overstrength factor of 1.5 recommended in the previous version of AISC Seismic Specification (2002). They found that the proposed overstrength factor used on capacity design principle is appropriate.

In the current AISC Seismic Specification (2005) the sources of overstrength are separated into two. An overstrength factor is utilized to take into account the effects of strain hardening. A R_y factor is utilized to consider the material overstrength. In addition, a resistance factor of 0.9 is used during member design which indirectly influences the amount of overstrength considered. As pointed out by Engelhardt and Popov (1989b) the use of a resistance factor while conducting a capacity design is an open judgment. The AISC Seismic Specification (2005) mandates that the beam-column provisions given in the AISC Specification for Structural Steel Buildings (2005), which include a resistance factor, be used in the design of members outside of the link. The AISC Seismic Specification (2005) recommends different overstrength values for the beam and the brace. According to this specification, the brace forces should be calculated considering an overstrength value of

1.25R_y. On the contrary, the forces on the beam outside of the link should be determined using an overstrength value of 1.1R_y. There are two special rules that need to be considered for the beam outside of the link. If the same section is used for the beam and the link then the material overstrength influences both members and can be neglected by considering an overall overstrength of 1.1. The commentary to the AISC Seismic Specification makes it clear that the recommended value of 1.1 is for beams acting compositely with a concrete slab. The idea here is that some of the forces will be counteracted by the composite slab and a reduced overstrength value, when compared with the one for braces, can be used. The very same commentary recommends that an overstrength value of 1.25 be used in cases where the beam outside of the link is not acting compositely with a concrete slab examples of which can be easily found in industrial construction.

For a typical steel with a yield strength of 345 MPa (50 ksi) such as A992 or S355, the recommended R_y value is 1.1 as per the AISC Seismic Specification (2005). A brace connected to a link section that is made up of this material should be designed considering an overall overstrength factor of 1.52 (1.25x1.1/0.9). Similarly, if the same section is used for the beam and the link, the beam should be designed considering an overall overtsrength of 1.22 (1.1/0.9) and 1.38 (1.25/0.9) for cases with and without a concrete slab, respectively.

Although the beams outside of the link are designed to remain elastic under combined forces, limited yielding at beam outside of the link is mostly inevitable. Engelhardt, Popov, and Tsai (1992) examined the results of the tests performed on University of California at Berkley and National Taiwan University to discuss the effect of yielding and instability on the beam outside of the link. The results of experiments indicated that yielding at the outside of the link does not cause adverse effect on EBFs. Moreover when the yielding is confined to brace connection panel particularly, the contribution of limited yielding at this region to energy dissipation capacity is noteworthy. However, the researchers observed that instability at beam outside of the link and the brace connection panel produces unfavorable behavior for EBFs. Lateral torsional buckling of the beam outside of the link and local flange buckling at the brace connection panel affects detrimentally the performance of EBFs and result in considerable decrease on strength and ductility of EBFs.

1.3 Scope of the Thesis

The primary aim of this thesis is to investigate the overstrength provisions recommended in the AISC Seismic Specification (2005). As mentioned before the members outside of the link should be designed considering the overtsrength of the link. The increase in forces and moments can exceed 50 percent due to overstrength. This increase in forces can be overcome by selecting bigger member sizes during the design of EBFs. This is particularly true for brace members. However, for the beam outside of the link, selecting a bigger member size is not always possible. If a bigger member is selected then this will influence the link size which in turn influences the amount of forces on the beam outside of the link. In general, designers experience difficulty in sizing the beam outside of the link due to the stringent overstrength provisions. If the selected beam/link size is inadequate alternative costly measures should be taken. These include increasing the brace size to reduce the amount of bending moment on the beam outside of the link or welding cover plates to the beam to increase its strength. Both measures can be avoided if limited yielding outside of the link is permitted. As indicated in the previous section, limited amount of yielding outside of the link may in fact help promote the system performance.

This thesis study was undertaken to address the issues related with the overstrength of links. In Chapter 2, the overstength of links is studied from a design standpoint and the severity of the overstrength problem is presented. In Chapter 3, a finite element analysis procedure which is adopted throughout the thesis is developed and its results are compared against previous experiments conducted by other researchers. In Chapter 4, the details of a parametric study are given. The parametric study includes 91 real design cases which does not satisfy the code requirements. Based on the findings from the parametric study, conclusions and recommendations are given in Chapter 5.

CHAPTER 2

EVALUATION OF LINK OVERSTRENGTH FROM A DESIGN STANDPOINT

In this chapter the link overstrength issue is evaluated from a design standpoint. Typical EBFs designed according to the AISC Seismic Provisions for Structural Steel Buildings (2005) are considered and the problems related with the overstength factor are studied using these designs. A computer program was developed to facilitate the EBF design. The details of this program are given in this chapter together with the results obtained.

2.1 EBF Design Procedure

The present study is limited to cases where one end of the link is connected to a column. For all designs a story height of 3810 mm (150 in.) were considered. The link length and bay width were considered as variables. For simplicity the clear distance between the column flanges were not considered. Span lengths (L) were varied between 1 to 2 times the story height (h) in 0.2h increments. Similarly, the link lengths (e) were varied between 0.2 to 1.0 times the story height by considering the following cases: e= 0.2h, 0.25h, 0.3h, 0.4h, 0.5h, 0.75h, 1.0h. Out of the 42 combinations of span and link lengths 34 cases were selected to represent the design space. Cases where the link length is greater than half of the span length and where the brace angle is excessively small or large were excluded from the parametric investigation. The resulting geometries are given in Table 2.1.

The average e/L ratio and brace angle for the selected geometries are 0.26 and 42.3 degrees, respectively. A yield strength (F_y) of 345 MPa (50 ksi) was assumed for the beam and the brace for all cases.

Table 2-1: EBF Geometries Considered in the Designs

L/h	e/h	e/L	Angle (degree)	L/h	e/h	e/L	Angle (degree)
1	0.2	0.200	51.3	1.6	0.3	0.188	37.6
1	0.25	0.250	53.1	1.6	0.4	0.250	39.8
1	0.3	0.300	55.0	1.6	0.5	0.313	42.3
1	0.4	0.400	59.0	1.6	0.75	0.469	49.6
1	0.5	0.500	63.4	1.8	0.2	0.111	32.0
1.2	0.2	0.167	45.0	1.8	0.25	0.139	32.8
1.2	0.25	0.208	46.5	1.8	0.3	0.167	33.7
1.2	0.3	0.250	48.0	1.8	0.4	0.222	35.5
1.2	0.4	0.333	51.3	1.8	0.5	0.278	37.6
1.2	0.5	0.417	55.0	1.8	0.75	0.417	43.6
1.4	0.2	0.143	39.8	2	0.2	0.100	29.1
1.4	0.25	0.179	41.0	2	0.25	0.125	29.7
1.4	0.3	0.214	42.3	2	0.3	0.150	30.5
1.4	0.4	0.286	45.0	2	0.4	0.200	32.0
1.4	0.5	0.357	48.0	2	0.5	0.250	33.7
1.6	0.2	0.125	35.5	2	0.75	0.375	38.7
1.6	0.25	0.156	36.5	2	1	0.500	45.0

For all these 34 geometries a set of beam (and link) sections were considered. The beam sections were selected from W-shapes which have a shear capacity between 445 kN (100 kips) and 2245 kN (500 kips). For the set of investigations that are presented in this chapter, sections that satisfy seismicly compact criterion were considered. AISC Seismic Provisions (2005) permits the use of compact sections for short links but not for long links. Investigation of cross sections that violate seismic compactness limits are investigated in later chapters. The resulting set of beam sections consisted of 91 W-shapes.

Either W-shapes or hollow structural sections (HSS) can be used as bracing members in EBFs. In order to make a fair comparison between the designs, only one type of cross-sectional shape was considered in this study. It was assumed that the bracing members are designed using square HSS members which are connected to the beam using a gusset plate. Usually a gusset plate is needed because the width of the HSS brace is greater than the flange width of the beam making direct connection impossible. According to the AISC Seismic Provisions (2005) braces in EBF should satisfy compactness criterion. A total of 60 square HSS sections were selected that satisfy the compactness limit.

The main function of the developed computer program is to design an optimum brace section for a given beam section and geometry. The optimum section is selected based on the minimum weight criterion. For some geometry and beam section combinations the brace members from the selected set of HSS may not be sufficient. These cases are excluded from the final statistical analysis.

A typical EBF design is based on considering a one-story portion of a frame as shown in Figure 2.1.

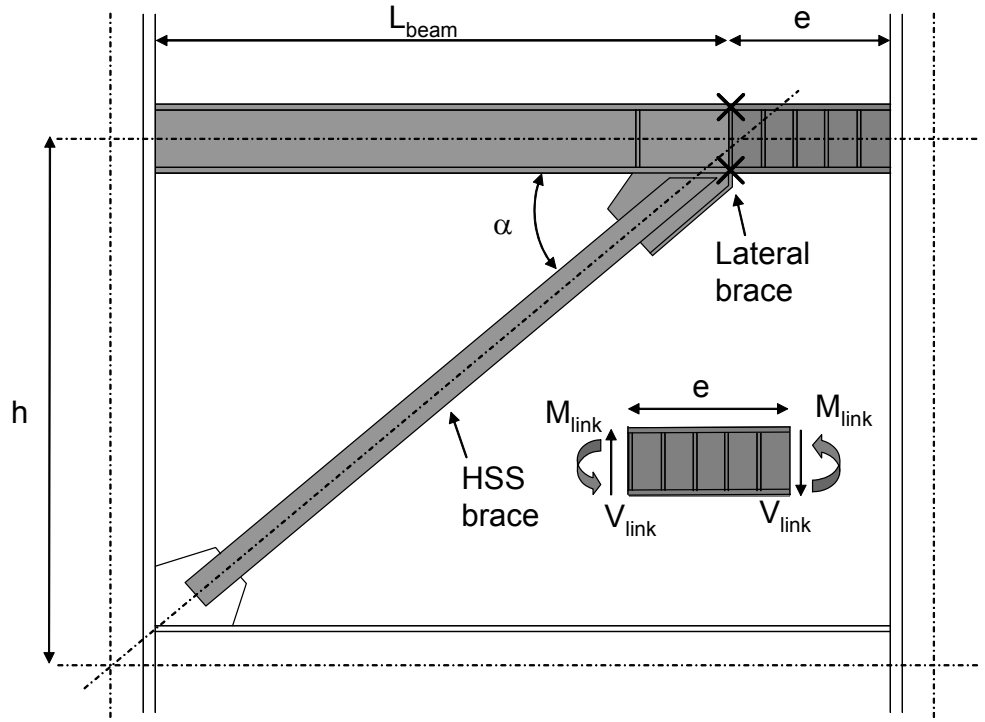

Figure 2.1: Typical EBF Geometry

The following steps are undertaken by the developed program to finalize the design of bracing member given the beam section and geometrical properties.

Based on the ratios of L/h and e/h, the span length (L), and the link length (e) are determined. The length of the beam outside of the link (L_{beam}), the length of the brace (L_{brace}), and the brace angle (α) are calculated as follows:

$$L_{beam} = L - e \tag{2.1}$$

$$\alpha = \arctan\left(\frac{h}{L_{beam}}\right) \tag{2.2}$$

$$L_{brace} = \frac{h}{\sin(\alpha)} \tag{2.3}$$

The plastic moment capacity of the section (M_p) and the plastic shear capacity (V_p) are determined according to the AISC Seismic Provisions (2005) as follows:

$$M_p = Z_{beam} F_y \tag{2.4}$$

$$V_p = 0.6 F_y t_w (d - 2t_f) \tag{2.5}$$

where t_w = web thickness of the beam, t_f = flange thickness of the beam, d = depth of the beam, Z_{beam} = plastic section modulus of the beam.

Depending on the link length, the link end moments and forces are determined using the following relationships.

$$For\ e < \frac{2M_p}{V_p} \qquad V_{link} = V_p \qquad M_{link} = \frac{eV_p}{2} \tag{2.6}$$

$$For\ e \geq \frac{2M_p}{V_p} \qquad V_{link} = \frac{2M_p}{e} \qquad M_{link} = M_p \tag{2.7}$$

where V_{link} = shear force produced at the link ends, M_{link} = moment produced at the link ends. The force distribution given in Equations 2.6 and 2.7 are based on the assumption that moments equalize at both ends of the link. This assumption can easily be violated for short links where e is less than $1.6M_p/V_p$. For these links, the moment at the column end can be significantly larger than the moment at the brace end. In addition, the link end moments and forces considered in Equations 2.6 and 2.7 do not consider any overstrength factor. The overstrength effects are added in later steps where design of individual members is conducted.

At this stage the program determines a brace section by minimizing its weight. Therefore, a trial and error procedure is utilized that starts from the brace with the lowest weight and proceeds until a suitable brace section is found. The brace section should be capable of supporting the applied axial load and bending moment. The following steps are undertaken to assure the stability of the brace member.

A thorough structural analysis has to be conducted to determine the forces and moments produced in the system. In order to facilitate the designs, a simplified method is utilized herein to predict the amount of tractions on the structural members. This method was verified using structural analysis results and is based on the free body diagram shown in Figure 2.2.

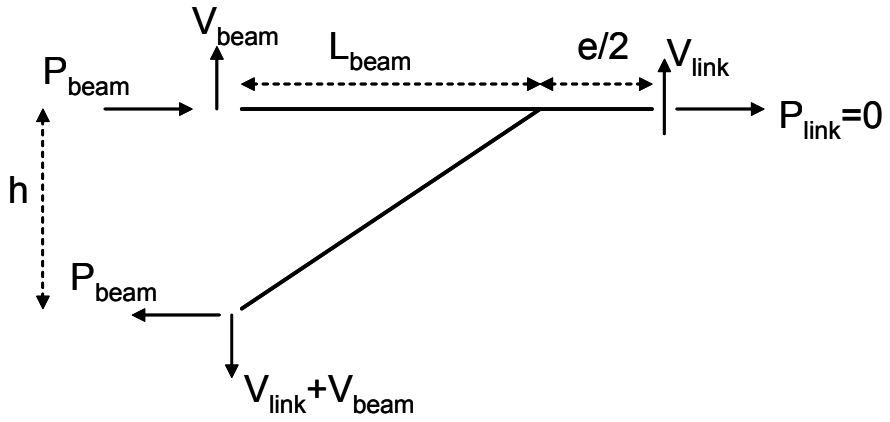

Figure 2.2: A Typical Force Distribution

One fundamental assumption used in this free body diagram is that the axial force in the link (P_{link}) is zero. The end moments of the beam and brace were taken equal to zero due to the pinned support at the ends. By taking moments with respect to the supported end of the brace, the axial force in the beam (P_{beam}) can be found as follows:

$$P_{beam} = \frac{V_{link}(L_{beam} + e/2)}{h} \tag{2.8}$$

Moment distribution method is utilized to determine the moments acting on the beam and the brace. This method requires calculation of moment distribution factors which can be determined as follows:

$$DF_{beam} = \frac{\frac{I_{beam}}{L_{beam}}}{\frac{I_{beam}}{L_{beam}} + \frac{I_{brace}}{L_{brace}}} \tag{2.9}$$

$$DF_{brace} = \frac{\frac{I_{brace}}{L_{brace}}}{\frac{I_{beam}}{L_{beam}} + \frac{I_{brace}}{L_{brace}}} \tag{2.10}$$

where DF_{beam} = moment distribution factor for the beam, DF_{brace} = moment distribution factor for the brace, I_{beam} = moment of inertia of the beam in the plane of bending, I_{brace} = moment of inertia of the brace in the plane of bending. In the derivation of the distribution factors, it was assumed that the moments distribute according to the stiffness of each member. The far ends of the beam and brace were assumed to be pinned, in other words identical.

The moment produced by the link at the brace end (M_{link}) is distributed to the brace and the beam outside of the link. By utilizing the distribution factor the moments on these members can be determined as follows:

$$M_{beam} = DF_{beam} M_{link} \tag{2.11}$$

$$M_{brace} = DF_{brace} M_{link} \times 1.25 \times R_y \tag{2.12}$$

where M_{beam} = moment acting on the beam at the brace-beam joint, M_{brace} = moment acting on the brace at the brace-beam joint, R_y = ratio of expected yield stress to the specified minimum yield stress. The distributed loads were not assumed on the beam.

After determining the moment acting on the beam the shear force in the beam (V_{beam}) can be determined as follows:

$$V_{beam} = \frac{M_{beam}}{L_{beam}} \tag{2.13}$$

The axial force in the brace (P_{brace}) can be calculated using the axial force and the shear force in the beam as follows:

$$P_{brace} = 1.25 \times R_y \times \sqrt{(P_{beam})^2 + (V_{beam} + V_{link})^2} \tag{2.14}$$

It is worthwhile to mention that the overstength of the link is included in the design of the brace member by multiplying the forces produced on the brace by 1.25 and R_y. The recommended R_y factor of 1.1 for F_y=345 MPa (50 ksi) is utilized in the program. It should be emphasized that the overstrength of the link is not considered in calculating the beam axial force. According to the AISC Seismic Provisions (2005), if a continuous section with same properties is used for the beam and the link, the R_y factor can be dropped. In fact an overstrength factor of 1.1 (or 1.25 for cases without a concrete deck) should be used for the beam but this factor is deliberately omitted from the equations. The ultimate objective is to find whether the beam has sufficient strength or not. For this purpose a PM ratio will be calculated and at that stage this ratio will be compared against the overstrength of the link. In

other words, the calculated PM ratios for the beam outside of the link do not include additional forces produced due to overstrength of the link.

The applied moment on the brace can increase due to second-order effects. This increase is accounted for by calculating the B_1 factor for the brace as recommended by the AISC Specification for Structural Steel Buildings (2005). The brace does not support any intermediate transverse loads other than its own weight which is negligible during the calculation of the B_1 factor. The moment variation on the brace is triangular where the beam end has the maximum moment and the other end has zero moment. For this type of a moment variation, the recommended C_m factor is 0.6 as per the AISC Specification (2005). Based on this C_m factor, the B_1 factor for the brace can be determined as follows:

$$\left(\frac{KL}{r}\right)_{brace} = \frac{1.0L_{brace}}{r_{brace}} \tag{2.15}$$

$$\left(F_{e1}\right)_{brace} = \frac{\pi^2 E}{\left(\frac{KL}{r}\right)^2_{brace}} \tag{2.16}$$

$$\left(P_{cr1}\right)_{brace} = \left(F_{e1}\right)_{brace} A_{brace} \tag{2.17}$$

$$\left(B_1\right)_{brace} = \frac{C_m}{1 - \frac{P_{brace}}{\left(P_{cr1}\right)_{brace}}} \geq 1.0 \tag{2.18}$$

where K = effective length factor, (KL/r) = effective slenderness, r_{brace} = radius of gyration of the brace member, F_{e1} = elastic critical Euler's buckling stress, P_{cr1} = elastic critical buckling load, A_{brace} = area of brace member, E = modulus of elasticity. In calculating the brace slenderness a K factor of 1.0 was assumed which is a conservative assumption. It should be noted that for majority of the cases the calculated B_1 factor turns out to be less than the lower bound of 1.0 because of the low value of C_m factor. Therefore, for most of the typical designs there is no moment amplification due to second order effects and the B_1 factor is essentially 1.0.

After determining the applied moments and forces, the next step is to calculate the nominal axial and moment capacities. Because square HSS sections do not suffer from lateral torsional buckling, the moment capacity of the brace $(M_n)_{\text{brace}}$ is directly equal to its plastic moment capacity.

$$\left(M_n\right)_{brace} = Z_{brace} F_y \tag{2.19}$$

The nominal axial capacity $(P_n)_{\text{brace}}$ is calculated as follows as per the AISC Specification (2005).

$$For \ \left(\frac{KL}{r}\right)_{brace} \le 4.71\sqrt{\frac{E}{F_y}} \qquad \left(F_{cr}\right)_{brace} = 0.658^{\frac{Fy}{(Fe1)_{brace}}} F_y \tag{2.20}$$

$$For \ \left(\frac{KL}{r}\right)_{brace} > 4.71\sqrt{\frac{E}{F_y}} \qquad \left(F_{cr}\right)_{brace} = 0.877\left(F_{e1}\right)_{brace} \tag{2.21}$$

$$\left(P_n\right)_{brace} = \left(F_{cr}\right)_{brace} A_{brace} \tag{2.22}$$

After determining the nominal capacities, a combined moment and axial load check is performed for the brace to ensure that the selected brace is adequate under the applied forces. This capacity check requires calculating a PM ratio which should be less than 1.0 for a satisfactory design.

$$For \ \frac{P_{brace}}{\phi(P_n)_{brace}} < 0.2 \qquad (PM)_{brace} = \frac{P_{brace}}{\phi 2(P_n)_{brace}} + \frac{(B_1)_{brace} M_{brace}}{\phi(M_n)_{brace}} \le 1.0 \tag{2.23}$$

$$For \ \frac{P_{brace}}{\phi(P_n)_{brace}} \ge 0.2 \qquad (PM)_{brace} = \frac{P_{brace}}{\phi(P_n)_{brace}} + \frac{8}{9}\frac{(B_1)_{brace} M_{brace}}{\phi(M_n)_{brace}} \le 1.0 \tag{2.24}$$

where ϕ = resistance factor which is 0.9 for members under compression and/or flexure.

By applying this outlined procedure, the program determines the most optimal brace section. The next step is to perform a PM ratio check for the beam outside of the link to determine whether this member satisfies the code provisions or not. When the beam outside of the link is not continuously supported laterally, it is susceptible to lateral torsional buckling. The nominal moment capacity of the beam outside of the link should be determined using the AISC Provisions (2005) as follows:

$$(M_n)_{beam} = M_p = Z_{beam}F_y \quad \text{when} \quad L_b \le L_p \tag{2.25}$$

$$(M_n)_{beam} = C_b\left[M_p - \left(M_p - 0.7S_xF_y\right)\left(\frac{L_b - L_p}{L_r - L_p}\right)\right] \le M_p \quad \text{when} \quad L_p < L_b \le L_r \tag{2.26}$$

$$(M_n)_{beam} = S_x\frac{C_b\pi^2 E}{\left(\frac{L_b}{r_{ts}}\right)^2}\sqrt{1+0.078\frac{J}{S_xh_o}\left(\frac{L_b}{r_{ts}}\right)^2} \le M_p \quad \text{when} \quad L_b > L_r \tag{2.27}$$

$$L_p = 1.76r_y\sqrt{\frac{E}{F_y}} \tag{2.28}$$

$$L_r = 1.95r_{ts}\frac{E}{0.7F_y}\sqrt{\frac{J}{S_xh_o}}\sqrt{1+\sqrt{1+6.76\left(\frac{0.7F_y}{E}\frac{S_xh_o}{J}\right)^2}} \tag{2.29}$$

$$r_{ts}^2 = \frac{\sqrt{I_yC_w}}{S_x} \tag{2.30}$$

where C_b = lateral torsional buckling modification factor, S_x = elastic section modulus for the beam bend about its major axis, L_b = unbraced length of the beam, h_o = distance between flange centroids, J = St. Venant's torsional constant, C_w = warping constant, I_y = moment of inertia with respect to minor axis.

The unbraced length of the beam should be determined depending on the location of lateral braces. It is required to provide lateral bracing at the brace end of the link according to AISC Seismic Provisions (2005). When the far end of the beam is connected to a column with a moment connection or a shear tab, this location is also considered to be laterally braced. When no lateral braces are used in between the brace end and the column end, L_b is equal to L_{beam}. Another important point in calculation of nominal moment capacity is the selection of an appropriate C_b factor. The variation of bending moment along the length of the beam is linear. The moment is maximum at the brace end and zero at the column end. If no lateral bracing is present then a C_b factor of 1.75 can be used. This value was determined by using the C_b factor equation presented in older versions of the AISC Specification. According to the current version, the recommended value for this loading is 1.67. It was decided to use the C_b factor given in the old specifications because the equation presented in the older versions is more suitable for this type of loading (i.e. moment at the ends without any transverse loads). The moment variation results in a significant amount of increase in the nominal moment capacity. In most cases the nominal moment capacity amplified by the C_b factor is greater than the plastic moment capacity. It should be emphasized that the C_b factor will reduce to 1.30 for cases in which a lateral brace is placed at the beam mid-span. In these cases however, the beam unbraced length is also reduced. Preliminary assessments were conducted using the full length (L_{beam}) as the unbraced length.

The nominal axial capacity of the beam $(P_n)_{beam}$ is calculated similar to the one for the brace as follows:

$$\left(\frac{KL}{r}\right)_{beam} = \frac{0.7L_{beam}}{r_y} \tag{2.31}$$

$$\left(F_e\right)_{beam} = \frac{\pi^2 E}{\left(\frac{KL}{r}\right)^2_{beam}} \tag{2.32}$$

$$For \ \left(\frac{KL}{r}\right)_{beam} \le 4.71\sqrt{\frac{E}{F_y}} \qquad \left(F_{cr}\right)_{beam} = 0.658^{\frac{Fy}{(Fe)_{beam}}} F_y \tag{2.33}$$

$$For \ \left(\frac{KL}{r}\right)_{beam} > 4.71\sqrt{\frac{E}{F_y}} \qquad (F_{cr})_{beam} = 0.877(F_e)_{beam} \tag{2.34}$$

$$(P_n)_{beam} = (F_{cr})_{beam} A_{beam} \tag{2.35}$$

where r_y = radius of gyration with respect to minor axis, A_{beam} = area of beam. In calculating the beam slenderness, a K factor of 0.7 was considered. This value is based on the theoretical solution for the case with one end pinned and the other end fixed. Test results by Engelhardt and Popov (1989b) show that the K factor varied between 0.6 and 0.7 for the specimens used in their study.

Second order effects are considered for the beam in a way similar to the one for the brace. The slenderness for the major axis bending was conservatively calculated using a K factor of 1.0. The C_m factor is taken as 0.6 for the same reasoning. Following expressions summarize the calculation procedure of B_1 factor for the beam.

$$(F_{e1})_{beam} = \frac{\pi^2 E}{\left(\frac{1.0 L_{beam}}{r_x}\right)^2_{beam}} \tag{2.36}$$

$$(P_{cr1})_{beam} = (F_{e1})_{beam} A_{beam} \tag{2.37}$$

$$(B_1)_{beam} = \frac{C_m}{1 - \frac{P_{beam}}{(P_{cr1})_{beam}}} \geq 1.0 \tag{2.38}$$

Similar to the observations for the braces, in general the lower bound value of 1.0 governs in the calculation of the B_1 factor.

The program calculates PM factors for the beam outside of the link based on the applied forces and nominal capacities. At this point two PM values are calculated. The first PM

value (PM_b) is based on considering the instability limit states. In other words, this value represents the case with discrete lateral braces. The second PM value (PM_y) is based on disregarding the instability limit states. In other words, this value represents the case with continuous lateral braces and provides a lower bound on the PM value. Following expressions are utilized in calculating PM ratios.

For discretely supported case:

$$For \quad \frac{P_{beam}}{\phi(P_n)_{beam}} < 0.2 \qquad (PM_b)_{beam} = \frac{P_{beam}}{\phi 2(P_n)_{beam}} + \frac{(B_1)_{beam} M_{beam}}{\phi(M_n)_{beam}} \tag{2.39}$$

$$For \quad \frac{P_{beam}}{\phi(P_n)_{beam}} \geq 0.2 \qquad (PM_b)_{beam} = \frac{P_{beam}}{\phi(P_n)_{beam}} + \frac{8}{9}\frac{(B_1)_{beam} M_{beam}}{\phi(M_n)_{beam}} \tag{2.40}$$

For continuously supported case:

$$For \quad \frac{P_{beam}}{\phi F_y A_{beam}} < 0.2 \qquad (PM_y)_{beam} = \frac{P_{beam}}{\phi 2 F_y A_{beam}} + \frac{(B_1)_{beam} M_{beam}}{\phi M_p} \tag{2.41}$$

$$For \quad \frac{P_{beam}}{\phi F_y A_{beam}} \geq 0.2 \qquad (PM_y)_{beam} = \frac{P_{beam}}{\phi F_y A_{beam}} + \frac{8}{9}\frac{(B_1)_{beam} M_{beam}}{\phi M_p} \tag{2.42}$$

The main purpose of these PM ratios is to check whether the beam outside of the link satisfies the code provisions or not.

Apart from these computations several auxiliary calculations are also performed by the program. These are detailed in later sections of the thesis.

2.2 Characteristics of Typical Designs

A total of 3094 cases were considered that include combinations of 91 W-sections and 34 frame geometries. The developed computer program selected the optimal HSS brace section for a given beam section size and frame geometry. As mentioned before, for some cases a

brace section cannot be found because of the high amounts of link end forces produced. These cases were excluded from the statistical analysis of typical designs. In addition, cases in which the link length (e) is smaller than $1.0M_p/V_p$ were also excluded from the final design set because these sections are too short and have excessive strain demands for typical drift limits. Overall 1782 cases were determined that represents the design space. Characteristics of these designs which are considered to be typical are investigated in this section.

The most important outcome of this parametric investigation is the resulting PM ratios for the beam outside of the link. For the design to be satisfactory the following inequalities have to be satisfied depending on whether a concrete deck is used to restrain the top flange of the beam or not.

$$(PM)_{beam} \times 1.1 \leq 1.0 \qquad \text{with concrete deck} \tag{2.43}$$

$$(PM)_{beam} \times 1.25 \leq 1.0 \qquad \text{without concrete deck} \tag{2.44}$$

In other words, the forces produced on the beam have to be amplified by the overstrength factor of 1.1 as recommended by the AISC Seismic Provisions (2005). This means the unfactored PM ratio should be below 1.1^{-1}=0.91. Similarly, if a concrete deck is not present the forces have to be amplified by 1.25 according to the Commentary to the AISC Seismic Provisions (2005). This means the unfactored PM ratio should be below 1.25^{-1}=0.8. The statistical analysis of the PM ratios (PM_b, and PM_y) for the beam outside of the link is presented in Figures 2.3 and 2.4 for cases where the beam is laterally unsupported and supported, respectively.

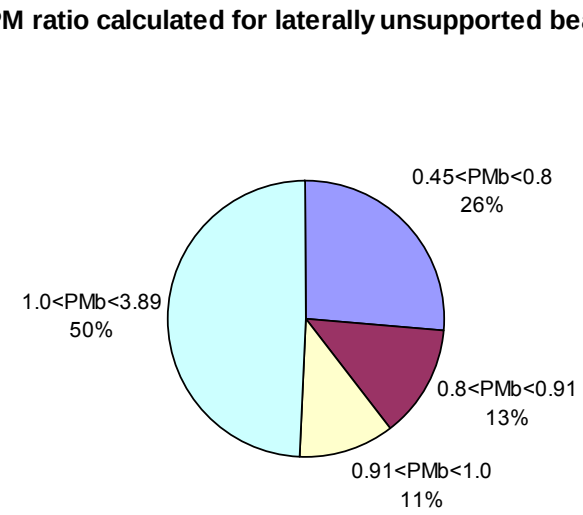

Figure 2.3: Statistical Analysis of PM Ratio for Laterally Unsupported Beams

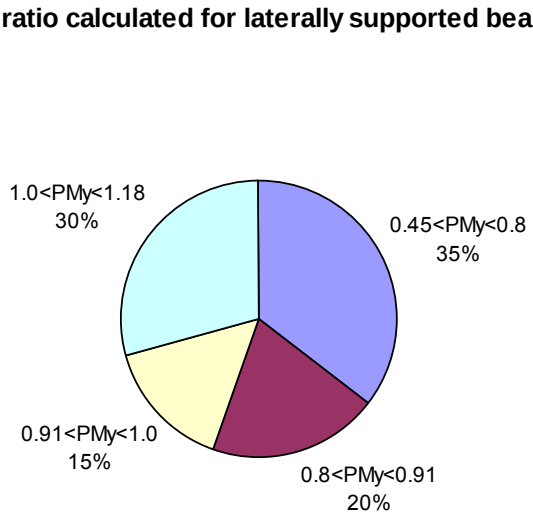

Figure 2.4: Statistical Analysis of PM Ratio for Laterally Supported Beams

The severity of the overstrength problem is evident from Figures 2.3 and 2.4. When the beam is discretely supported the instability effects are significant. For these cases only 26 percent of the cases satisfied the code provisions if no concrete deck is present. This number increases to 39 percent if a concrete deck is utilized. In either case more than 60 percent of the designs are inadmissible. The maximum PM ratio can reach to 3.89 for the cases considered.

If the beam is laterally supported continuously, the instability failure modes are prevented but the beam can plastify under the action of high axial force and moment. The statistical analysis results reveal that PM ratios for laterally supported beams are less than the ones for unsupported beams as expected. For these cases 35 percent of the designs without concrete deck satisfy code limits while 55 percent satisfies the code when a concrete deck is present. More than 40 percent of the cases do not satisfy the code provisions. The maximum PM ratio can reach to 1.18 for the cases considered. It should be emphasized that the PM_y values provide a lower bound on the PM ratio in general. Even if discrete lateral supports are placed to the beam outside of the link the lowest PM ratio that can be reached is PM_y.

The variation of distribution factors (DF_{beam}, DF_{brace}) for the beam and the brace were investigated. The analysis results reveal that the distribution factors are significantly dependent on the brace angle. The variations of distribution factors are given in Figures 2.5 and 2.6.

When the brace angle increases the forces produced on the brace typically decreases. When the forces are decreased a smaller brace section can be sufficient to support the loads. Selecting a smaller section results in a decrease in the brace stiffness, and therefore; a decrease in its distribution factor. As the brace angle increases the distribution factor for the beam reaches to unity as shown in Figure 2.5 whereas the distribution factor for the brace reaches to zero as shown in Figure 2.6. This means that for larger brace angles majority of the moment produced by the link is resisted by the beam outside of the link. When the brace angle gets closer to 30 degrees both distribution factors converge to 0.5 implying that the moment produced by the link is equally resisted by the beam outside of the link and the brace.

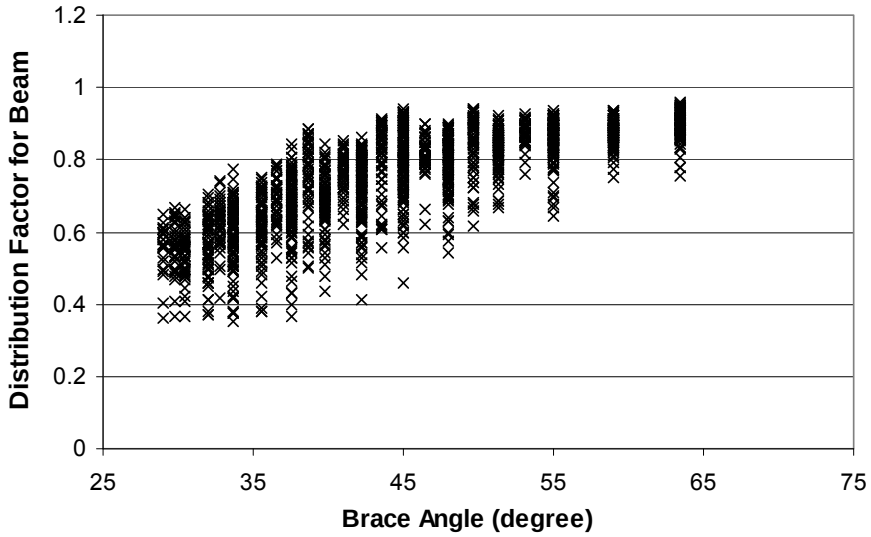

Figure 2.5: Distribution Factor for the Beam

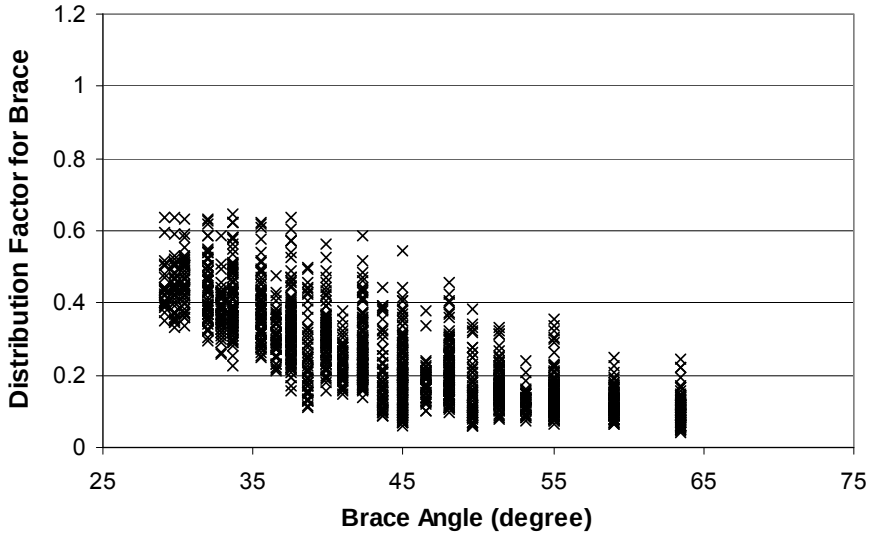

Figure 2.6: Distribution Factor for the Brace

In order to provide general information on the resulting brace sizes, the slenderness of the braces were evaluated. A plot of brace slenderness function of the brace angle is given in Figure 2.7. According to this figure the brace slenderness values varied between 27 and 93 with average of 51. All of the braces have a slenderness value that falls into the inelastic buckling range. These braces were designed using a *K* factor of unity. This was a conservative assumption. Designers may choose a value less than unity based on the end conditions which are not easily represented by ideal boundary conditions. The resulting brace sizes suggest that using a lower K factor such as 0.8 does not significantly alter the final brace size. For low slenderness values the axial strength obtained from the column strength curve is not significantly influenced by the slenderness of the brace.

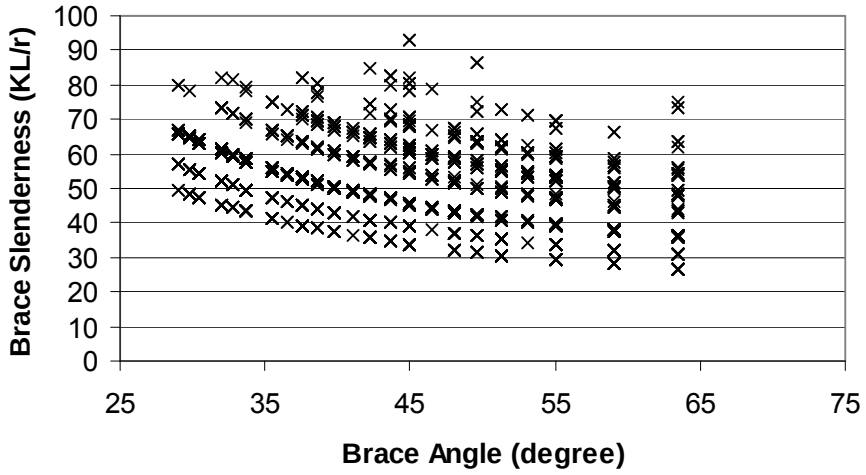

Figure 2.7: Slenderness of Brace Members

Distribution factors are related with the relative stiffness of the connected members. In addition to their stiffness, strength of the beam and brace were compared for typical designs. The plastic moment capacity provided at the beam-brace connection was studied by calculating strength ratios. For the beam this ratio corresponds to the plastic moment capacity of the beam divided by the sum of the plastic moment capacities of the beam and the brace. Similar calculations were performed for the brace and this time the plastic moment capacity of the brace was normalized by the sum of capacities. The results are presented in

Figures 2.8 and 2.9. It is evident from these figures that the same conclusions from the investigation of stiffness can be derived for strength also. For shallow angles the strength ratios converge to 0.5 implying that both the beam and the brace are contributing equally to the resistance of the joint. When the brace angle is increased the strength of the beam dominates over the strength of the brace. The investigation on strength will be useful in later sections when the total moment capacity provided at the joint is examined closely.

The PM ratio for the beam was investigated further to observe if the problematic designs can be related to the geometry or the beam properties. For this purpose the PM ratio based on yielding (i.e. laterally supported case) was considered. Figures 2.10, 2.11, and 2.12 show the dependence of the PM ratio on the e/L ratio, the brace angle, and the $e/(M_p/V_p)$ ratio, respectively.

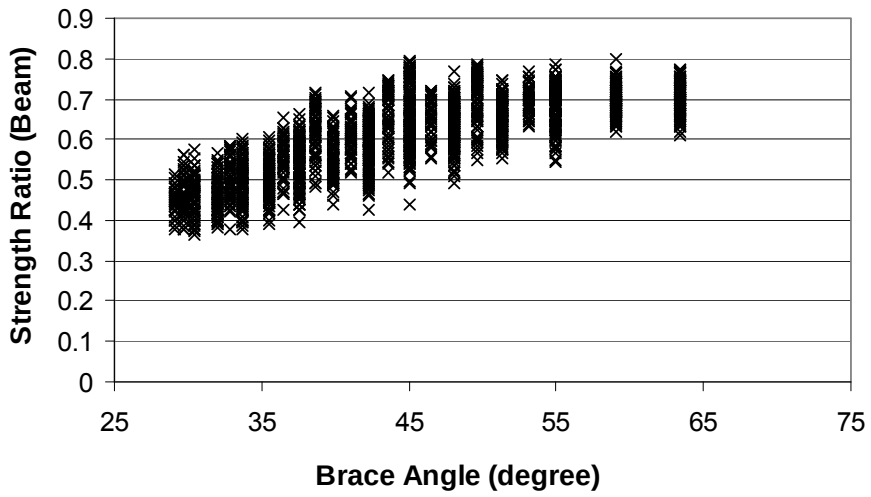

Figure 2.8: Strength Ratio for the Beam

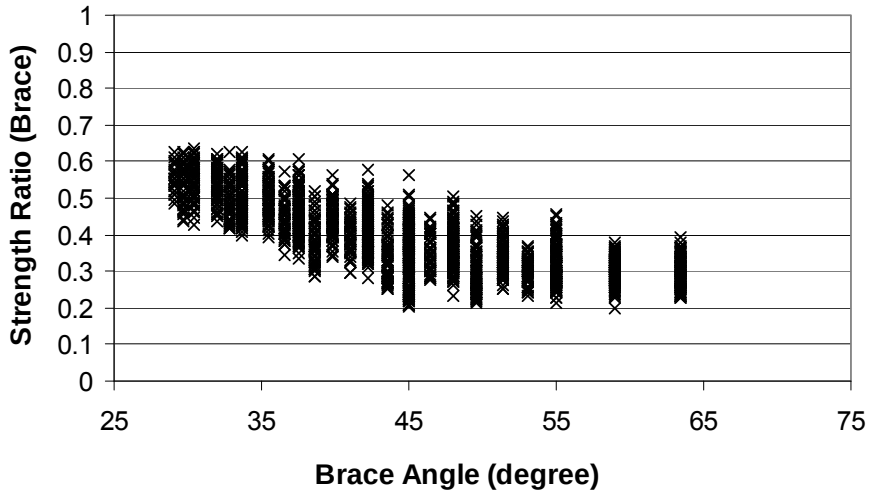

Figure 2.9: Strength Ratio for the Brace

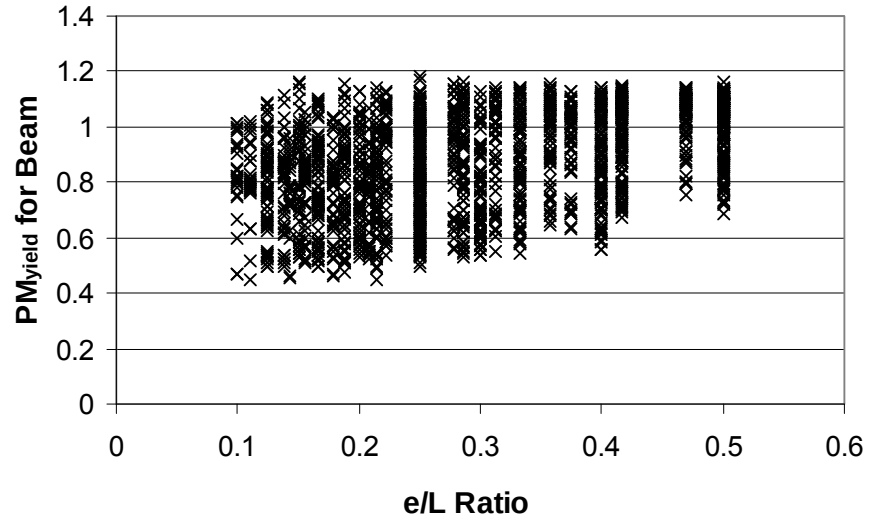

Figure 2.10: PM Ratio as a Function of e/L

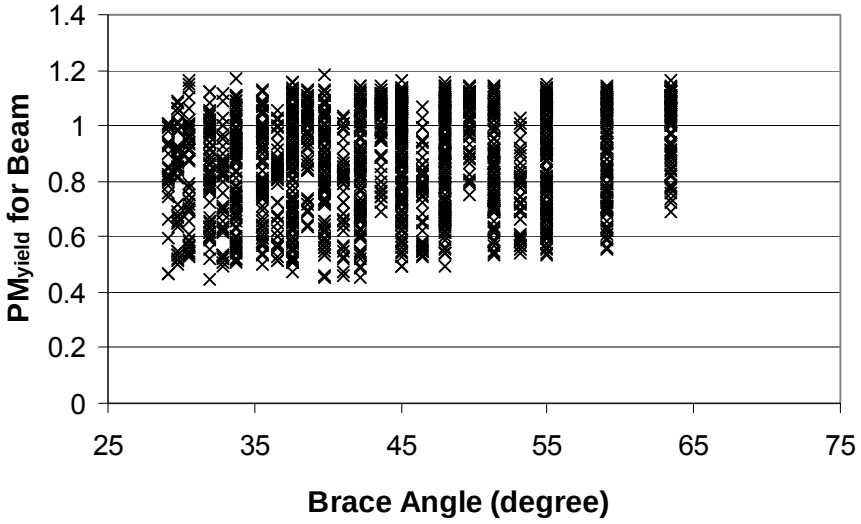

Figure 2.11: PM Ratio as a Function of the Brace Angle

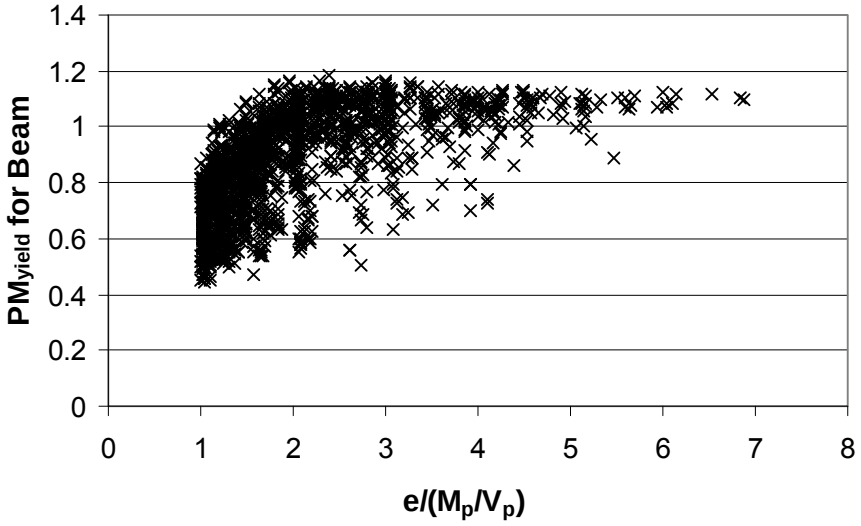

Figure 2.12: PM Ratio as a Function of $e/(M_p/V_p)$

Based on Figures 2.10 and 2.12 it can be concluded that the PM ratio is not very much dependent on the e/L ratio or the brace angle. All e/L ratios or the brace angles produced PM ratios in excess of 0.8. On the contrary, Figure 2.12 reveals that the PM ratio depends to a certain extent on the normalized link length ($e/(M_p/V_p)$). Flexural yielding links with normalized link lengths greater than 3.0 produced PM ratios in excess of 0.8 while shear yielding links with normalized link lengths less than 1.6 generally produced PM ratios below 0.8. From this point it seems that the flexural yielding links are more problematic. This is due to the fact that significantly high moments are produced at the link ends which in turn transmit higher moments to the beam outside of the link.

The stability of the beam outside of the link is usually governed by its slenderness (L_{beam}/r_y). The effects of slenderness on the calculated PM ratios are investigated in Figure 2.13. Based on this figure, the PM_b ratios increase significantly with increasing in slenderness when the L_{beam}/r_y ratio is greater than 100. For lower slenderness values the PM_b ratios generally fall within a narrow band.

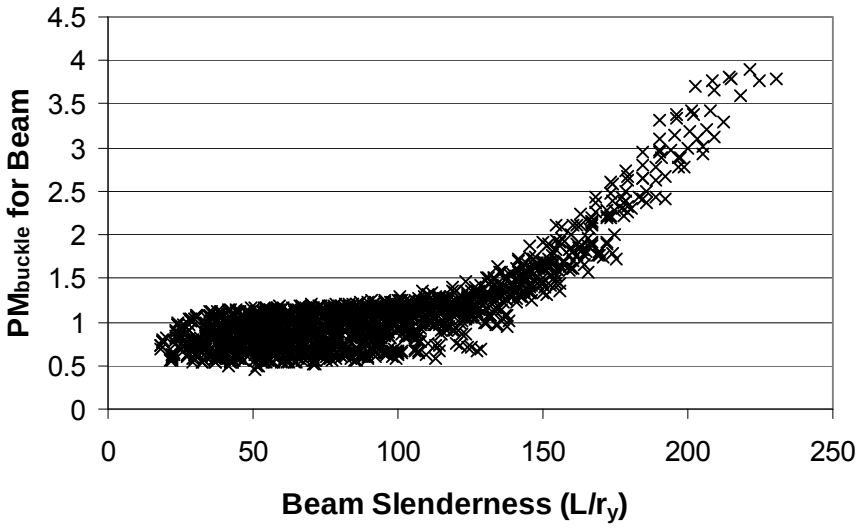

Figure 2.13: PM ratio as a function of beam slenderness

2.3 Investigation of Beam Plastification

Analysis results of the previous section revealed that 65 percent of the cases investigated as a part of this study have PM_y values greater than 0.8 even if the beam outside of the link is fully supported. This means that the beam outside of the link can form a plastic hinge at the connection region. The primary focus of the study presented in this section is to investigate the consequences of beam yielding. When the beam yields, the forces and moments will redistribute. The redistribution can occur inside the link. In other words, the moments at both ends of the link will change significantly and majority of the moments can occur at the column side. Another possibility is that the moments will be redistributed between the beam and the brace where the brace will take an increased share of the link end moment. The latter redistribution type is investigated herein by using a simplified load distribution model.

The free body diagram of the simplified load distribution model is shown in Figure 2.14. In this model it is assumed that the strain hardened link will produce a shear force equal to $1.25xR_yxV_{link}$. The most critical loading is the one that creates tension on the beam and compression on the brace.

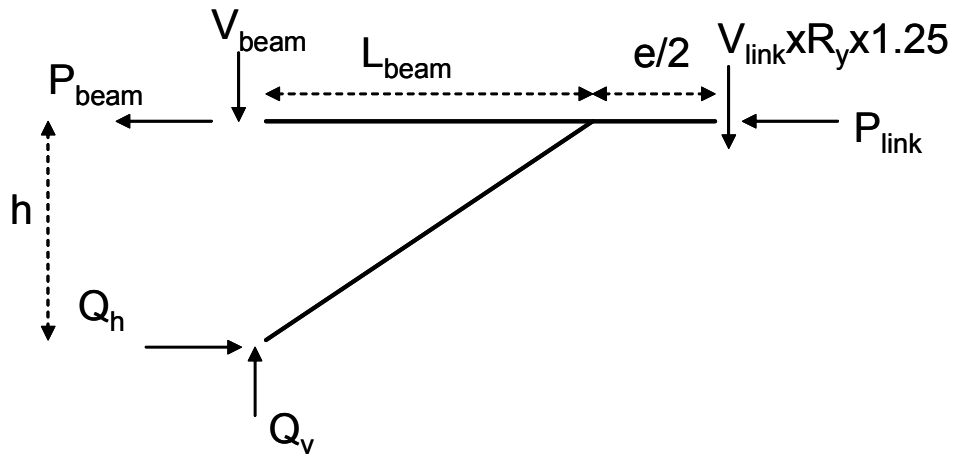

Figure 2.14: Distribution of forces considering beam yielding

The link end moment produced by this shear force can be calculated as follows:

$$M_{link} = 1.25 \times R_y \times V_{link} \frac{e}{2} \tag{2.45}$$

This moment distribution is based on the assumption that moments equalize at both ends of the link and may not be accurate for short links as explained earlier.

It is assumed that when the link shear reaches to $R_y x V_{link}$ the beam outside of the link reaches to its capacity and does not take any extra force. Based on this assumption the maximum amount of axial force on the beam can be calculated as follows:

$$P_{beam} = \frac{R_y V_{link} \left(L_{beam} + e/2\right)}{h} \tag{2.46}$$

In reality the beam axial force can be smaller if the PM ratio of the beam is large or greater if the PM ratio is small. This way of calculating the axial force gives a good approximation of the force level that is expected at the onset of beam yielding.

The horizontal reaction at the brace support (Q_h) can be directly found from equilibrium as follows:

$$Q_h = \frac{1.25 \times R_y \times V_{link} \left(L_{beam} + e/2\right)}{h} \tag{2.47}$$

Equilibrium of the forces in the horizontal direction gives the axial force produced in the link (P_{link}) as follows:

$$P_{link} = Q_h - P_{beam} \tag{2.48}$$

The moment on the beam can be found using moment distribution as follows:

$$M_{beam} = DF_{beam} M_{link} \tag{2.49}$$

It should be emphasized that this moment value is bounded by the maximum moment capacity of the beam $(M_{beam})_{max}$ which can be computed as follows:

$$For\ \frac{P_{beam}}{R_y P_y} < 0.2 \qquad (M_{beam})_{\max} = H_f R_y M_p \left(1 - \frac{P_{beam}}{2R_y P_y}\right) \tag{2.50}$$

$$For\ \frac{P_{beam}}{R_y P_y} \geq 0.2 \qquad (M_{beam})_{\max} = \frac{9}{8} H_f R_y M_p \left(1 - \frac{P_{beam}}{R_y P_y}\right) \tag{2.51}$$

where P_y is the squash load of the beam expressed as follows:

$$P_y = F_y A_{beam} \tag{2.52}$$

Preliminary finite element analysis results showed that after the beam plastifies it can still undergo strain hardening if the behavior is not governed by any instability limit states. In this model it is assumed that the bending moment increases due to strain hardening while the axial force remains constant. A hardening factor (H_f) is utilized in the model to take into account the effects of strain hardening during the computations. This factor can range between unity and 1.25.

By considering the equilibrium of the brace-beam joint, the moment on the brace can be calculated as follows:

$$M_{brace} = M_{link} - M_{beam} \tag{2.53}$$

The shear in the beam outside of the link can be found as follows:

$$V_{beam} = \frac{M_{beam}}{L_{beam}} \tag{2.54}$$

The vertical reaction at the brace support (Q_v) can be calculated as follows:

$$Q_v = R_y \times 1.25 \times V_{link} + V_{beam} \tag{2.55}$$

Finally, the axial force on the brace is the vectorial sum of the two reaction forces and can be found as follows:

$$P_{brace} = \sqrt{Q_h^2 + Q_v^2} \tag{2.56}$$

Based on this new set of forces, the PM ratio of the brace can be re-calculated using Equations 2.23 and 2.24.

This model was implemented into the computer program to investigate the consequences of beam yielding. The first set of investigations was performed using a hardening factor equal to unity which represents no strain hardening. The variation of the PM factor for the brace with several different factors is given in Figures 2.15, 2.16, and 2.17. According to Figure 2.15 the PM factor for the brace significantly increases when the PM ratio for the beam is greater than unity. This is an expected outcome. When the force demands on the beam is high and the beam is incapable of supplying enough resistance, the brace member has to take the extra forces produced after yielding of the beam.

Figures 2.16 and 2.17 can be investigated to understand the problematic cases with high PM ratios. According to Figure 2.16, the PM ratios tend to be higher when the distribution factor for the brace is lower. Low distribution factors belong to the cases with very tiny braces. In these cases the beam tries to redistribute the extra moments to the brace but the brace is not sizeable enough to counteract these moments.

According to Figure 2.17 cases with large e/L ratios are more problematic compared to the ones with smaller e/L ratios. Cases with large e/L ratios generally represent the moment yielding links. In these cases the braces are subjected to low axial forces and their sections are relatively smaller. This in turn results inadequate braces when the beam starts to yield.

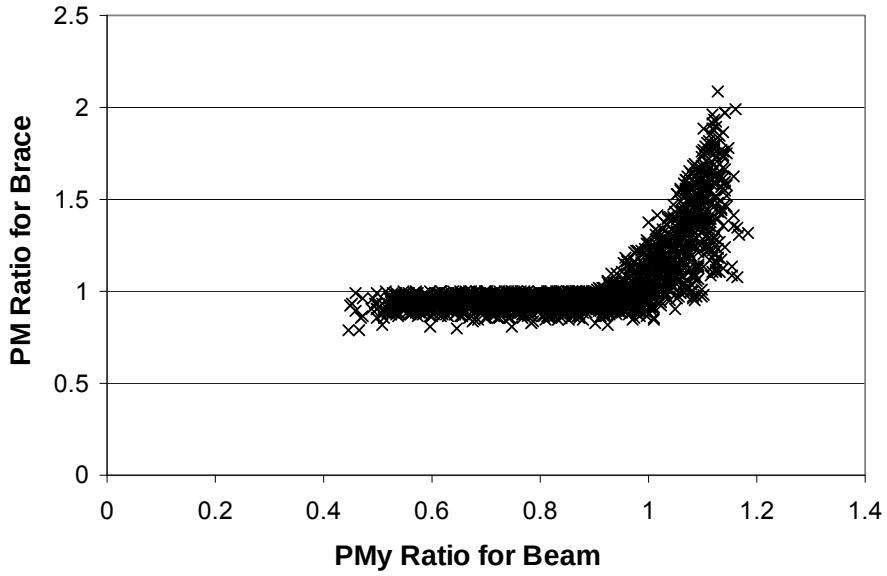

Figure 2.15: Variation of PM ratio for the brace as a function of PM ratio for the beam

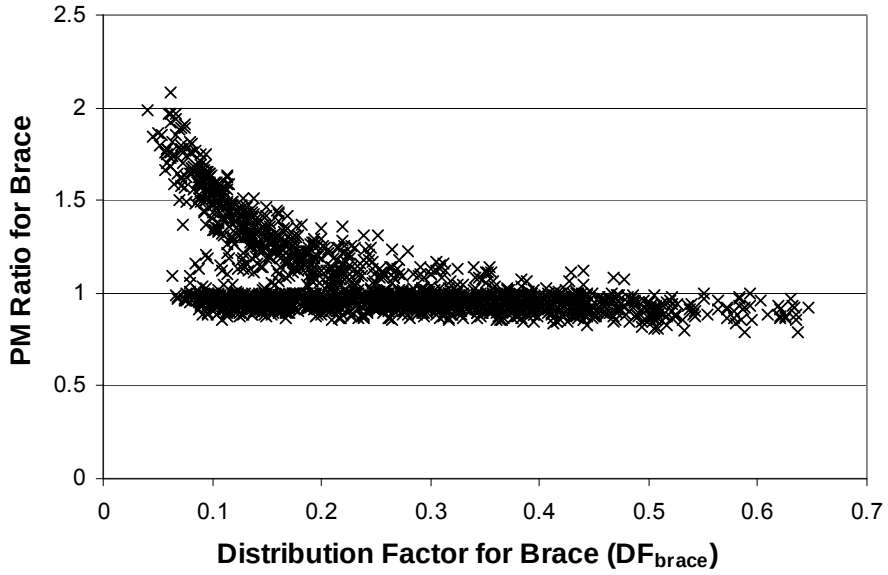

Figure 2.16: Variation of PM ratio for the brace as a function of distribution factor for brace

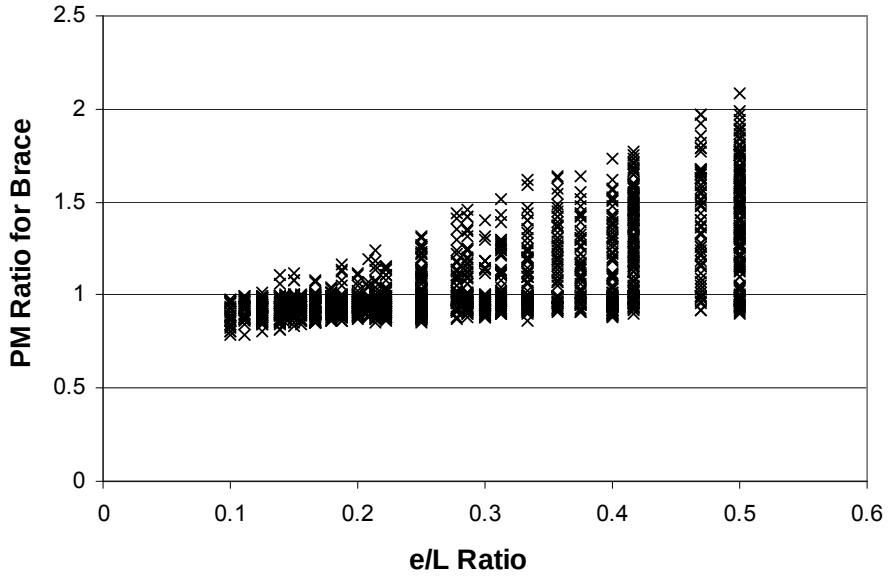

Figure 2.17: Variation of PM ratio for the brace as a function of e/L ratio

The effects of the hardening factor was studied by considering an extreme case with H_f=1.25. The resulting PM values were plotted against the PM values for the beam in Figure 2.18. It is evident from these results that the strain hardening in the beam reduces the PM values of the brace by a significant margin.

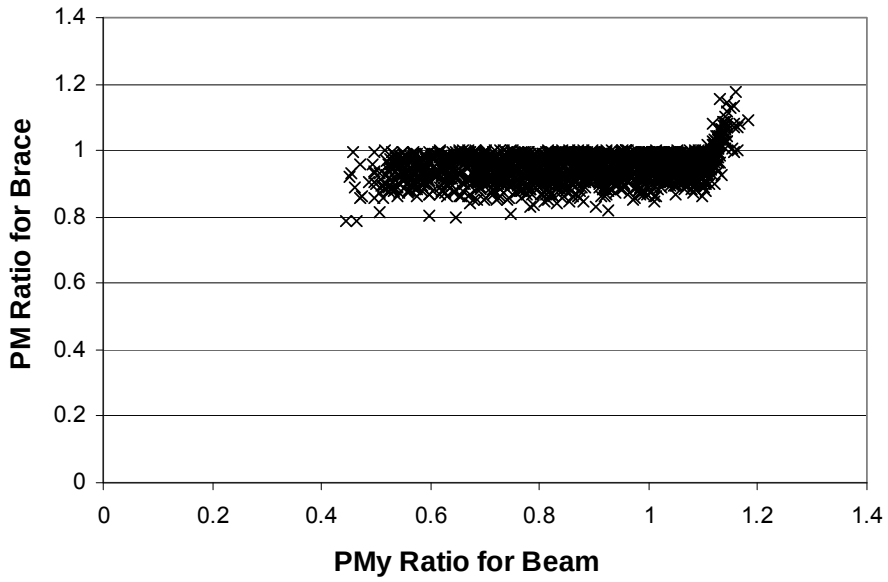

Figure 2.18: Variation of PM ratio for the brace as a function of PM ratio for the beam

CHAPTER 3

NUMERICAL MODELING DETAILS AND VERIFICATION

In this chapter the finite element modeling details are given alongside with the verification of the models. Majority of previous research on EBFs has included tests on isolated links. There are a few experimental studies reported to date on EBF sub-assemblages which can be used for model verification purposes. The study conducted by Engelhardt and Popov (1989b) is considered as a benchmark in this thesis and the test results obtained by these researchers were used in calibrating the finite element models.

In late 1980's Engelhardt and Popov (1989b) investigated the potential use of long, flexural yielding links in seismic resistant EBFs. A total of fourteen 2/3 scale sub-assemblages were subjected to cyclic loads as a part of this study. The sub-assemblage configuration and dimensions were selected to model a portion of a single-diagonal EBF with links attached to the columns. These researchers stated that the objectives of this study were to provide an assessment of the key issues affecting the use of long links in EBFs, to identify the potential range of applicability of long link EBF systems and to develop preliminary design recommendations for EBFs with long links. Following sections present details of the study conducted by Engelhardt and Popov (1989b).

3.1 Benchmark Experiments of Engelhardt and Popov (1989b)

The schematic of the test set-up used in the experiments is given in Figure 3.1. In this test setup the beam section can have a variable length. Two typical lengths were used and these were named as "Setup A" and "Setup B". The dimensions of the members were determined by scaling down the prototype designs. The beam was connected to a column at the link end. The other end of the beam was supported as shown in Figure 3,1 and these supports actually contained load cells to measure the magnitude of support reactions. A brace was attached to the beam and the length of the brace corresponds to one-half of the brace in the prototype.

Column and brace members were also supported at their ends with attachments details that contain load cells to measure the reaction forces. Some auxiliary attachments were also utilized to prevent out-of-plane movement of the structural members. In particular, an assembly was utilized to provide lateral supports to the beam outside of the link. The location of this assembly can be adjusted depending on the location of lateral supports. Cyclic loads were applied by using a loading ram which is connected to the column.

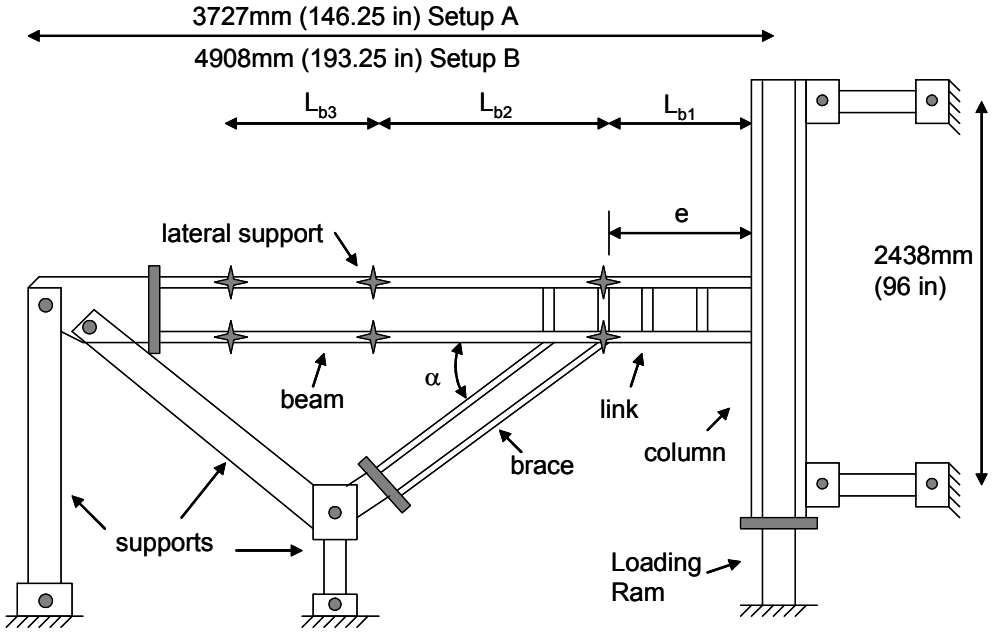

Figure 3.1: Schematic of the Test Set-up used by Engelhardt and Popov (1989b)

The prime variables investigated in this testing program were link length, beam section properties, location of stiffeners, brace-beam angle, beam flexural stiffness, beam lateral support spacing, link-to-column connection details, and brace-to-link connection details. Two beam sections, W12x16 and W12x22, were used throughout the testing program. These sections represent reasonable upper and lower bound for flange width-thickness ratio. A survey conducted by the researchers revealed that the column sections were typically on the order of 1 to 6 times rigid than the link sections. Based on this range, a W10x77 section was used in all experiments. Different details were utilized for the brace-to-link and link-to-

column connections. The brace was either directly welded to the flange of the beam or in some cases a gusset plate was utilized to connect the beam to the brace.

Among the 14 specimens tested by the researchers, only 3 were utilized in the verification study. These specimens were Specimen 3, Specimen 6, and Specimen 7. Each of these specimens has unique characteristics in terms of their behavior. Specimen 3 showed stable behavior during the loading history and did not exhibit any strength degradation. Specimen 6 suffered from severe local buckling at the brace connection panel and showed gradual strength degradation. Specimen 7 suffered from lateral torsional buckling and showed severe loss of strength after lateral buckling. Basically all detrimental failure modes, local buckling and lateral buckling, are accounted for by selecting these specimens.

The researchers considered some typical prototype designs where the brace angle varied between 28^{o} and 51^{o}. The prototype design dimensions for the three specimens are given in Table 3.1.

Table 3-1: Details of Prototype Designs

Specimen Number	**Link Length, e mm (in)**	**Span Length, L m (ft)**	**Beam Length Outside of Link mm (in)**	**Beam Brace Angle degrees**	**L/e**	**Story Height m (ft)**
3	1270 (50)	4.26 (14)	2997 (118)	51.2	3.4	3657 (12)
6	1676 (66)	7.62 (25)	5943 (234)	33.2	4.5	3657 (12)
7	1117 (44)	7.92 (26)	6807 (268)	28.4	7.1	3657 (12)

Based on the prototype designs given in Table 3.1, the resulting specimen dimensions were derived by scaling down the values. The dimensions and the sections used for these three specimens are given in Table 3.2. In addition, material and geometrical properties of the links are given in Table 3.3. A set of lateral supports were provided to each specimen depending on its length. The general layout of the lateral supports is shown in Figure 3.1 and their locations are given in Table 3.4.

Table 3-2: Actual Specimen Dimensions and Structural Sections

Specimen Number	Beam Section	Link Length mm (in)	Brace Section	Brace Angle (degree)	Set-up	Column Section
3	W12x22	838 (33)	TS 7x4x5/16	51.2	A	W10x77
6	W12x16	1117 (44)	W10x26	33.2	B	W10x77
7	W12x16	737 (29)	TS 4x5x1/4	28.4	B	W10x77

Table 3-3: Geometrical and Material Properties of Link Sections

Specimen Number	Beam Section	Flange Slenderness bf/2tf	Yield Strength, Fy flange MPa (ksi)	Yield Strength, Fy web MPa (ksi)	Actual e/(Mp/Vp)
3	W12x22	4.7	316 (46)	393 (57)	2.4
6	W12x16	7.5	358 (52)	413 (60)	3.4
7	W12x16	7.5	303 (44)	351 (51)	2.3

Table 3-4: Location of Lateral Supports

Specimen Number	L_{b1} mm (in)	L_{b1}/r_y	L_{b2} mm (in)	L_{b2}/r_y	L_{b3} mm (in)	L_{b3}/r_y
3	838 (33)	39	2057 (81)	96		
6	1117 (44)	57	1879 (74)	96	1168 (46)	60
7	736 (29)	38	1879 (74)	96	1549 (61)	79

Each of these three specimens had different stiffening arrangements and connection types. Stiffening and connection details are given in Figures 3.2, 3.3, and 3.4. As shown in these figures, ribs were utilized in connecting the link to the column in specimens 6 and 7. All three specimens have different brace to beam connection details. In specimen 3, the tubular brace is directly welded to the beam. Specimen 6 also utilized direct welding but the type of the brace used was a W-shape brace instead of a tubular one. In specimen 7, a gusset plate was utilized to connect a tubular section to the beam.

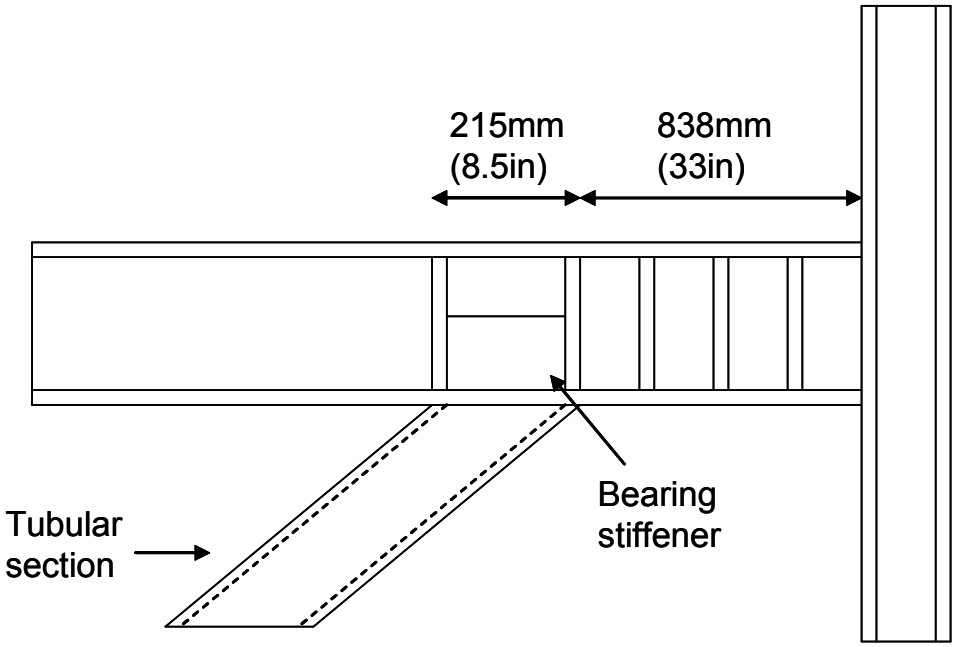

Figure 3.2: Stiffening and Connection Details for Specimen 3

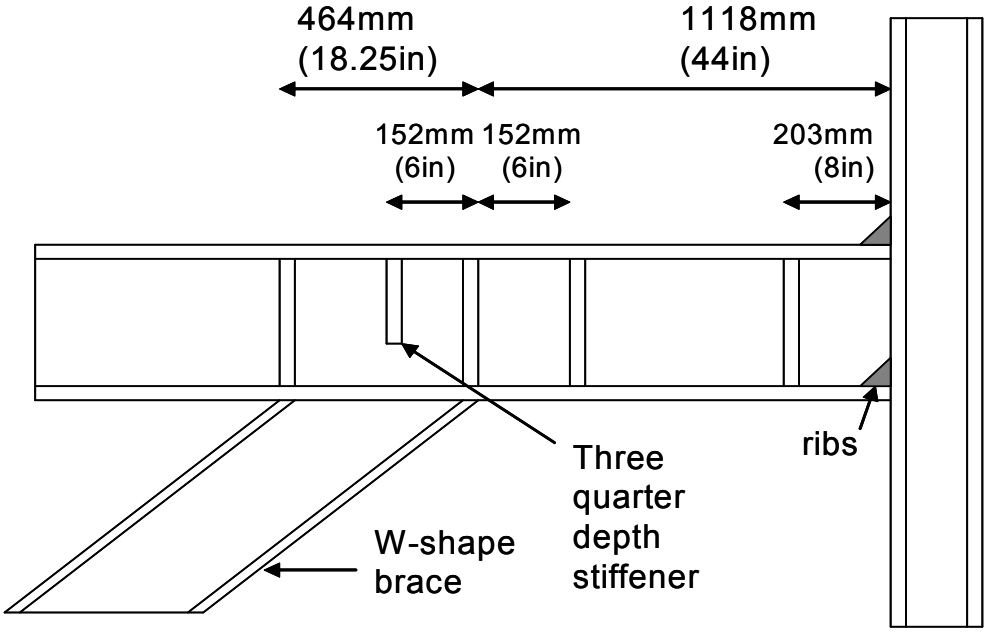

Figure 3.3: Stiffening and Connection Details for Specimen 6

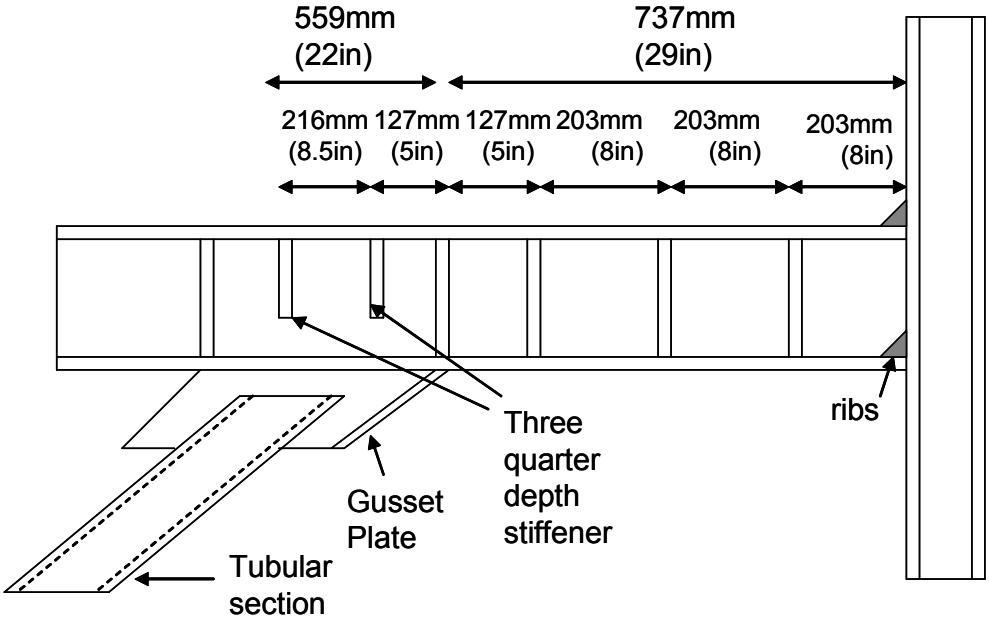

Figure 3.4: Stiffening and Connection Details for Specimen 7

During the design of the specimens the brace members were selected to satisfy the strength equations presented in the steel design code of that time. For the design of specimen 7, however, the strength requirements were intentionally violated. The brace section for this specimen was purely designed for axial compression without taking into account the bending moment. The reason for omitting the bending moment was to increase the bending moment on the beam outside of the link and promote failure in this region of the sub-assembly. The PM ratios for the three specimens were not reported by the researchers but were calculated using the interaction equations presented in Chapter 2. The PM ratios were calculated to be 1.06, 0.73, 1.60 for specimens 3, 6, and 7, respectively.

The reported failure modes for the three specimens and the amount of plastic rotation at the onset of strength degradation are given in Table 3.5. According to the AISC Seismic Specification (2005) regulations the expected plastic rotations from specimens 3, 6, and 7 are 0.032, 0.02, and 0.038 radians, respectively. According to the experimental results specimen 3 performed as expected and its rotation capacity is twice the required rotation capacity. Specimen 6 suffered from local buckling both at the brace connection panel and the flanges

of the link but these buckles actually occurred after the required rotation capacity was reached. Specimen 7 was not able to reach the required plastic rotation capacity due to lateral torsional buckling of the beam outside of the link.

Table 3-5: Failure Modes of Specimens

Specimen Number	Primary Failure Modes	Additional Failure Modes	Plastic Rotation Capacity (rad)
3	Fracture of link flange at link-column connection		0.073
6	Fracture of link flange at link-column connection at the ends of reinforcing ribs	Flange buckling in brace connection panel; flange buckling in link adjacent to ribs	0.033
7	Fracture of link flange at link-column connection at the ends of reinforcing ribs; lateral torsional buckling of beam		0.017

3.2 Finite Element Modeling Details

A commercially available finite element package ANSYS (2006) was used to conduct finite element analysis of the three specimens. The beam outside of the link, the link, the column, the brace, the gusset plate, the ribs, and the stiffeners were all modeled by 8-node shell elements (shell93). Two-node truss elements (link8) were used to model the stiff link between the ends of the beam and the brace. Finite element meshes for specimens 3, 6 and 7 are given in Figures 3,6, 3.7, and 3.8, respectively. The global coordinate axis is also given in Figure 3.6. The material properties reported by Engelhart and Popov (1989b) were used in the models. The modulus of elasticity of steel was assumed to be 200 GPa (29000 ksi) and the Poisson's ratio was assumed to be 0.3. The nonlinear material behavior was modeled using Von Mises yield criterion and utilizing bilinear kinematic hardening. The hardening modulus beyond the yield point was assumed to be 2 GPa (290 ksi) which is equal to 1 percent of the initial elastic modulus. Out-of-plane movement of the model was prevented by applying displacement boundary conditions (u_x=0) at the points of lateral supports. The movement of free ends of the beam and the brace was prevented in three of the principal directions.

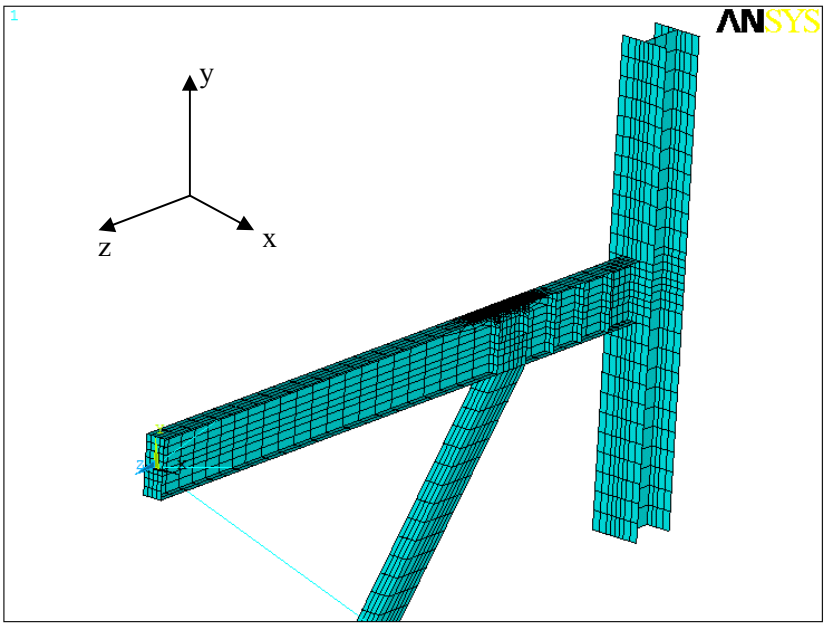

Figure 3.5: Finite Element Model of Specimen 3

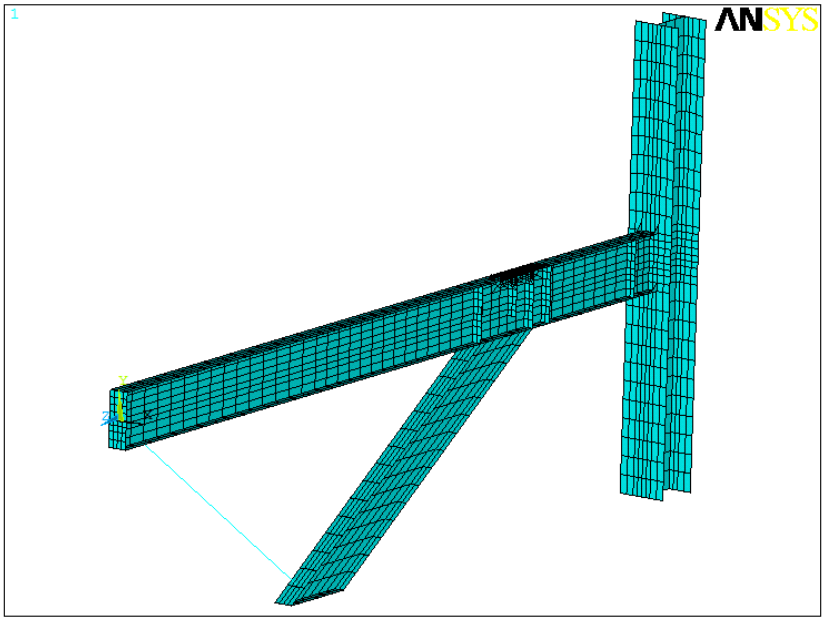

Figure 3.6: Finite Element Model of Specimen 6

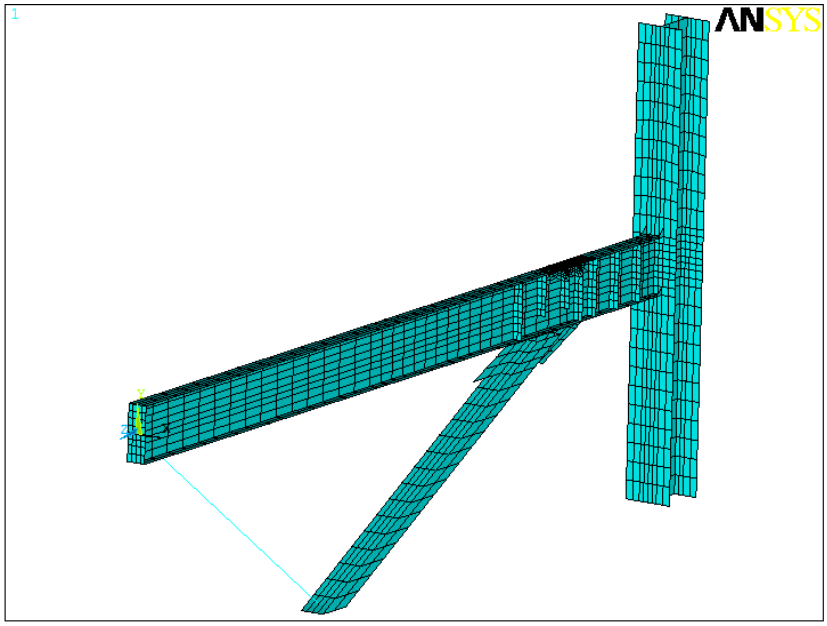

Figure 3.7: Finite Element Model of Specimen 7

Both ends of the column were prevented from movement in the z-direction. Displacements were applied in the y-direction at the bottom end of the column. Particularly, a single node that is located at the junction of flange and web was forced to displace vertically in order to achieve the loading protocol utilized during the experiments. It is worthwhile to note that applying displacements to more than one node creates a rotational restraint and concentrated moments at the bottom of the column which in turn alters the boundary conditions significantly.

Newton-Raphson method was utilized to trace the load displacement history. Geometrical nonlinearities were included in the analysis to capture instabilities. In general, a monotonic analysis for each specimen was conducted first to find out the relationship between applied displacement and link rotation angle. Vertical displacements of the nodes that lie on the centroid of the link cross section were monitored at the two ends of the link. These vertical displacements were used to calculate the link rotation angle. After conducting a monotonic analysis, a separate cyclic analysis was conducted using the link rotation histories adopted by Engelhardt and Popov (1989b). In cases where the beam suffers from lateral torsional

buckling, it is difficult to apply the correct amount of displacement to achieve the target rotation angle. Because the system softens significantly, the amount of vertical displacement required to achieve the target rotation becomes excessive. High amounts of vertical displacement demands on models that experience lateral torsional buckling can result in numerical instabilities and convergence problems which cause early termination of the analysis. In these situations the displacement demand was reduced for cycles that cause compression on the beam outside of the link.

Comparisons of experimental findings and numerical results are given in Figures 3.8 to 3.13. Experimental observations and the finite element analysis results are presented separately for clarity of comparisons. The experimental observations were plotted by digitizing the data presented by Engelhardt and Popov (1989b). Results are presented in terms of link shear force versus total rotation. It is evident from the comparisons that analysis results conform to the experimental observations. Based on the analysis results, specimen 3 showed stable hysteretic behavior without any sign of instability. Specimen 6 suffered from local buckling at the brace connection panel and also at the link ends. Local buckling was liable for strength degradation which was observed for this specimen. Specimen 7 suffered from lateral torsional buckling and had a very limited rotation capacity. Due to the aforementioned reasons on numerical instability, the positive displacements which cause compression on the beam outside of the link were cut short. To achieve convergence in the models the displacements in that direction were limited. This in turn resulted in the discrepancy in link rotations between the actual case and numerical analysis. Nevertheless, the finite element model is accurately capturing lateral torsional buckling behavior.

Typical deformed shapes and failures of specimens are presented in Figures 3.14 to 3.16. It can be easily recognized from Figure 3.15 that specimen 6 experiences severe local buckling at the brace connection panel. In addition, lateral torsional buckling of the beam outside of the link can be seen from Figure 3.16.

Based on comparisons of the actual and predicted behavior, it can be concluded that finite element models are capable of simulating the response of specimens. The finite element models capture both local and global instabilities with sufficient accuracy and can be used to study the response of the beam outside of the link.

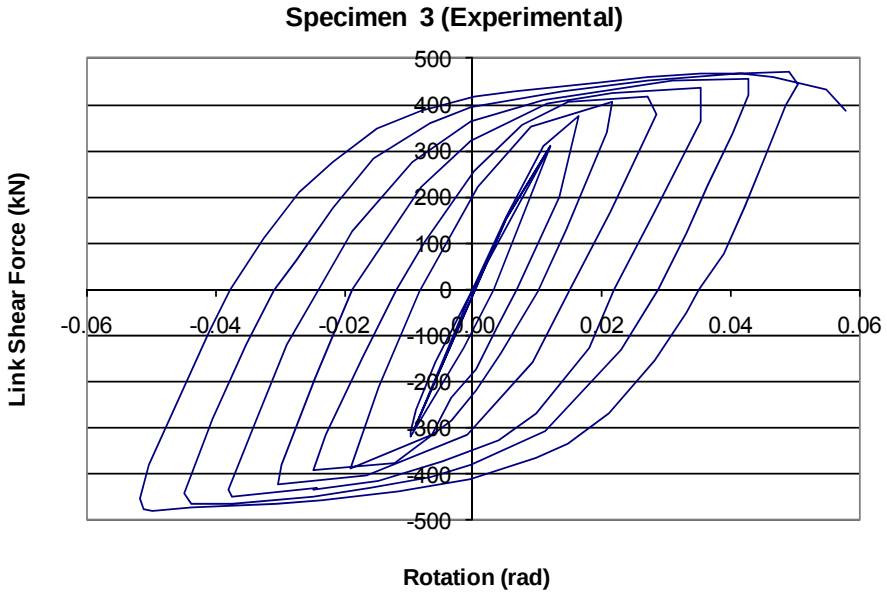

Figure 3.8: Experimental Behavior of Specimen 3

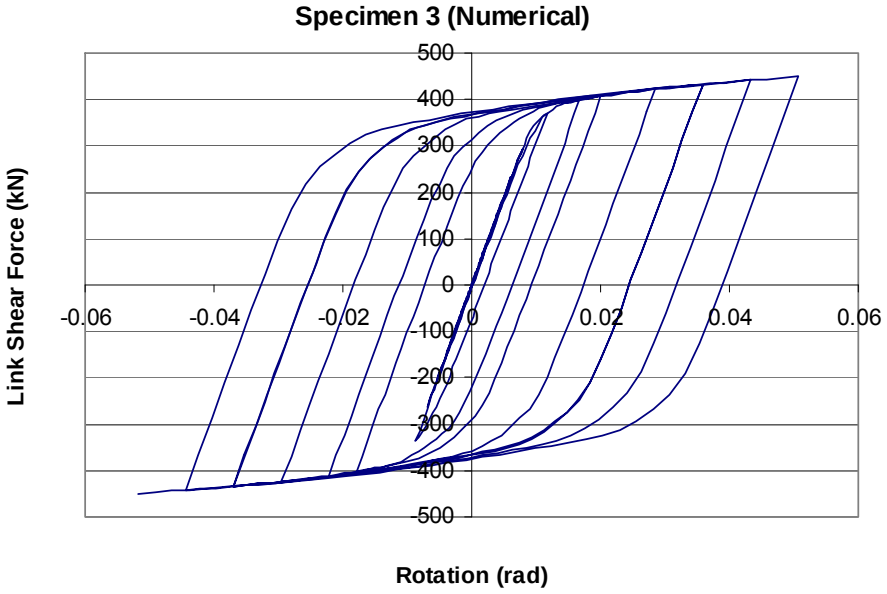

Figure 3.9: Numerical Simulation Results for Specimen 3

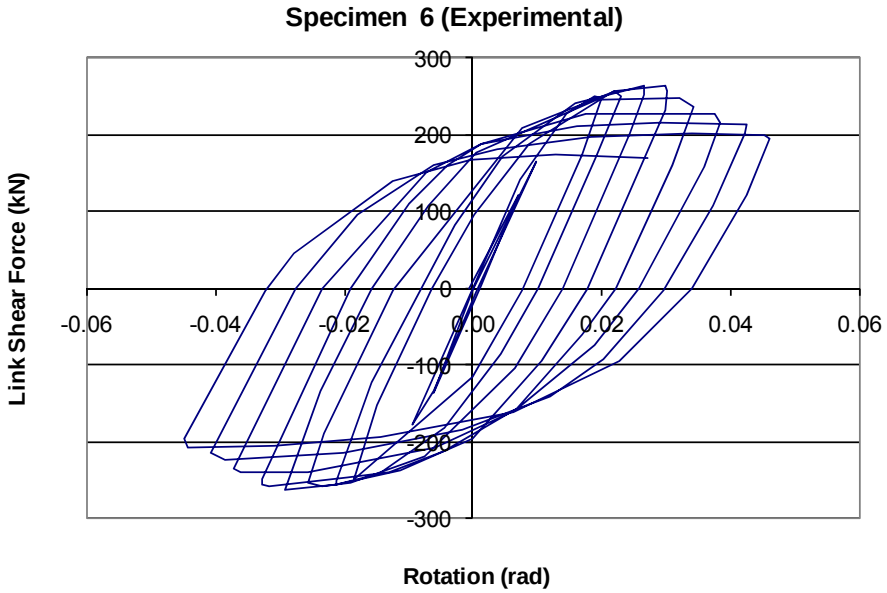

Figure 3.10: Experimental Behavior of Specimen 6

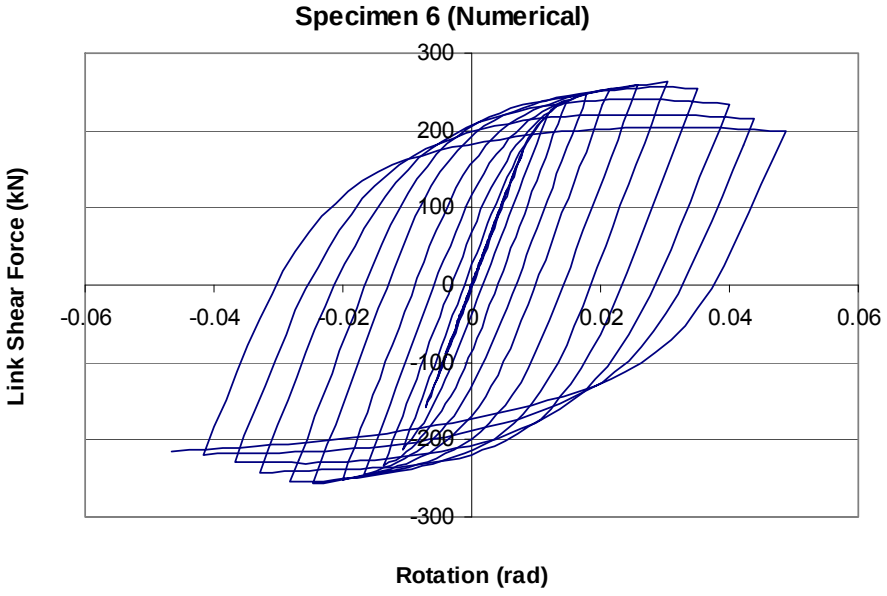

Figure 3.11: Numerical Simulation Results for Specimen 6

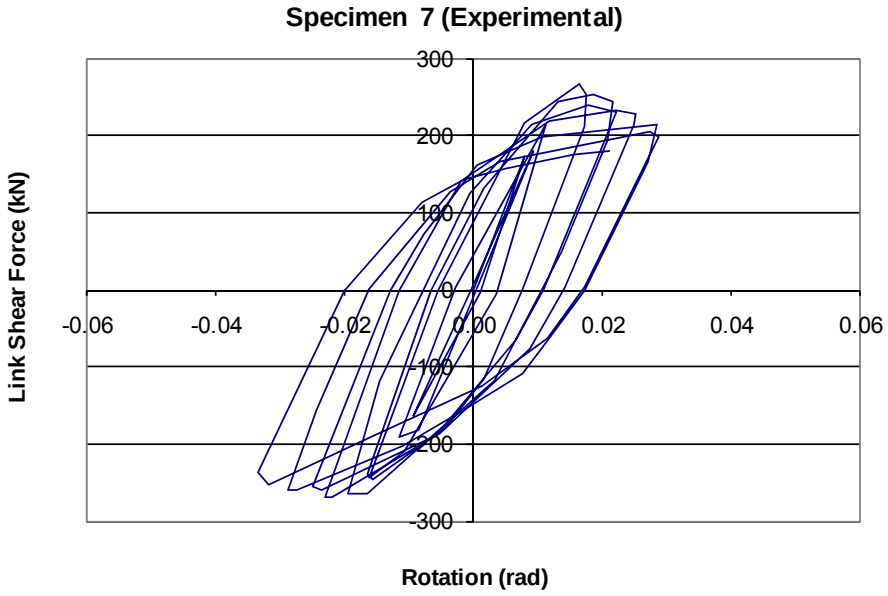

Figure 3.12: Experimental Behavior of Specimen 7

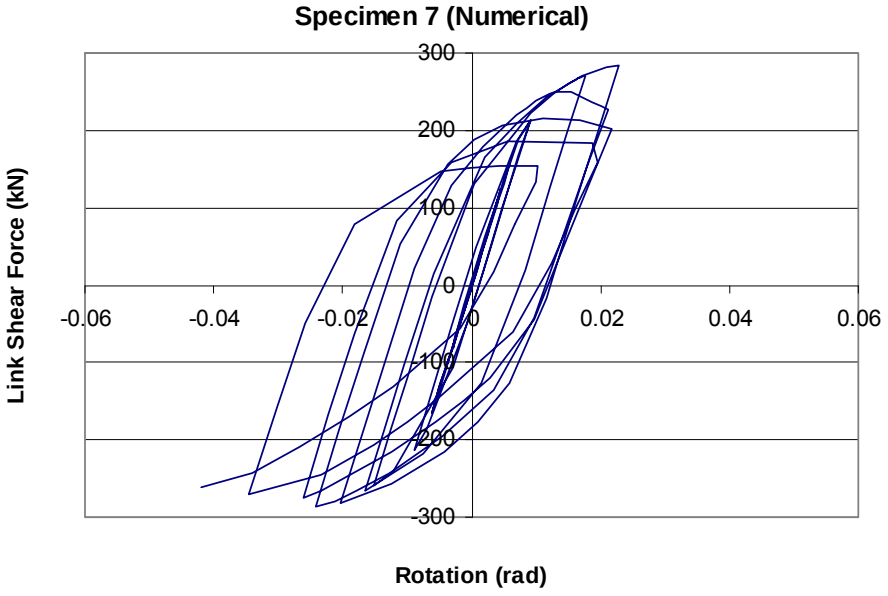

Figure 3.13: Numerical Simulation Results for Specimen 7

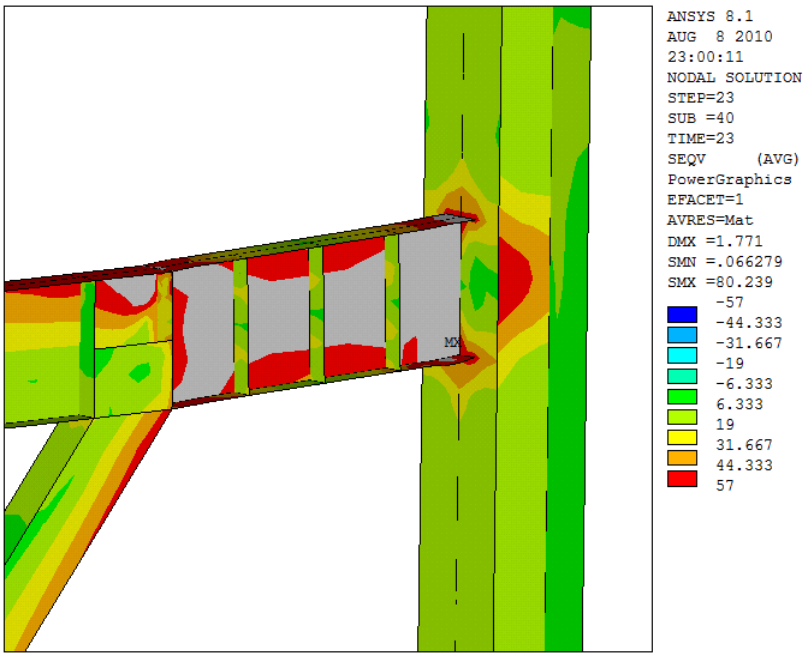

Figure 3.14: Stable behavior of Specimen 3

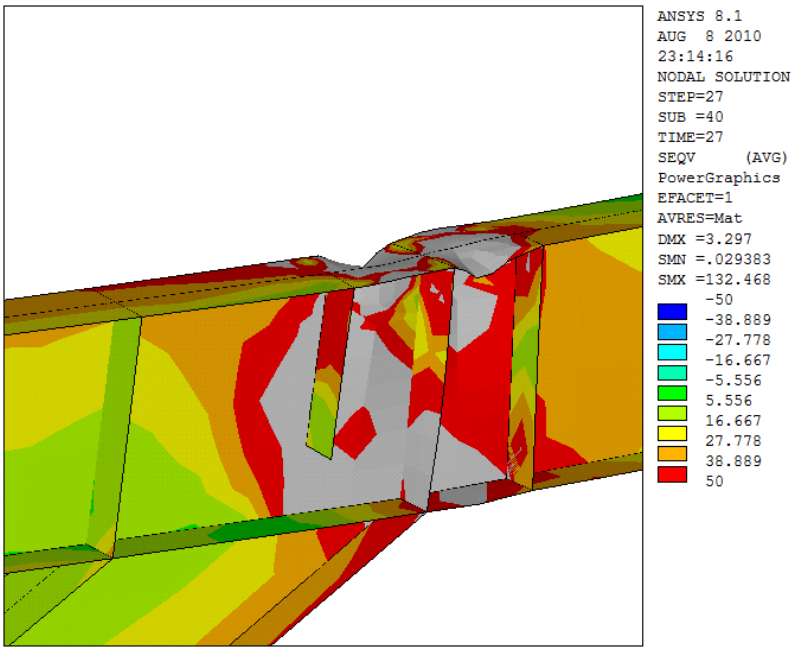

Figure 3.15: Local flange buckling on brace cconnection panel on Specimen 6

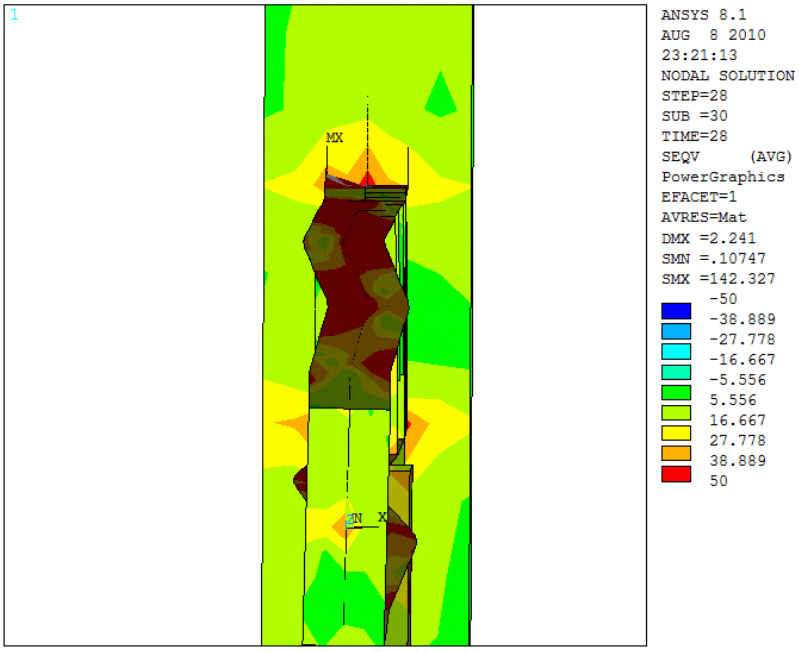

Figure 3.16: Lateral Torsional Buckling of the Beam outside of the Link on Specimen 7

CHAPTER 4

PARAMETRIC STUDY

In this chapter the link overstrength issue is evaluated by making use of finite element analysis. Designs which do not satisfy the code requirements were selected and analyzed to investigate their behavior. In this chapter the details of the prototype design selection and the results of the numerical investigation are presented in detail.

4.1 Selection of Design Cases

The developed computer program details of which are given in Chapter 2 was extensively utilized in selecting the cases for numerical analysis. A single story, single bay EBF geometry shown in Figure 2.1 was considered to be typical for all designs. As mentioned before, a story height of 3180 mm (150 in) was considered. The L/h and e/h values presented in Table 2.1 were utilized but the design space was further reduced by imposing constraints on the brace angle (α) and the e/L ratio. Based on the study of Engelhardt and Popov (1989b) the maximum values of the brace angle and the e/L ratio were considered to be 52^o and 0.32, respectively. Brace angles in excess of this maximum is not very practical. In addition, e/L ratios greater than 0.3 results in designs which exhibit moment resisting frame behavior rather than eccentrically braced frame behavior because of the excessively long link lengths.

The idea here is to select the problematic designs that do not satisfy the code provisions. A detailed analysis of resulting designs was presented in Chapter 2 and it was demonstrated that vast majority of cases are problematic. A systematic selection procedure should be applied to distinguish between designs that show acceptable and unacceptable performance. An extensive set of preliminary analysis was conducted to understand the most influential parameters that affect the system performance. Based on this set of analysis it was observed that the global and local slenderness of the beam outside of the link and its PM value are the

governing parameters over the others. The global lateral stability of the beam outside of the link is primarily governed by its slenderness with respect to its minor axis, L/r_y, where L is the length of the beam outside of the link and r_y is the minor axis radius of gyration. In addition, the local instability of the brace connection panel is influenced by the slenderness of the beam flange usually expressed as $b_f/2t_f$, where b_f is the flange width and t_f is the flange thickness.

Lateral and local instabilities of the beam were studied separately to understand the influence of slenderness measures, namely L/r_y and $b_f/2t_f$. The effects of flange slenderness on local buckling of the brace connection panel can be investigated independent of the lateral instability by considering cases with continuous lateral supports. On the other hand, investigating lateral instability without the effects of local buckling requires selecting beam sections with very stocky flanges. This may induce further reductions in the design space and can lead to omitting some potentially detrimental design cases. Therefore, no particular emphasis was given to the flange slenderness in studying the lateral instability of the beam outside of the link. The analysis cases were divided into two sets. The first set consists of 51 cases and was primarily used to study lateral instability. The second set consists of 40 cases and was utilized to study local instability. Some of the results from the first set were also useful in studying the local instabilities and these were combined with the results of the second set.

In order to study the lateral instability of the beam outside of the link, two lateral support arrangements were considered. In the first arrangement the beam is laterally unsupported whereas in the second arrangement a lateral support is placed at the mid-span of the beam. Design cases considering these two arrangements were combined together to form a design space. It should be emphasized that in presenting slenderness values a K factor of unity is considered while a K factor of 0.7 was used in calculating PM values for the beam as explained in Chapter 2. When a plastic hinge forms at the end of the beam the boundary conditions for stability changes from fixed to pinned. This observation was the primary motive in considering a K factor of unity. It is also worthwhile emphasizing that the complete length is utilized for slenderness calculations for laterally unsupported cases while the half-length is utilized in similar calculations for cases with a single lateral support at the mid-length. The resulting combined design space is plotted in Figure 4.1. As mentioned in

Chapter 2, cases where the PM ratio considering instability effects (PM_b) is greater than 0.8 are problematic from a design point of view. Figure 4.1 shows only a region of the design space where the PM ratio is limited to 1.6. As presented in Figure 2.13 the PM ratios can be greater than 1.6 when the slenderness of the beam is in excess of 150.

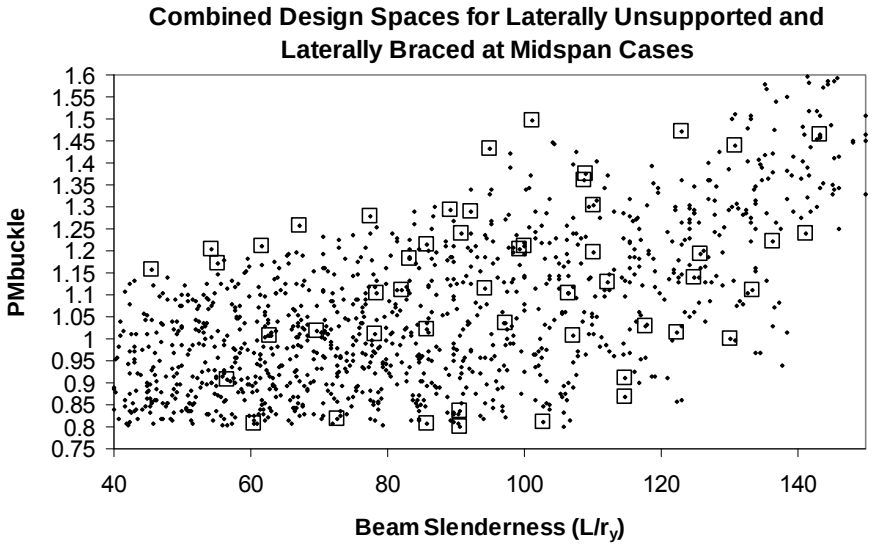

Figure 4.1: Design Space for Investigating Lateral Instability

A total of 51 cases were selected by considering the design space given in Figure 4.1. The selected cases are shown with boxes in the same figure. For a particular region of beam slenderness, the most problematic cases with high PM ratios were included in the analysis set. In addition, cases with PM ratios close to unity and 0.8 were also included. As shown in Figure 4.1 the boundaries of the design space are well covered by this selection. Among the 51 cases selected 12 of them have lateral supports at mid-span and the rest are laterally unsupported.

A similar procedure was adopted in selecting the second set of analysis cases. The influence of the normalized link length ($e/(M_p/V_p)$) was considered to be influential in studying the local buckling of the brace connection panel. Therefore, the designs were separated into

three categories according to the normalized link length. The first category represents primarily shear links where the normalized link length is between 1.5 and 1.7. The second category belongs to intermediate length links with a normalized link length between 1.9 and 2.1. The final category belongs to moment yielding links with normalized link lengths greater than 2.6. The use of compact sections for links with a normalized link length less than 1.6 is allowed as per the AISC Seismic Specification (2005). Links with compact sections having normalized link lengths less than 1.6 were also included in the first category. The design spaces for all three categories and the selected sections are plotted in Figures 4.2, 4.3 and 4.4. As mentioned before, all the cases considered in the study of local buckling have laterally supported beams. Therefore, the PM value is directly influenced by yielding and lateral instability effects do not have to be taken into account. In presenting the design spaces the PM_y value based on yielding of the cross section was utilized. As shown in these figures designs with varying $b_f/2t_f$ and PM_y values were selected to cover the boundaries of the design spaces. General features of the selected cases are given in Tables 4.1 and 4.2.

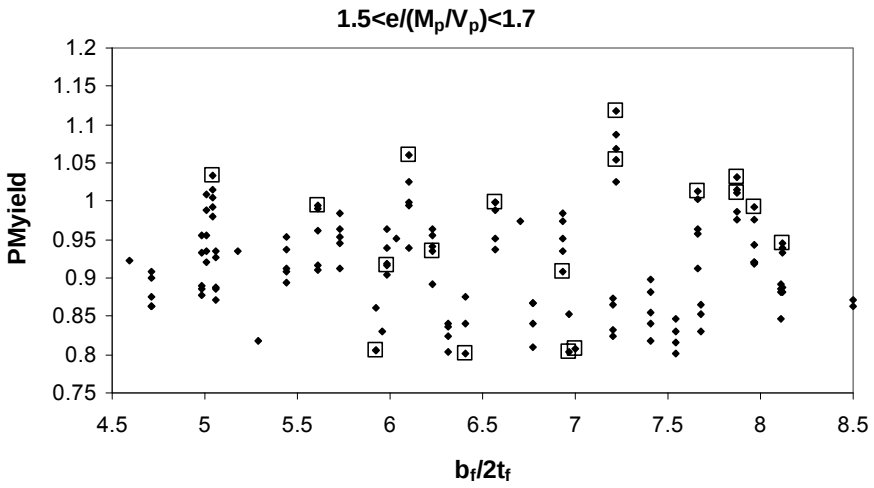

Figure 4.2: Design Space for Investigating Local Instability (Short Links)

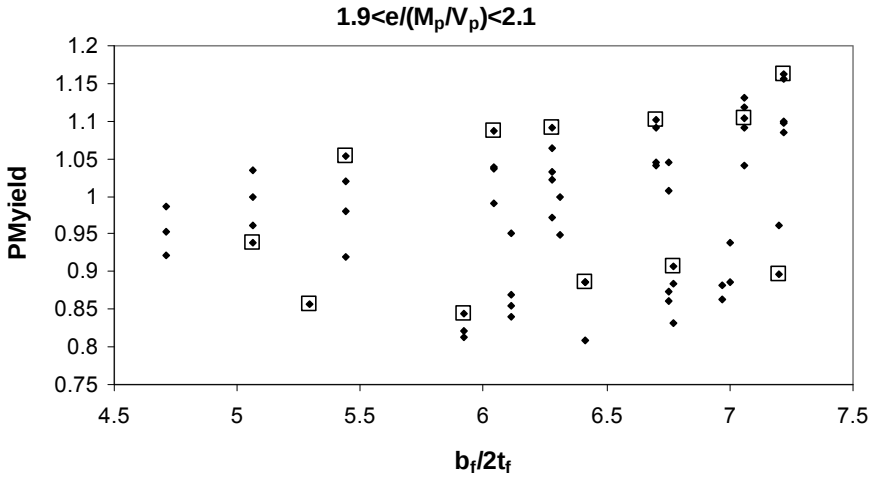

Figure 4.3: Design Space for Investigating Local Instability (Intermediate Links)

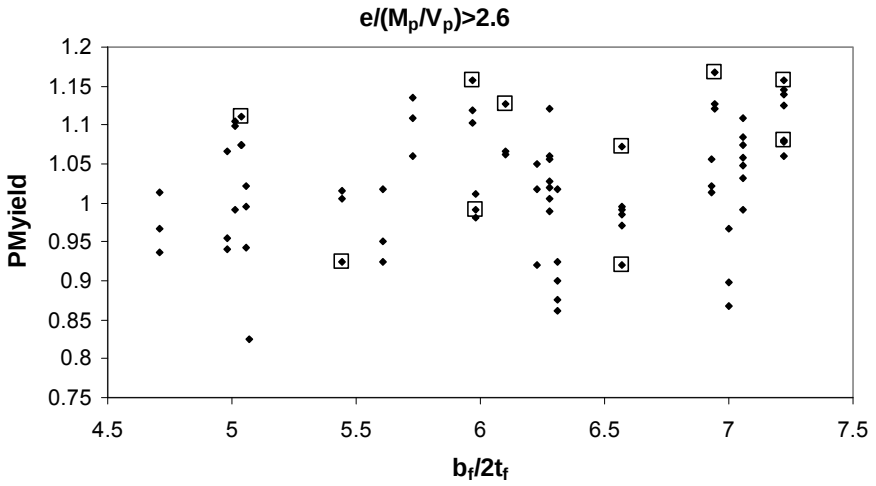

Figure 4.4: Design Space for Investigating Local Instability (Long Links)

Table 4-1: Analysis Cases Set 1

Case #	Beam (W)	Brace (HSS)	Column (W)	L/r_y	$b_f/2t_f$	$e/(M_p/V_p)$	PM_b	PM_y	e/L	L/h	Angle	Expected Rotation	Actual Rotation	Failure State
1	16X40	12X12X1/2	14X53	143.3	6.93	1.691	1.47	0.91	0.17	1.8	33.7	0.075	0.0021	LTB
2	18X71	14X14X5/8	14X109	141.2	4.71	1.03	1.24	0.76	0.11	1.8	32.0	0.080	0.0111	LTB
3	21X44	9X9X1/2	14X82	131.0	7.22	3.269	1.44	1.15	0.31	1.6	42.3	0.020	0.002	LTB
4	12X50	12X12X1/2	14X61	130.1	6.31	1.517	1.00	0.71	0.15	2.0	30.5	0.080	0.11	LTB
5	24X55	12X12X5/8	14X120	123.1	6.94	1.798	1.47	1.14	0.21	1.4	42.3	0.068	0.004	LTB
6	12X50	12X12X5/8	14X61	122.4	6.31	2.023	1.01	0.78	0.20	2.0	32.0	0.055	0.08	LTB+LB
7	21X62	12X12X5/8	14X120	110.2	6.70	2.471	1.30	1.11	0.28	1.8	37.6	0.028	0.012	LTB
8	14X48	12X12X1/2	14X61	117.8	6.75	2.461	1.03	0.84	0.25	2.0	33.7	0.028	0.044	LB
9	12X50	12X12X1/2	14X61	114.8	6.31	2.529	0.91	0.76	0.25	2.0	33.7	0.024	0.061	LB
10	12X50	12X12X1/2	14X61	114.8	6.31	1.517	0.87	0.68	0.17	1.8	33.7	0.080	0.122	NLB
11	24X62	12X12X5/8	14X145	108.7	5.97	2.278	1.36	1.16	0.29	1.4	45.0	0.039	0.005	LTB
12	12X35	10X10X3/8	14X43	107.1	6.31	1.813	1.01	0.87	0.21	1.4	42.3	0.067	0.103	NLB
13	14X82	14X14X5/8	14X90	102.8	5.92	1.247	0.81	0.66	0.15	2.0	30.5	0.080	0.122	NLB
14	18X50	9X9X5/8	14X82	90.9	6.57	2.133	1.24	1.13	0.29	1.4	45.0	0.048	0.049	LTB
15	12X35	9X9X3/8	14X43	97.4	6.31	2.417	1.04	0.95	0.29	1.4	45.0	0.031	0.044	LB
16	14X82	16X16X5/8	14X90	90.7	5.92	2.079	0.83	0.73	0.25	2.0	33.7	0.051	0.08	LB
17	14X82	12X12X5/8	14X90	90.7	5.92	1.247	0.80	0.70	0.17	1.8	33.7	0.080	0.122	NLB
18	24X76	14X14X5/8	14X176	85.9	6.61	2.231	1.22	1.11	0.31	1.6	42.3	0.042	0.033	LB
19	14X53	10X10X1/2	14X61	85.9	6.11	2.405	1.02	0.96	0.31	1.6	42.3	0.032	0.061	LB
20	8X58	9X9X5/8	14X61	85.7	5.07	2.189	0.81	0.73	0.25	1.6	39.8	0.045	0.112	NLB
21	14X48	8X8X5/8	14X61	78.5	6.75	1.969	1.11	1.04	0.29	1.4	45.0	0.058	0.065	LB
22	14X53	10X10X1/2	14X61	78.1	6.11	1.924	1.01	0.95	0.29	1.4	45.0	0.061	0.083	LB
23	14X74	12X12X5/8	14X90	72.6	6.41	1.624	0.82	0.77	0.25	1.6	39.8	0.079	0.084	NLB
24	27X102	16X16X5/8	14X283	69.8	6.03	1.546	1.02	0.95	0.29	1.4	45.0	0.080	0.134	NLB
25	18X86	14X14X5/8	14X132	62.7	7.20	1.958	1.01	0.96	0.31	1.6	42.3	0.059	0.068	LB

Table 4-1 (continued)

Case #	Beam (W)	Brace (HSS)	Column (W)	L/r_y	$b_f/2t_f$	$e/(M_p/V_p)$	PM_b	PM_y	e/L	L/h	Angle	Expected Rotation	Actual Rotation	Failure State
26	14X74	12X12X1/2	14X90	60.5	6.41	1.624	0.81	0.78	0.29	1.4	45.0	0.079	0.084	NLB
27	18X97	12X12X5/8	14X159	56.6	6.41	1.539	0.91	0.88	0.29	1.4	45.0	0.080	0.128	NLB
28	14X48	12X12X1/2	14X61	133.5	6.75	1.477	1.11	0.78	0.15	2.0	30.5	0.080	0.04	LTB
29	12X35	9X9X1/2	14X43	136.4	6.31	2.417	1.22	0.94	0.22	1.8	35.5	0.031	0.02	LTB
30	14X53	12X12X5/8	14X61	125.0	6.11	1.924	1.14	0.87	0.20	2.0	32.0	0.061	0.082	LTB
31	14X38	10X10X1/2	14X61	125.8	6.57	1.779	1.19	0.93	0.19	1.6	37.6	0.069	0.05	LTB
32	18X40	9X9X1/2	14X61	112.2	5.73	1.523	1.13	0.95	0.21	1.2	46.5	0.080	0.052	LTB
33	21X62	12X12X5/8	14X120	110.2	6.70	1.483	1.20	0.97	0.19	1.6	37.6	0.080	0.052	LTB
34	14X38	9X9X1/2	14X61	106.5	6.57	1.779	1.10	0.95	0.21	1.4	42.3	0.069	0.106	LB
35	21X68	14X14X5/8	14X132	100.0	6.04	1.909	1.21	1.04	0.25	1.6	39.8	0.061	0.09	LTB
36	14X48	9X9X5/8	14X61	94.2	6.75	1.969	1.11	1.01	0.25	1.6	39.8	0.058	0.064	LB
37	21X73	14X14X5/8	14X145	99.4	5.60	1.878	1.20	1.04	0.25	1.6	39.8	0.063	0.07	LTB
38	21X83	14X14X5/8	14X159	82.0	5.00	1.866	1.11	1.02	0.29	1.4	45.0	0.064	0.13	NLB
39	21X68	12X12X5/8	14X132	83.3	6.04	1.909	1.18	1.09	0.29	1.4	45.0	0.061	0.09	LTB+LB
40	21X44	14X14X5/8	14X82	101.2	7.22	1.961	1.50	1.16	0.15	2.0	30.5	0.058	0.001	LTB
41	16X31	12X12X1/2	14X43	109.0	6.28	2.065	1.38	1.02	0.15	2.0	30.5	0.052	0.002	LTB
42	24X55	16X16X5/8	14X120	95.1	6.94	1.798	1.43	1.15	0.15	2.0	30.5	0.068	0.002	LTB
43	18X35	12X12X1/2	14X53	92.2	7.06	2.052	1.29	1.09	0.17	1.8	33.7	0.053	0.02	LTB
44	21X44	14X14X5/8	14X82	89.3	7.22	1.961	1.29	1.10	0.17	1.8	33.7	0.058	0.011	LTB
45	21X44	12X12X5/8	14X82	77.4	7.22	1.961	1.28	1.15	0.19	1.6	37.6	0.058	0.05	LTB
46	24X55	12X12X5/8	14X120	67.2	6.94	2.397	1.26	1.18	0.25	1.6	39.8	0.032	0.023	LB
47	24X55	12X12X5/8	14X120	61.6	6.94	1.798	1.21	1.14	0.21	1.4	42.3	0.068	0.072	LB
48	24X62	12X12X5/8	14X145	54.3	5.97	2.278	1.21	1.16	0.29	1.4	45.0	0.039	0.052	LB
49	18X35	9X9X1/2	14X53	55.3	7.06	2.052	1.17	1.13	0.25	1.2	48.0	0.053	0.031	LB
50	18X50	9X9X5/8	14X82	45.5	6.57	2.133	1.16	1.13	0.29	1.4	45.0	0.048	0.049	LB
51	14X48	8X8X5/8	14X61	39.3	6.75	1.969	1.06	1.04	0.29	1.4	45.0	0.058	0.065	LB

Table 4-2: Analysis Cases Set 2

Case #	Beam (W)	Brace (HSS)	Column (W)	L/r_y	$b_f/2t_f$	$e/(M_p/V_p)$	PM_b	PM_y	e/L	L/h	Angle	Expected Rotation	Actual Rotation	Failure State
101	21X44	14X14X5/8	14X82	202.4	7.22	1.961	3.71	1.16	0.15	2.0	30.5	0.058	0.0533	LB
102	18X35	12X12X5/8	14X53	209.0	7.06	2.052	3.67	1.10	0.15	2.0	30.5	0.053	0.0292	LB
103	21X62	12X12X5/8	14X120	84.7	6.70	1.977	1.20	1.10	0.29	1.4	45.0	0.057	0.0517	LB
104	21X68	12X12X5/8	14X132	83.3	6.04	1.909	1.18	1.09	0.29	1.4	45.0	0.061	0.0905	NLB
105	18X60	12X12X5/8	14X90	107.1	5.44	2.042	1.24	1.05	0.25	1.6	39.8	0.053	0.0864	LB
106	18X65	16X16X5/8	14X99	142.0	5.06	2.058	1.44	0.94	0.20	2.0	32.0	0.053	0.086	LB
107	16X31	9X9X1/2	14X43	141.0	6.28	2.065	1.61	1.09	0.21	1.4	42.3	0.052	0.053	LB
108	16X77	14X14X5/8	14X99	78.9	6.77	2.045	0.98	0.91	0.28	1.8	37.6	0.053	0.084	NLB
109	18X86	16X16X5/8	14X132	74.1	7.20	1.958	0.97	0.90	0.28	1.8	37.6	0.059	0.068	LB
110	18X97	16X16X5/8	14X159	62.3	6.41	1.924	0.93	0.89	0.31	1.6	42.3	0.061	0.088	LB
111	16X89	16X16X5/8	14X120	78.3	5.92	2.032	0.92	0.85	0.28	1.8	37.6	0.054	0.098	LB
112	16X100	16X16X5/8	14X132	65.7	5.29	1.998	0.90	0.86	0.31	1.6	42.3	0.056	0.124	NLB
113	24X55	12X12X5/8	14X120	167.9	6.94	2.997	2.36	1.17	0.25	2.0	33.7	0.020	0.0124	LB
114	21X44	9X9X5/8	14X82	154.8	7.22	3.269	1.94	1.16	0.28	1.8	37.6	0.020	0.012	LB
115	24X62	12X12X5/8	14X145	141.3	5.97	2.848	1.69	1.16	0.28	1.8	37.6	0.020	0.0216	LB
116	21X50	10X10X1/2	14X90	126.9	6.10	3.067	1.36	1.13	0.31	1.6	42.3	0.020	0.02	LB
117	21X57	12X12X5/8	14X109	166.7	5.04	2.797	2.11	1.11	0.25	2.0	33.7	0.020	0.02	LB
118	14X38	10X10X1/2	14X61	145.2	6.57	2.965	1.33	0.92	0.25	2.0	33.7	0.020	0.027	LB
119	18X60	14X14X5/8	14X90	133.9	5.44	2.552	1.25	0.92	0.25	2.0	33.7	0.023	0.046	LB
120	18X55	12X12X1/2	14X90	98.8	5.98	2.639	1.11	0.99	0.31	1.6	42.3	0.020	0.047	LB
121	21X44	12X12X5/8	14X82	166.7	7.22	2.615	2.20	1.08	0.22	1.8	35.5	0.020	0.012	LB
122	18X50	10X10X1/2	14X82	100.0	6.57	2.667	1.19	1.07	0.31	1.6	42.3	0.020	0.029	LB
123	21X44	12X12X5/8	14X82	184.5	7.22	1.634	2.95	1.12	0.14	1.8	32.8	0.078	0.111	NLB
124	21X44	12X12X5/8	14X82	160.7	7.22	1.634	2.11	1.05	0.16	1.6	36.5	0.078	0.111	NLB
125	12X45	9X9X1/2	14X61	100.0	7.00	1.543	0.93	0.81	0.19	1.6	37.6	0.080	0.123	NLB

Table 4-2 (continued)

Case #	Beam (W)	Brace (HSS)	Column (W)	L/r_y	$b_f/2t_f$	$e/(M_p/V_p)$	PM_b	PM_y	e/L	L/h	Angle	Expected Rotation	Actual Rotation	Failure State
126	18X50	12X12X5/8	14X82	154.5	6.57	1.6	1.84	1.00	0.15	2.0	30.5	0.080	0.126	NLB
127	16X40	12X12X1/2	14X53	143.3	6.93	1.691	1.47	0.91	0.17	1.8	33.7	0.075	0.086	NLB
128	14X68	12X12X5/8	14X90	97.6	6.97	1.632	0.93	0.80	0.20	2.0	32.0	0.078	0.12	NLB
129	21X50	14X14X5/8	14X90	201.9	6.10	1.534	3.39	1.06	0.13	2.0	29.7	0.080	0.131	NLB
130	16X45	12X12X1/2	14X61	143.3	6.23	1.694	1.46	0.94	0.17	1.8	33.7	0.074	0.12	NLB
131	18X97	16X16X5/8	14X159	79.2	6.41	1.539	0.89	0.80	0.22	1.8	35.5	0.080	0.128	NLB
132	16X50	8X8X5/8	14X68	84.9	5.61	1.677	1.07	0.99	0.25	1.2	48.0	0.075	0.125	NLB
133	18X55	12X12X5/8	14X90	116.8	5.98	1.583	1.16	0.92	0.19	1.6	37.6	0.080	0.126	NLB
134	14X82	12X12X5/8	14X90	72.6	5.92	1.663	0.86	0.81	0.25	1.6	39.8	0.076	0.12	NLB
135	21X57	14X14X5/8	14X109	166.7	5.04	1.678	2.16	1.03	0.17	1.8	33.7	0.075	0.109	NLB
136	16X36	9X9X1/2	14X61	113.5	8.12	1.56	1.15	0.95	0.18	1.4	41.0	0.080	0.127	NLB
137	21X55	14X14X5/8	14X109	147.4	7.87	1.588	1.84	1.03	0.15	2.0	30.5	0.080	0.109	NLB
138	24X68	14X14X5/8	14X159	120.3	7.66	1.426	1.36	1.01	0.17	1.8	33.7	0.080	0.13	NLB
139	16X26	10X10X1/2	14X43	214.3	7.97	1.528	3.54	0.99	0.11	1.8	32.0	0.080	0.107	NLB
140	21X55	12X12X5/8	14X109	112.7	7.87	1.588	1.27	1.01	0.19	1.6	37.6	0.080	0.109	NLB

4.2 Modeling Details and Analysis Procedure

The numerical modeling details explained in Chapter 3 were adopted with minor changes. The specimens experimented by Engelhardt and Popov (1989b) had half length braces. Full length braces were modeled in the present study. In all models a gusset plate was utilized to connect the brace to the beam. The brace was oriented in such a way that the beam and brace centerlines (workpoint) meet at the link end. The AISC Seismic Provisions allows for the workpoint being located inside the link but not outside. If the workpoint is located inside the link, the resulting eccentricity modifies the moment distribution inside the link. In order to avoid this modification the workpoint was located at the link end.

Preliminary analysis results showed that the column size have a significant effect on the system performance. The elastic moment distribution between the link ends is directly influenced by the column size. For intermediate and long links the link end moments tend to equalize after yielding of the link. However, for short links there can be significant differences between the link end moments even after the link yields. A study by Engelhardt and Popov (1989b) revealed that the rigidity of the column sections used in practice is 1 to 6 times the rigidity of the link section. Based on this observation a rigidity ratio of unity was considered in selecting the column size where appropriate. Selecting a smaller column size is a conservative approach. Flexible columns provide less resistance at the column end of the link resulting in greater moments occurring at the braced end. Selecting a flexible column has the drawback of having undesirable yielding of the column and its panel zone. In order to avoid premature yielding, the column is modeled with elastic material properties throughout the parametric study.

At the far end of the beam a single node lying at the center of the cross section was restrained against movement in all three orthogonal directions. In other words, there was no rotational restraint provided at this end leading to a pin connection. A thick stiffener was modeled at the far end of the brace. A single node lying at the center of this stiffener was restrained against movement in three orthogonal directions. Similar to the beam end, no rotational restraint was present at the far end of the brace. For both the beam and the brace ends the twist of the cross sections were prevented by restraining the out of plane movement

of two nodes that were located on the top and bottom flanges. While the twists of the sections were prevented there was no restraint against warping.

Stiffeners were placed inside the link according to the recommendations given in the AISC Seismic Provisions (2005). There are no specific rules for stiffening of the brace connection panel therefore; no stiffeners were modeled in this region. The braced end of the link was laterally supported by restraining the out of plane movement of both flanges. A similar restraint was provided for cases where there is a lateral brace at the mid-length of the beam outside of the link.

In general the link stiffeners were placed on one side of the link according to AISC Seismic Provisions (2005). This kind of a placement produces unsymmetrical finite element models. Although the models did not possess a plane of symmetry, preliminary finite element analysis runs revealed that geometrical imperfections need to be introduced for some cases in order to trigger lateral buckling. A geometrical imperfection equal to $L/1000$ (where L is the distance between lateral supports) at the mid-length was considered in all cases. The imperfections were introduced by modeling an initially crooked beam. The geometrical locations of the nodes that lie on a cross section at the mid-length of the beam were adjusted according to the level of imperfection. For the cases with intermediate lateral supports the initial imperfections were applied on both segments of the beam outside of the link. In general the shapes of the imperfections resemble a half sine-wave and a full sine-wave for the laterally unsupported and the supported cases, respectively.

An important aspect in numerical analysis of the selected EBF systems is the applied loading. Results depend on the adopted loading procedure. In this thesis a rational loading procedure developed for EBFs were adopted. This loading procedure is primarily for qualifying cyclic tests of link-to-column connections and is detailed in the AISC Seismic Provisions (2005). According to this procedure the link is subjected to several loading cycles by controlling the total link rotation angle (γ_{total}). The γ_{total} imposed on the system is as follows: 6 cycles at γ_{total}=0.00375 rad; 6 cycles at γ_{total}=0.005 rad; 6 cycles at γ_{total}=0.0075 rad; 6 cycles at γ_{total}=0.01 rad; 4 cycles at γ_{total}=0.015 rad; 4 cycles at γ_{total}=0.02 rad; 2 cycles at γ_{total}=0.03 rad; 1 cycle at γ_{total}=0.04 rad; 1 cycle at γ_{total}=0.05 rad; 1 cycle at γ_{total}=0.07 rad; 1 cycle at γ_{total}=0.09 rad; and continue at loading increments of γ_{total}=0.01 rad, with one cycle

of loading at each step. The early cycles usually produce elastic response of the link. In order to reduce the computational cost, the early cycles were omitted and the loading was started at a total link rotation of 0.01 radians. The applied loading procedure is given in Figure 4.5.

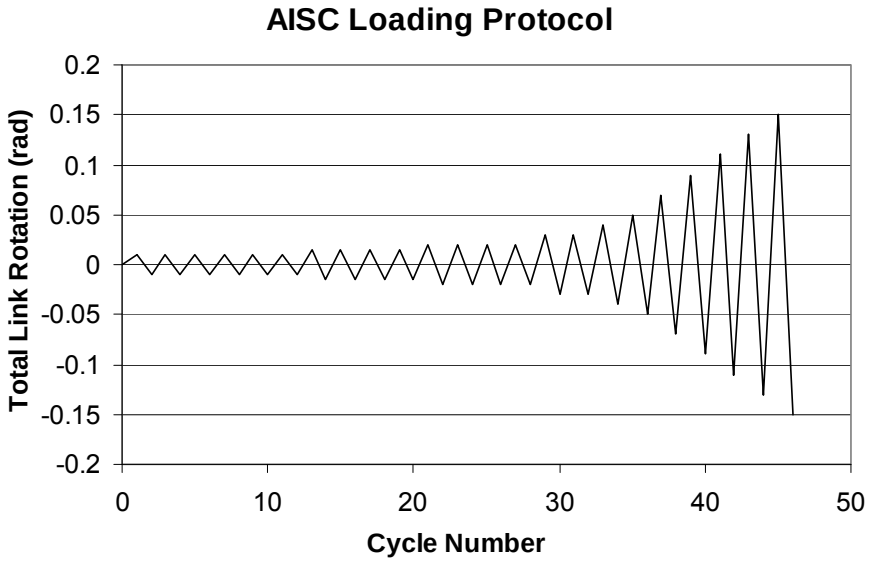

Figure 4.5: Adopted Loading Protocol

Steel with a nominal yield strength of F_y=345 MPa (50 ksi) was considered for both the beam and the brace. This value of yield strength is representative of A992 and S355 steels used in United States and Europe, respectively. In order to simulate the overstrength in material properties an R_y value of 1.1 was considered based on the recommendations of the AISC Seismic Provisions (2005) and an actual yield strength of 380 MPa (55 ksi) was used in the numerical analysis. A hardening modulus equal to E/100 (2GPa (290ksi)) was considered in all analysis.

4.3 Results of the Parametric Study

Several quantities were monitored during a typical analysis. These include shear force on the link, vertical displacements at link ends, and reaction forces at the ends of the beam, the column and the brace. The reaction forces were used to calculate the axial forces and moments applied at the beam, the brace and the link. In calculating the moments, second order effects are included. In other words, equilibrium equations were derived based on the deformed geometry and the secondary bending moments created due to the axial forces were taken into account.

For majority of the cases investigated, the loading history described in Figure 4.5 was applied. For some cases where a lateral instability of the beam was observed, the analysis was terminated at lower link rotation levels. In post processing the results, variation of link shear, moment at the beam end, moment at the brace end, axial force in the beam, axial force in the brace, link moment at the column end, link moment at the braced end were plotted against the plastic rotation angle of the link. Representative graphs for these quantities are given in Figures 4.6 through 4.12 for analysis case 15. In addition, variation of PM values for the brace and the beam were calculated for the entire loading history and their maximums were recorded. After each analysis was completed deformed shapes and von Mises stresses were investigated in detail to understand the instability mode of the beam outside of the link. In general, the deformed shapes and the global link shear behavior classify the global response of the system. Typical global responses include lateral torsional buckling (LTB) of the beam outside of the link, local buckling in the brace connection panel (LB), local buckling of either the web or flanges of the link, and stable behavior (NLB). Stable behavior is usually associated with yielding of the brace connection panel together with the yielding of the link. Typical global link shear responses for different system performances are given in Figures 4.6, 4.13, and 4.14. The response presented in Figure 4.6 is dominated by local buckling at the link ends followed by local buckling in the brace connection panel. Similarly the response presented in Figure 4.13 is for a system experiencing lateral buckling of the beam at very early stages of loading. Note that the entire loading history was not applied to this case and the analysis was terminated shortly after lateral instability was observed. A stable response is presented in Figure 4.14 where there was no instability observed in the system until the end of the selected loading protocol.

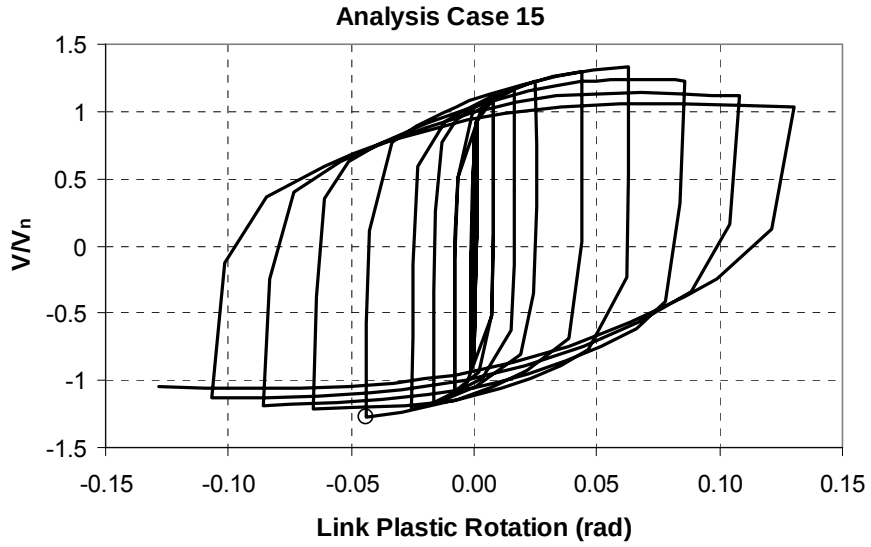

Figure 4.6: A Typical Link Shear Response

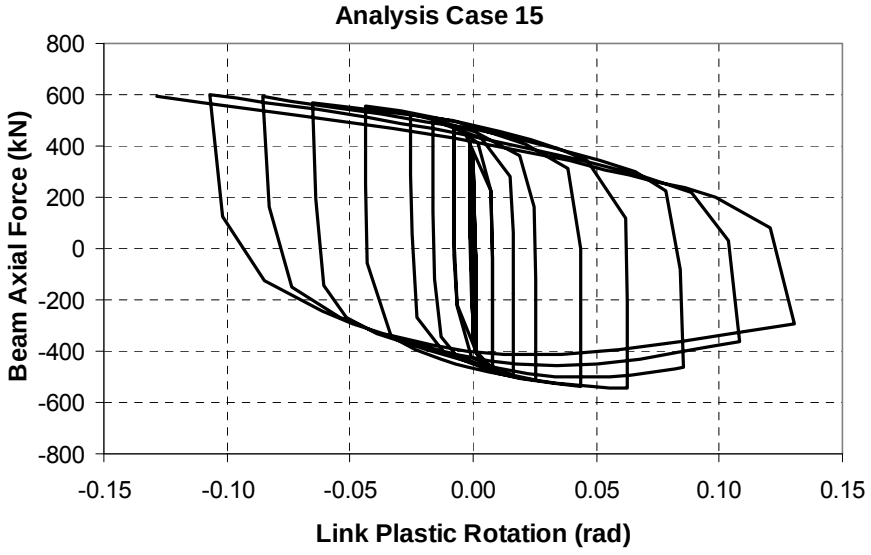

Figure 4.7: A Typical Beam Axial Force Response

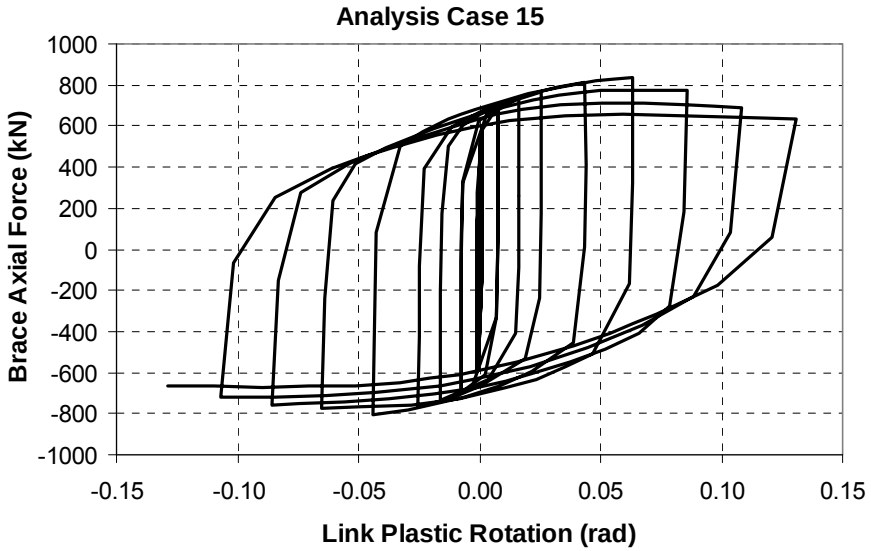

Figure 4.8: A Typical Brace Axial Force Response

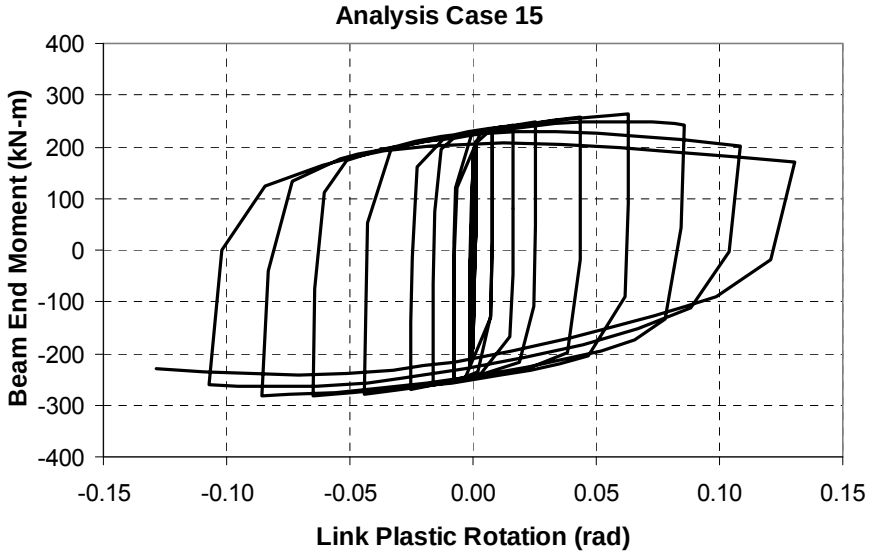

Figure 4.9: A Typical Beam End Moment Response

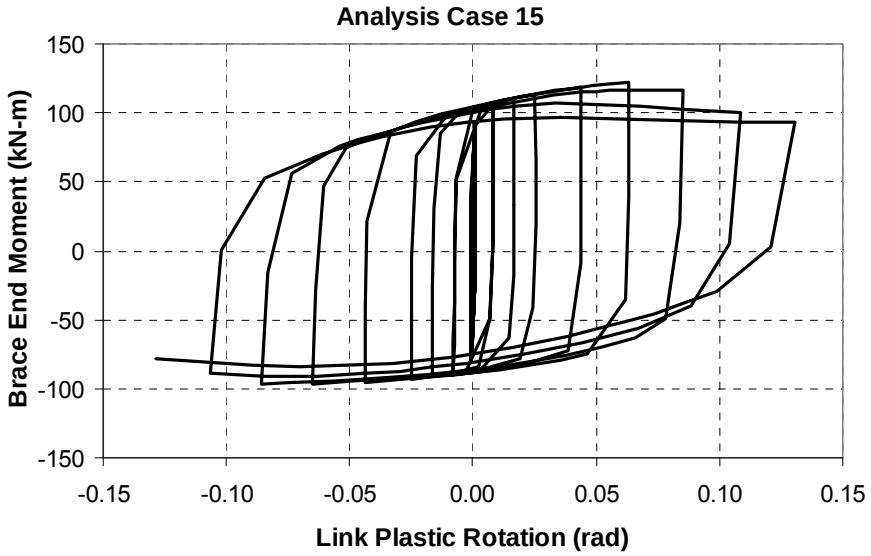

Figure 4.10: A Typical Beam End Moment Response

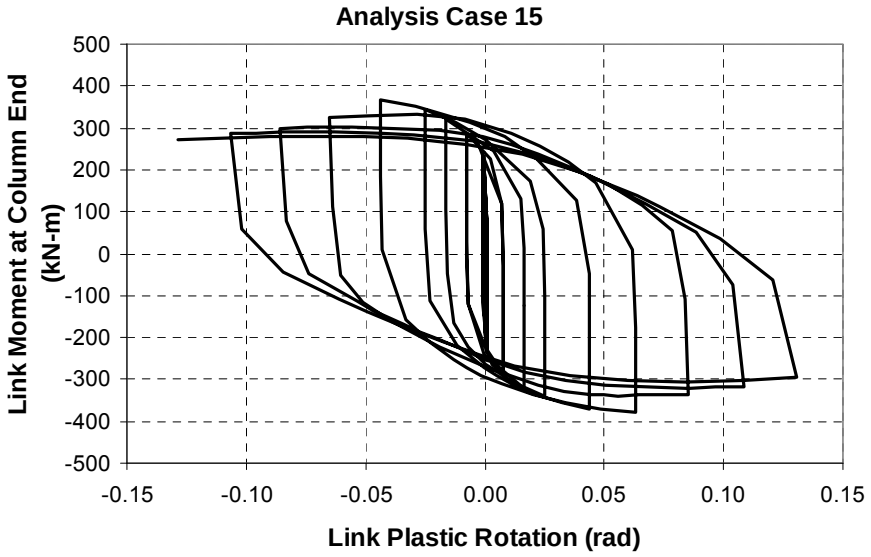

Figure 4.11: A Typical Link Moment at Column End Response

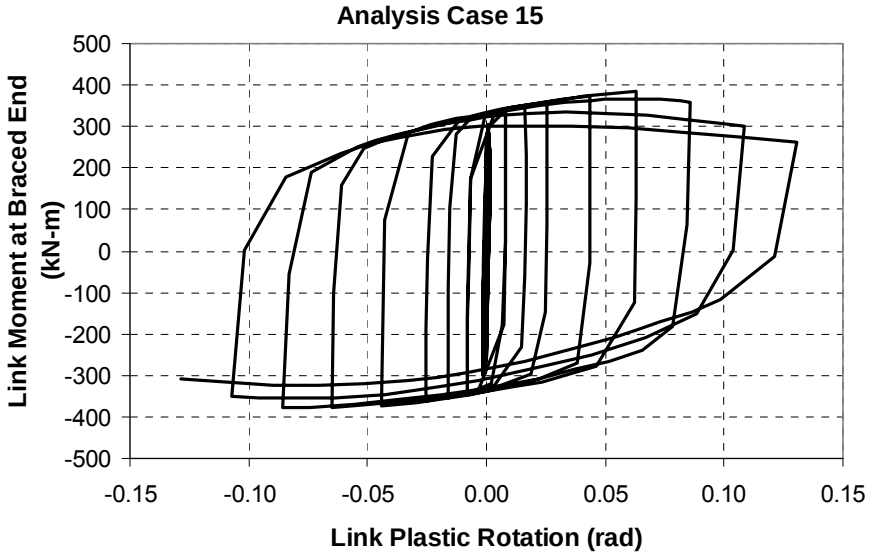

Figure 4.12: A Typical Link Moment at Braced End Response

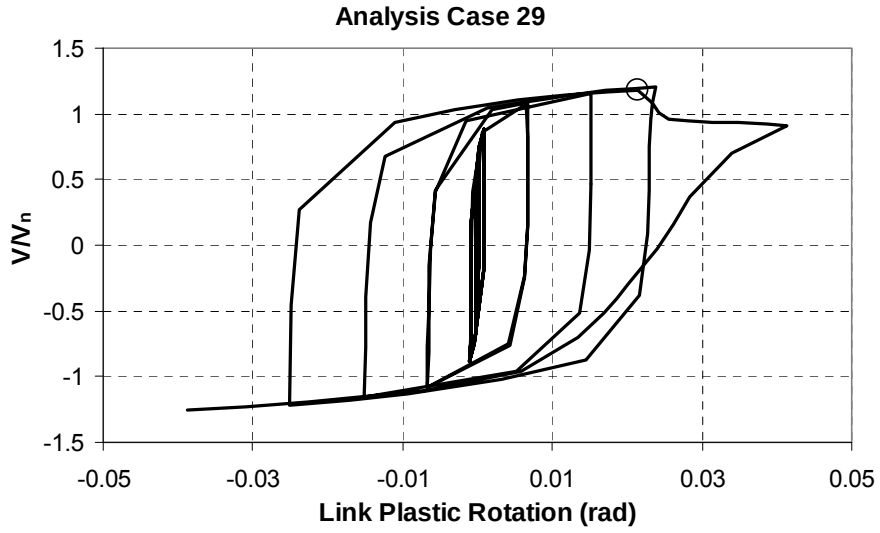

Figure 4.13: A Typical Normalized Link Shear Response for a System Experiencing Lateral Instability

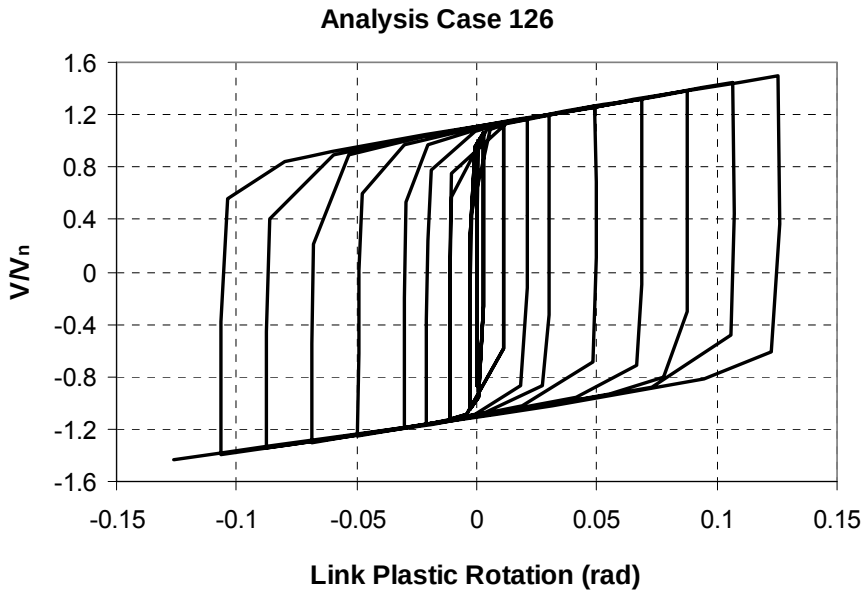

Figure 4.14: A Typical Normalized Link Shear Response for a System with Stable Response

The deformed finite element meshes and the von Mises stress distributions for the three cases presented in Figures 4.6, 4.13, and 4.14 are given in Figures 4.15 through 4.17, respectively. Figure 4.15 shows local buckles occurring at the link ends and the brace connection panel. The global instability of the beam outside of the link is evident from Figure 4.16. Similarly, Figure 4.17 shows a stable link response with yielding concentrated on the link and some minor yielding of the brace connection panel.

Link plastic rotations at the system failure level were recorded for all analysis cases. In general, these rotation levels were quantified based on the last stable loading cycle. As shown with a circle in Figure 4.6, analysis case 15 was able to sustain a plastic rotation cycle at 0.04 radians but strength degradation was observed when the link experiences 0.07 radians of plastic rotation. The observed strength degradation was an indication of instabilities in the system and the last cycle at which no strength degradation is observed was recorded as the plastic rotation at failure. These values are given in Tables 4.1 and 4.2. Detailed investigations of the response of systems are presented in the following sections.

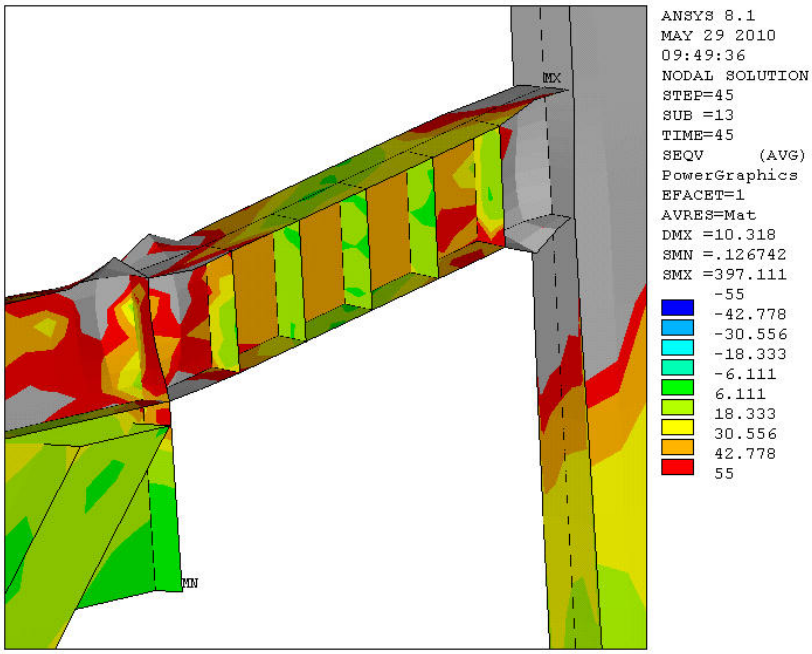

Figure 4.15: Local Instability in the Brace Connection Panel and Link Ends

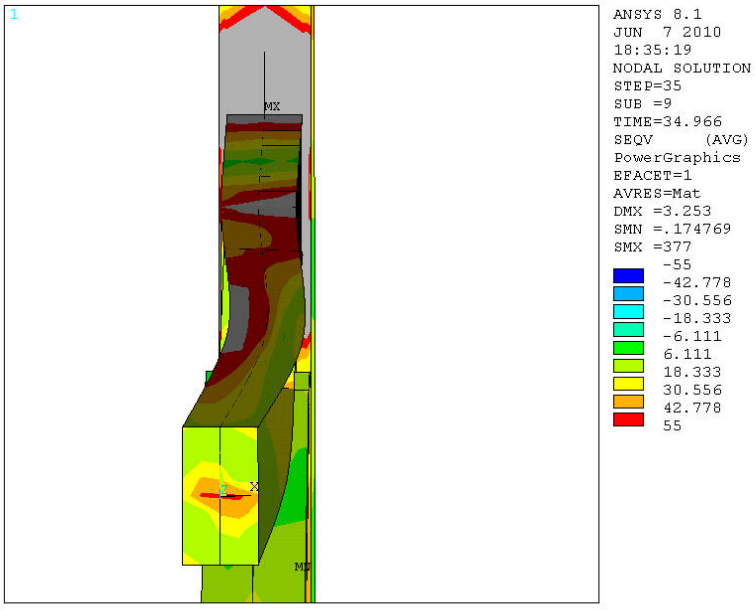

Figure 4.16: Lateral Torsional Buckling of the Beam outside of the Link

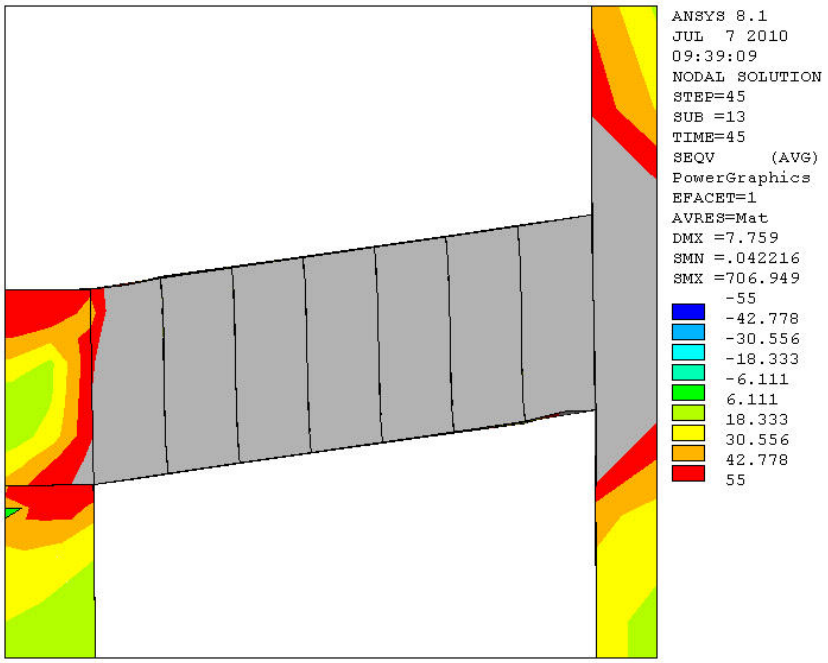

Figure 4.17 : Stable System Response with Yielding of the Link and Brace Connection Panel

4.4 Investigation of Lateral Instabilities

Lateral torsional instability of structural members subjected to bending and axial compression is ensured by keeping the PM ratio below unity at the design stage. As was shown in Chapter 2, the PM ratio should be kept below 0.8 if 25 percent overstrength due to strain hardening is expected. When the member is properly designed (i.e. PM<0.8) formation of a plastic hinge at the beam end is not likely. All the cases that belong to the first set of analysis have PM ratios in excess of 0.8. Therefore, yielding and/or lateral instabilities of the beam outside of the link are expected. Because the AISC Seismic Specification (2005) enforces capacity design principles for the beam outside of the link, there are no specific rules for its lateral bracing. If certain amount of yielding at the beam ends is allowed by designing the member with a PM ratio greater than 0.8, then lateral bracing may be needed to ensure the stability of this member. Beams used in moment resisting frames (MRFs) form plastic hinges at their ends during a seismic event. Due to their inherent behavior, lateral bracing guidelines were developed for beams in MRFs and

these primarily depend on the ductility demand. AISC Seismic Provisions (2005) classifies moment resisting frames into three categories namely; Special Moment Frames (SMF), Intermediate Moment Frames (IMF), and Ordinary Moment Frames (OMF). The ductility demands for the beams are the highest in SMF and lowest in OMF. AISC Seismic Provisions (2005) does not provide any special rules for lateral beam bracing for OMF. However, for MFR and IMF unbraced length (L) between lateral braces shall not exceed the values Equation 4.1.

$$\begin{aligned} L &< 0.086 r_y \frac{E}{F_y} \quad (MRF) \\ L &< 0.17 r_y \frac{E}{F_y} \quad (IMF) \end{aligned} \tag{4.1}$$

The limits given in Equation 4.1 can be conveniently written in terms of a slenderness ratio (L/r_y). For a steel with a yield strength of F_y=345 MPa (50 ksi) the slenderness limits are 50 and 98.6 for MRFs and IMFs, respectively.

Fifty-one cases that belong to the first set of analyses were classified according to their lateral stability behavior. First, these cases were divided based on whether lateral instability was observed or not. The cases that exhibit instability were further divided into two categories based on whether instability occurred before or after the code specified target plastic rotation. The PM_b ratio versus the slenderness for these three cases is plotted in Figure 4.18. According to this figure combined evaluation of PM ratio and slenderness is a good measure for predicting the lateral instability of the beam outside of the link. A boundary shown in bold dashed lines were placed on this figure to distinguish between safe and unsafe designs. The analysis results revealed that all cases having a PM_b ratio less than unity are not susceptible to lateral instability. In other words, considering link overstrength and reducing the PM limit to 0.8 turns out to be a stringent requirement. Cases with PM ratios in between 0.8 and 1.0 produce laterally stable behavior although the beam outside of the link experiences yielding. Furthermore for cases having PM ratios in excess of unity the behavior can be divided into two regimes. When the slenderness of the beam outside of the link is less than 75, it shows laterally stable behavior. Lateral instability is a threat for cases having slenderness ratios in excess of 75 and PM ratios greater than unity.

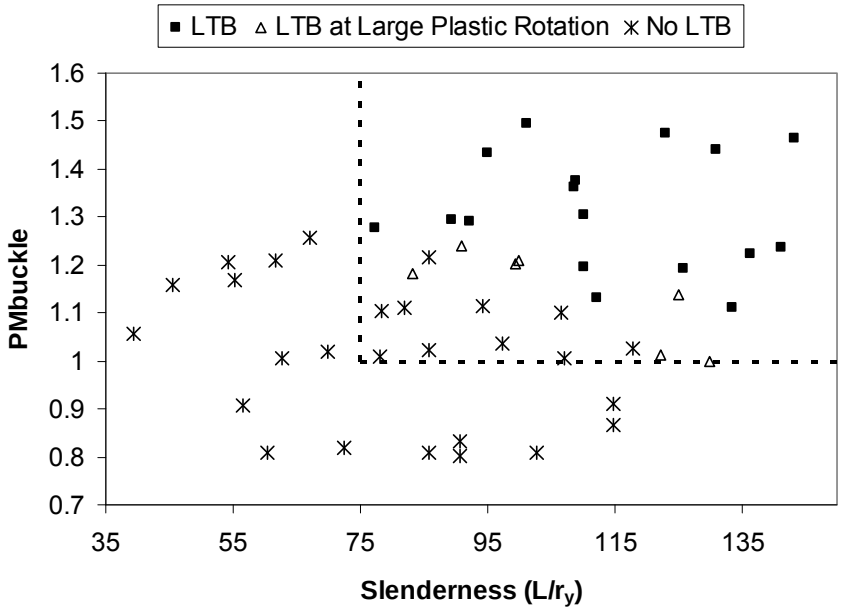

Figure 4.18: PM versus Slenderness for Cases Showing Laterally Stable and Unstable Behavior

The boundaries in Figure 4.18 are provided to give a safe estimate of the behavior. All cases, in which the beam become lateral unstable after reaching the target rotation, are included in the unsafe region. This approach is overly-conservative and the boundaries can also be shifted so that the unsafe region is defined by PM>1.1 and L/r_y>85. Cases with PM values in between unity and 1.1 can still provide stable behavior because of the margin of safety injected into the PM ratio by introducing a resistance factor(ϕ) of 0.9.

In light of the data presented in Figure 4.18, it is recommended that the beam outside of the link can be designed by disregarding the overstrength of the link. If the beam outside of the link has a PM ratio greater than unity for a selected link section, then lateral bracing should be provided where the unbraced length between braces should satisfy the following requirement.

$$L < 0.13 r_y \frac{E}{F_y} \tag{4.2}$$

A detailed investigation of the factors that lead these conclusions will be presented in later sections of the thesis.

4.5 Investigation of Local Instabilities

A similar investigation was conducted to study the local instability of the brace connection panel. If the beam outside of the link is designed to have a PM ratio below 0.8, then it is expected that the brace connection panel will show a stable behavior. The single most important factor in assessing the local instability of the brace connection panel is the flange slenderness measured as $b_f/2t_f$. In addition, preliminary analyses revealed that normalized link length also has an effect on the behavior. In long and intermediate length links, significant amount of bending moments are produced at the link ends. These moments in turn are transferred to the brace connection panel and impose significant amount of bending strains in its flanges. When the data in Tables 4.1 and 4.2 are investigated, it observed that brace connection local buckling is present in majority of the cases. However, a careful examination of the behavior reveals that in most of these cases the local buckles occur at rotation levels that are in excess of the target rotation. In studying the local buckling response the analysis cases were divided into two categories. First of all the cases where lateral torsional buckling was observed were removed from the data set. Second, the two sets of analysis were combined. The combined data set was sorted according to the results in terms of local buckling. The first category belongs to cases where local buckling of the brace connection panel occurs at plastic rotation levels that are less than the target rotation. The second category belongs to cases which either showed no local buckling or local buckling at plastic rotation levels that are in excess of the target plastic rotation. These two categories are plotted in Figure 4.19. Similar to Figure 4.18, a boundary was placed to distinguish between safe and unsafe designs. It is worthwhile to note that PMy values are used in the assessment of local buckling because the analysis cases either were laterally supported or showed no lateral instability.

Examination of Figure 4.19 reveals that 9 out of 63 cases suffered from local buckling prior to reaching the target plastic rotation levels. These cases usually belong to the region where the PM_y ratio is above unity and the flange slenderness is greater than 6.6 ($0.27(E/F_y)^{1/2}$). The

AISC flange slenderness limit for seismicly compact sections is $0.30(E/F_y)^{1/2}$ which gives a ratio of 7.22 for a steel with a yield strength of F_y=345 MPa (50 ksi).

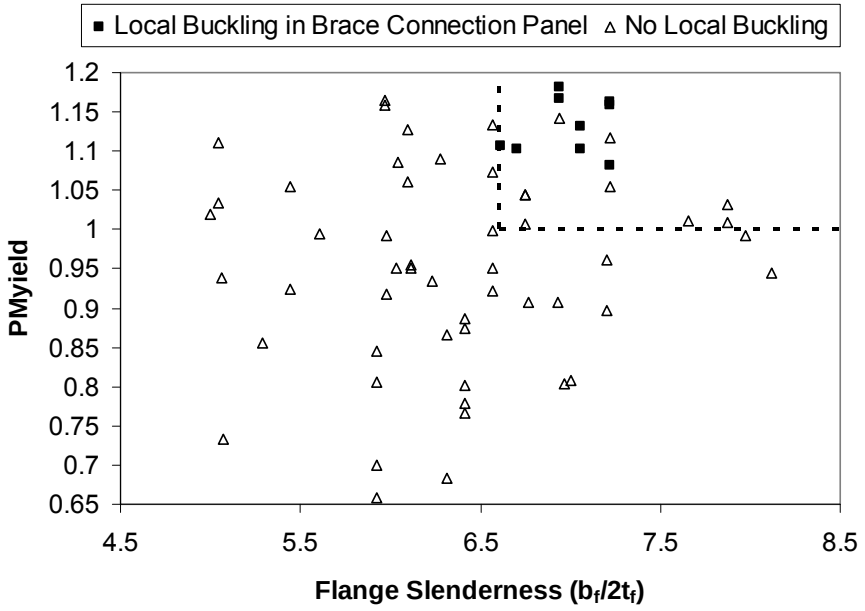

Figure 4.19: PM versus Slenderness for Cases Showing Locally Stable and Unstable Behavior

Based on the analysis results it is recommended that the flange slenderness for the beam outside of the link should be less than $0.27(E/F_y)^{1/2}$ if the PM ratio is to be greater than unity. For cases with PM ratios less than unity local buckling of the brace connection may happen at large plastic rotation levels. The boundary at PM equals to unity was set using some conservatism. This boundary can safely be shifted to PM_y=1.1. In fact all cases except one which showed local buckling have PM_y ratios greater than 1.1. The reason for having systems with stable behavior and PM ratios in excess of unity can be attributable to the resistance factor used in calculation of the PM factor.

4.6 Link Overstrength

Overstrength of the link is one of the most important factors influencing the stability of an EBF system. As mentioned earlier, overstength can be primary due to two sources. The link material may possess higher yield strength than considered at the design stage and this can be accounted for by considering a R_y factor. In the present study a R_y factor of 1.1 was used at the design stage as well as during the analysis phase. The second and more influencing factor is the overstrength due to strain hardening. Unfortunately, the strain hardening process is highly dependent on the loading protocol and the target strain. The AISC Seismic Provisions (2005) provide a single value for overstrength due to strain hardening regardless of the target plastic rotation and the link properties. This is merely a conservative assumption and as mentioned earlier the recommended overstrength factor is 1.25 if the beam outside of the link is not acting compositely with a concrete slab. In addition, there is an additional factor of safety embedded in the PM calculations. The resistance factor of 0.9 used in the PM calculations are actually accounting for some level of overstrength. When the two factors are combined the overall link overstrength considered during the design stage turns out to be 1.38 (1.25/0.9).

The overstength possessed by the analysis cases was investigated to understand the legality of the overstrength factor recommended by the AISC Specification (2005). For each analysis the nominal shear strength of the link (V_n or V_{link}) which was calculated at the design stage is reported in Tables 4.3 and 4.4. This value does include overstrength due to actual material properties. In addition, the maximum value of link shear force recorded during the analysis phase was reported in the same tables. Two values for each analysis were reported based on the direction of loading. Positive loading produces compression on the beam outside of the link while negative loading produces tension. Results were separated into two depending on the system performance. Cases in Table 4.3 are for the ones that experience lateral torsional buckling whereas cases in Table 4.4 are for the ones that show laterally stable behavior. Overstrength possessed by each link was calculated by normalizing the maximum link shear with the nominal shear strength of the link and are reported in these tables. Statistical measures such as the average, standard deviation, maximum and minimum are also included. Clearly there is a difference between the average overstrength possessed by the two sets. Systems that experienced lateral torsional buckling exhibited less overstrength compared to

the systems that showed laterally stable behavior. This is natural because the lateral instability prevented further increase in the capacity of the system. The focus should be given to systems that showed laterally stable behavior. For these systems the average overstrength is 1.36 and 1.30 for positive and negative loading directions, respectively. Again these values combine material overstrength with the overstrength due to strain hardening. Overstrength due to strain hardening alone is 1.23 (1.36/1.1). This value is clearly less than the anticipated value of 1.38. This suggests that the amount of link overstrength considered in the specifications can be overly conservative. It is worthwhile to investigate the influence of link properties on the overstrength. The most influencing factor is the normalized link length ($e/(M_p/V_p)$). The variation of overtrength due to strain hardening is plotted against the normalized link length in Figure 4.20. The analysis results were combined with the experimental observations of Okazaki et al. (2005). According to this figure the amount of overstrength reduces significantly as the normalized link length increases. Majority of the analysis cases fall below the AISC limit. The reason for having less overstength in long links is apparent because such links have less rotation capacity. At low rotation levels local buckles at the link ends are produced which in turn limit the increase in shear capacity of these links. Only shear yielding links with normalized lengths less than 1.6 reached to the overstrength level recommended by the AISC Specification (2005). Based on these observations it is recommended that a criterion which takes into account the normalized link length should be developed for design purposes. The limit recommended by the AISC Specification (2005) can be used for short links but this limit is overly conservative for long and intermediate links.

4.7 Quality of Estimates – Beam and Brace Axial Force

Stability of the beam and the brace are directly influenced by the forces acting on them. EBF systems, in general, are indeterminate and certain level of force redistribution is always present. The PM factors for the beam and the brace were calculated based on assumed force distributions. In this and the following sections, the quality of the force estimations was evaluated. The estimated axial force on the beam and the brace are given in Tables 4.3 and 4.4. It should be mentioned the beam axial force is not amplified, in other words it was found by utilizing the force distribution law and the nominal link shear capacity. On the contrary,

the brace axial force was found by considering an increase of 1.1x1.25=1.38 in the nominal link shear capacity due to overtsrength.

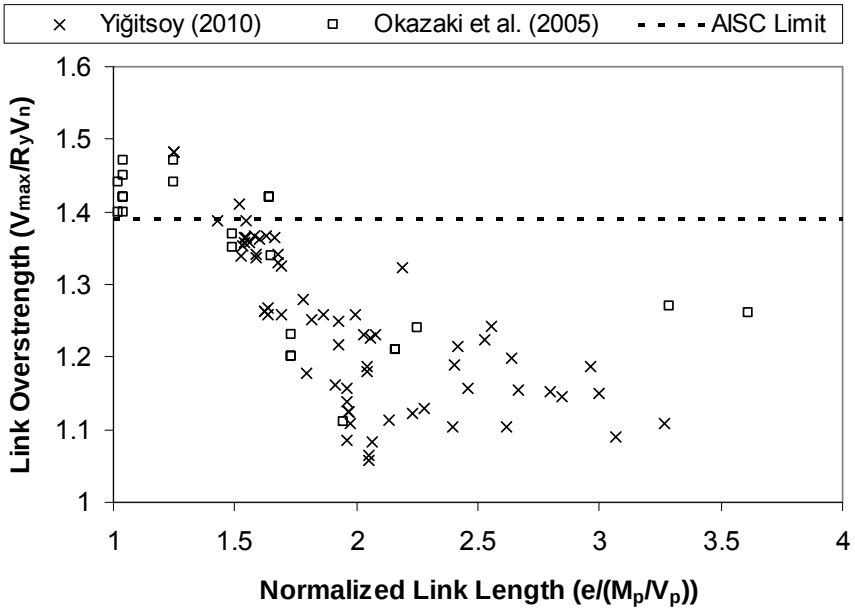

Figure 4.20: Overstrength as a Function of Normalized Link Length

The maximum values for each analysis case is reported in Tables 4.3 and 4.4 for both the positive and the negative loading. In order to assess the quality of the predictions the ratio of the actual axial force to the estimated axial force was calculated. In order to make a fair comparison, the estimated axial force was amplified by the actual overstrength possessed by the link which is also given in the very same tables. In finding the ratio for the brace the estimated axial force was further divided by 1.38 to take into account the overstrength considered during the design phase. When the statistical measures for these ratios are studied it can be found that the axial force predictions for the brace have an average ratio close to unity. This suggests that the brace forces are accurately predicted and the difference between the actual forces and the estimated forces only stem from the differences between the actual and predicted overstrengths.

Table 4-3: Comparison of Estimated and Actual Response Quantities (LTB Cases)

Case #	e/(Mp/Vp)	Estimated Vlink (kN)	Actual (+) Vmax (kN)	Actual (-) Vmax (kN)	Overstrength (+)	Overstrength (-)	Estimated Pbeam (kN)	Actual (+) Pbeam (kN)	Actual (-) Pbeam (kN)	Ratio (+)	Ratio (-)	Estimated Pbrace (kN)	Actual (+) Pbrace (kN)	Actual (-) Pbrace (kN)	Ratio (+)	Ratio (-)
1	1.691	610	618	765	1.01	1.25	1007	965	1268	0.95	1.00	1644	1223	1499	1.01	1.00
2	1.03	1115	1317	1886	1.18	1.69	1895	2077	3154	0.93	0.98	3054	2615	3727	1.00	0.99
3	3.269	566	574	681	1.01	1.20	764	698	867	0.90	0.94	1403	1014	1219	0.98	0.99
4	1.517	539	792	787	1.47	1.46	997	1343	1441	0.92	0.99	1575	1681	1677	1.00	1.00
5	1.798	1191	1223	1459	1.03	1.23	1488	1406	1735	0.92	0.95	2731	2033	2397	1.00	0.99
6	2.023	533	703	663	1.32	1.24	959	1116	1241	0.88	1.04	1529	1450	1383	0.99	1.00
7	2.471	854	983	1041	1.15	1.22	1324	1401	1512	0.92	0.94	2262	1882	1988	0.99	0.99
11	2.278	1134	1228	1330	1.08	1.17	1361	1343	1535	0.91	0.96	2603	2028	2184	0.99	0.98
14	2.133	749	916	872	1.22	1.16	898	996	1125	0.91	1.08	1724	1521	1463	0.99	1.00
28	1.477	572	721	747	1.26	1.31	1059	1250	1339	0.94	0.97	1672	1535	1597	1.00	1.00
29	2.417	379	454	498	1.20	1.31	607	672	836	0.93	1.05	1011	876	961	1.00	0.99
30	1.924	621	801	765	1.29	1.23	1118	1317	1410	0.91	1.02	1787	1668	1597	1.00	1.00
31	1.779	541	663	667	1.23	1.23	784	885	1090	0.92	1.13	1342	1188	1205	0.99	1.00
32	1.523	708	898	1032	1.27	1.46	761	885	1112	0.92	1.00	1504	1383	1575	1.00	0.99
33	1.483	1055	1490	1521	1.41	1.44	1530	1784	2286	0.83	1.04	2629	2478	2731	0.92	0.99
35	1.909	1132	1472	1437	1.30	1.27	1585	1824	2211	0.88	1.10	2784	2607	2531	0.99	0.98
37	1.878	1197	1566	1495	1.31	1.25	1676	1922	2331	0.88	1.11	2947	2767	2651	0.99	0.99
39	1.909	1132	1503	1428	1.33	1.26	1358	1548	1855	0.86	1.08	2596	2451	2357	0.98	0.99
40	1.961	925	841	858	0.91	0.93	1711	1441	1486	0.93	0.94	2702	1784	1824	1.00	1.00
41	2.065	534	512	641	0.96	1.20	987	894	1139	0.94	0.96	1559	1090	1361	1.00	1.00
42	1.798	1191	1143	1250	0.96	1.05	2203	1890	2139	0.89	0.93	3480	2393	2651	0.98	1.00
43	2.052	657	725	721	1.10	1.10	1084	1121	1125	0.94	0.95	1771	1419	1414	1.00	1.00
44	1.961	925	974	970	1.05	1.05	1526	1486	1499	0.92	0.94	2488	1895	1899	0.99	1.00
45	1.961	925	1094	1050	1.18	1.14	1341	1446	1463	0.91	0.96	2296	1957	1890	0.99	1.00
				Av	**1.18**	**1.24**			Av	**0.91**	**1.00**			Av	**0.99**	**1.00**
				StD	**0.15**	**0.16**			StD	**0.03**	**0.06**			StD	**0.02**	**0.01**
				Max	**1.47**	**1.69**			Max	**0.95**	**1.13**			Max	**1.01**	**1.00**
				Min	**0.91**	**0.93**			Min	**0.83**	**0.93**			Min	**0.92**	**0.98**

Table 4-4: Comparison of Estimated and Actual Response Quantities (Non LTB Cases)

Case #	e/(Mp/Vp)	Estimated Vlink (kN)	Actual (+) Vmax (kN)	Actual (-) Vmax (kN)	Overstrength (+)	Overstrength (-)	Estimated Pbeam (kN)	Actual (+) Pbeam (kN)	Actual (-) Pbeam (kN)	Ratio (+)	Ratio (-)	Estimated Pbrace (kN)	Actual (+) Pbrace (kN)	Actual (-) Pbrace (kN)	Ratio (+)	Ratio (-)
8	2.461	465	592	574	1.27	1.23	814	947	1032	0.92	1.03	1319	1214	1179	0.99	1.00
9	2.529	427	574	547	1.35	1.28	746	903	1041	0.90	1.09	1206	1174	1125	1.00	1.00
10	1.517	539	836	805	1.55	1.49	890	1245	1317	0.90	0.99	1450	1632	1579	1.00	1.00
12	1.813	459	632	600	1.38	1.31	573	712	761	0.90	1.01	1046	1045	1001	1.00	1.00
13	1.247	857	1397	1352	1.63	1.58	1585	2366	2473	0.92	0.99	2504	2980	2891	1.00	1.01
15	2.417	379	507	485	1.34	1.28	455	547	600	0.90	1.03	866	836	805	0.99	1.00
16	2.079	824	1116	1059	1.35	1.28	1442	1677	1962	0.86	1.06	2325	2268	2171	0.99	1.00
17	1.247	857	1397	1352	1.63	1.58	1414	2095	2215	0.91	0.99	2314	2753	2678	1.00	1.01
18	2.231	1186	1463	1401	1.23	1.18	1601	1739	2673	0.88	1.41	2916	2553	2482	0.98	0.99
19	2.405	516	676	645	1.31	1.25	697	810	956	0.89	1.10	1268	1197	1143	0.99	0.99
20	2.189	443	645	618	1.45	1.39	620	756	903	0.84	1.04	1084	1134	1099	0.99	1.00
21	1.969	572	707	681	1.24	1.19	686	756	885	0.89	1.08	1315	1165	1130	0.99	0.99
22	1.924	621	854	787	1.38	1.27	745	858	1005	0.84	1.06	1419	1397	1303	0.98	1.00
23	1.624	758	1054	1019	1.39	1.34	1062	1326	1477	0.90	1.04	1862	1886	1828	1.00	1.01
24	1.546	1748	2669	2562	1.53	1.47	2098	2624	3038	0.82	0.99	4008	4390	4208	0.99	0.99
25	1.958	1080	1352	1308	1.25	1.21	1458	1615	2108	0.88	1.19	2640	2393	2317	1.00	1.00
26	1.624	758	1054	1027	1.39	1.35	910	1121	1285	0.89	1.04	1727	1753	1712	1.00	1.01
27	1.539	1204	1806	1735	1.50	1.44	1444	1806	2166	0.83	1.04	2766	2962	2847	0.98	0.98
34	1.779	541	761	729	1.41	1.35	676	836	916	0.88	1.01	1238	1245	1205	0.98	0.99
36	1.969	572	707	676	1.24	1.18	801	894	987	0.90	1.04	1412	1259	1214	0.99	1.00
38	1.866	1356	1877	1766	1.38	1.30	1627	1904	2260	0.85	1.07	3096	3051	2896	0.98	0.99
46	2.397	993	1205	1170	1.21	1.18	1391	1526	1672	0.90	1.02	2454	2139	2091	0.99	0.99
47	1.798	1191	1543	1454	1.30	1.22	1488	1721	1833	0.89	1.01	2731	2549	2411	0.99	0.99
48	2.278	1134	1410	1388	1.24	1.22	1361	1486	1784	0.88	1.07	2603	2304	2291	0.98	0.99
49	2.052	657	765	725	1.16	1.10	690	729	801	0.91	1.05	1397	1174	1121	0.99	1.00
50	2.133	749	916	885	1.22	1.18	898	992	1156	0.90	1.09	1724	1517	1481	0.99	1.00
51	1.969	572	707	676	1.24	1.18	686	756	881	0.89	1.09	1315	1165	1130	0.99	1.00

Table 4-4 (continued)

Case #	e/(Mp/Vp)	Estimated Vlink (kN)	Actual (+) Vmax (kN)	Actual (-) Vmax (kN)	Overstrength (+)	Overstrength (-)	Estimated Pbeam (kN)	Actual (+) Pbeam (kN)	Actual (-) Pbeam (kN)	Ratio (+)	Ratio (-)	Estimated Pbrace (kN)	Actual (+) Pbrace (kN)	Actual (-) Pbrace (kN)	Ratio (+)	Ratio (-)
101	1.961	925	1103	1027	1.19	1.11	1711	1877	1850	0.92	0.97	2702	2335	2184	1.00	1.00
102	2.052	657	770	721	1.17	1.10	1216	1321	1281	0.93	0.96	1921	1628	1535	1.00	1.00
103	1.977	1055	1285	1223	1.22	1.16	1266	1357	1868	0.88	1.27	2416	2108	2015	0.98	0.99
104	1.909	1132	1446	1370	1.28	1.21	1358	1517	1899	0.87	1.16	2596	2371	2255	0.98	0.99
105	2.042	912	1183	1121	1.30	1.23	1277	1468	1672	0.89	1.07	2245	2082	1988	0.98	0.99
106	2.058	986	1330	1250	1.35	1.27	1775	2135	2286	0.89	1.02	2831	2749	2602	0.99	1.00
107	2.065	534	636	609	1.19	1.14	667	734	752	0.92	0.99	1222	1050	1023	0.99	1.01
108	2.045	890	1161	1103	1.31	1.24	1379	1552	1895	0.86	1.11	2336	2188	2099	0.99	1.00
109	1.958	1080	1374	1294	1.27	1.20	1674	1877	2393	0.88	1.19	2832	2598	2469	0.99	1.00
110	1.924	1204	1610	1543	1.34	1.28	1625	1850	2455	0.85	1.18	2927	2829	2718	0.99	1.00
111	2.032	1038	1406	1339	1.35	1.29	1609	1846	2246	0.85	1.08	2715	2651	2540	0.99	1.00
112	1.998	1173	1624	1557	1.38	1.33	1584	1810	2215	0.83	1.05	2844	2833	2731	0.99	1.00
113	2.997	795	1005	956	1.26	1.20	1391	1610	1975	0.92	1.18	2273	2073	1984	0.99	1.00
114	3.269	566	689	672	1.22	1.19	877	983	1210	0.92	1.16	1506	1317	1294	0.99	1.00
115	2.848	907	1143	1085	1.26	1.20	1406	1610	2139	0.91	1.27	2408	2184	2086	0.99	1.00
116	3.067	653	783	814	1.20	1.25	881	974	1259	0.92	1.15	1615	1397	1454	0.99	0.99
117	2.797	765	970	939	1.27	1.23	1339	1539	1917	0.91	1.17	2185	1681	1646	0.83	0.84
118	2.965	365	476	449	1.30	1.23	638	756	872	0.91	1.11	1038	983	934	1.00	1.00
119	2.552	729	996	947	1.37	1.30	1277	1566	1695	0.90	1.02	2070	2042	1953	0.99	1.00
120	2.639	664	876	854	1.32	1.29	897	1054	1263	0.89	1.10	1628	1543	1517	0.99	1.00
121	2.615	707	858	823	1.21	1.16	1132	1268	1441	0.92	1.09	1884	1655	1588	0.99	1.00
122	2.667	599	761	734	1.27	1.22	809	939	1125	0.91	1.14	1479	1352	1312	0.99	1.00
123	1.634	925	1281	1214	1.39	1.31	1549	1966	1984	0.92	0.98	2515	2518	2402	0.99	1.00
124	1.634	925	1290	1228	1.39	1.33	1364	1726	1761	0.91	0.97	2310	2317	2224	0.99	1.00
125	1.543	489	734	698	1.50	1.43	710	939	1027	0.88	1.01	1217	1326	1268	1.00	1.00

Table 4-4 (continued)

Case #	e/(Mp/Vp)	Estimated Vlink (kN)	Actual (+) Vmax (kN)	Actual (-) Vmax (kN)	Overstrength (+)	Overstrength (-)	Estimated Pbeam (kN)	Actual (+) Pbeam (kN)	Actual (-) Pbeam (kN)	Ratio (+)	Ratio (-)	Estimated Pbrace (kN)	Actual (+) Pbrace (kN)	Actual (-) Pbrace (kN)	Ratio (+)	Ratio (-)
126	1.6	799	1197	1139	1.50	1.43	1478	2006	2046	0.91	0.97	2339	2531	2424	0.99	1.00
127	1.691	610	845	801	1.38	1.31	1007	1277	1272	0.92	0.96	1644	1655	1566	1.00	1.00
128	1.632	696	1045	1005	1.50	1.45	1252	1655	1828	0.88	1.01	2005	2184	2108	1.00	1.00
129	1.534	1000	1490	1428	1.49	1.43	1876	2571	2575	0.92	0.96	2949	3176	3051	0.99	1.00
130	1.694	689	1005	956	1.46	1.39	1137	1508	1543	0.91	0.98	1858	1962	1868	0.99	1.00
131	1.539	1204	1797	1717	1.49	1.43	1926	2460	2807	0.86	1.02	3201	3425	3269	0.99	0.98
132	1.677	763	1125	1090	1.48	1.43	801	1041	1112	0.88	0.97	1629	1730	1681	0.99	0.99
133	1.583	876	1317	1268	1.50	1.45	1271	1712	1788	0.90	0.97	2176	2362	2282	0.99	1.00
134	1.663	857	1285	1245	1.50	1.45	1200	1570	1770	0.87	1.02	2106	2286	2224	0.99	1.00
135	1.678	1070	1566	1459	1.46	1.36	1765	2344	2313	0.91	0.96	2886	3056	2851	1.00	1.00
136	1.56	592	884	838	1.49	1.42	755	1014	1059	0.90	0.99	1362	1468	1401	0.99	1.00
137	1.588	989	1459	1352	1.48	1.37	1829	2451	2469	0.91	0.99	2893	3091	2869	1.00	1.00
138	1.426	1248	1904	1828	1.53	1.47	2059	2811	2918	0.89	0.97	3374	3723	3581	0.99	1.00
139	1.528	501	738	689	1.47	1.38	851	1165	1143	0.93	0.98	1371	1463	1370	1.00	1.00
140	1.588	989	1454	1352	1.47	1.37	1434	1886	1939	0.89	0.99	2460	2615	2442	0.99	1.00
				Av	**1.36**	**1.30**			Av	**0.89**	**1.06**			Av	**0.99**	**0.99**
				StD	**0.12**	**0.11**			StD	**0.03**	**0.09**			StD	**0.02**	**0.02**
				Max	**1.63**	**1.58**			Max	**0.93**	**1.41**			Max	**1.00**	**1.01**
				Min	**1.16**	**1.10**			Min	**0.82**	**0.96**			Min	**0.83**	**0.84**

The average ratios for the beam, however, are 0.89 and 1.06 for positive and negative loadings, respectively. The deviation from unity is in acceptable limits and is attributable to the neglect of link axial force in calculating the beam axial force. Detailed analysis of the data revealed that when the beam outside of the link yields, additional link shear forces are transmitted to the link rather than the beam as an axial force. This concept was explained in Chapter 2. Because the axial force on the beam can no longer increase due to plastic hinge formation, the actual forces on this member are on average 10 percent less than the estimated ones.

4.8 Quality of Estimates – Beam and Brace Moments

Similar types of investigations were performed for the moments acting on the beam and the brace. Another important factor in the investigations is the amount of link end moments. As explained in Chapter 2, it was assumed that the moments equalize at the link ends when the link experiences plastic deformations. This assumption was validated by experimental results in the past for long links. For short links, however, the moment variation can be significantly different. First of all the actual link end moment at the braced end was compared with the estimated link end moments. The estimations and the actual quantities are presented in Tables 4.5 and 4.6. Analysis cases were separated into two categories depending on the failure of the systems. The ratio of actual moment to the estimated moment is also tabulated. Again, in these ratios the actual overstrength of the beam was taken into account by multiplying the estimated moment value with the actual overstrength of the system observed during the analysis. Statistical analysis of the results reveals that for both failure categories and direction of loading the ratios are close to unity. These observations suggest that the assumed moment distribution law is acceptable in terms of predicting the link end moments.

When moments acting on the beam and the brace were investigated, it was found that the predictions for these member tractions are not as good as the ones for the link end moment. This suggests that there exists moment redistribution between the beam and the brace. First of all, the ratios in Tables 4.5 and 4.6 show that the moment acting on the beam are less than the estimated moment. This is more pronounced for positive loading where the beam is under compression. The average ratios for this loading are 0.82 and 0.84, for LTB and non

LTB cases, respectively. The same ratios are 0.95 and 0.99 for the negative loading where the beam is under tension. The difference in actual and estimated beam end moments can be attributable to yielding of the beam. When a plastic hinge forms at the beam end or at the brace connection panel, the beam can no longer sustain additional moments and the moments are solely carried by the brace member. The difference between the ratios for positive and negative loading can be attributable to the second order effects. As shown in Figure 4.21, the axial load on the beam reduces the beam end moment when the beam is under compression and increases it when the beam is under tension. Usually the second order moments due to lateral translation are neglected during the design because it is assumed that the brace fully restrains the movement between the beam ends. In reality, however, due to elastic frame deformations, certain amount of vertical deflection at the brace connection panel is inevitable. Fortunately, due to this displacement, a second order moment that counteracts the first order moment is produced when the beam is under compression. The opposite is true when the beam is under tension.

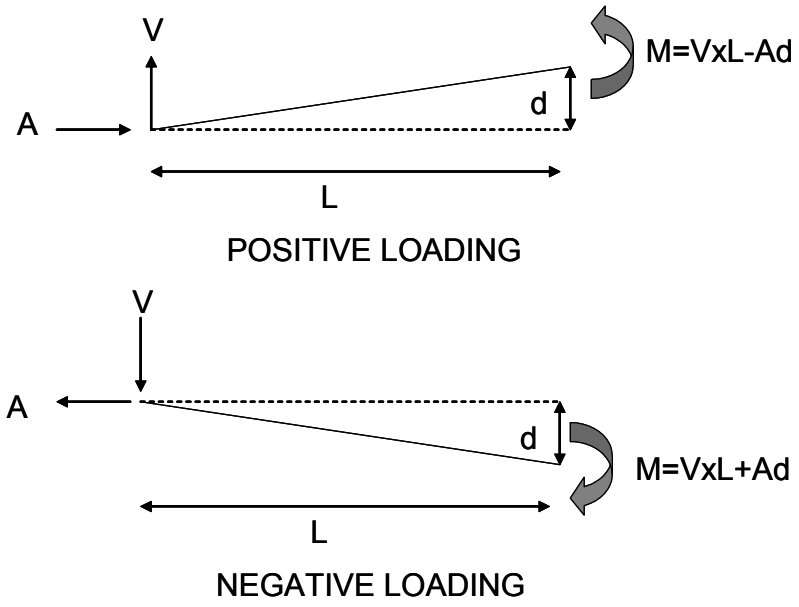

Figure 4.21: Second Order Effects on Beam End Moments

When the brace end moments are examined, it is evident that the behaviors for the two different categories are distinct. Cases that suffered from lateral torsional buckling showed significant increases in brace end moments. This is natural because after the beam fails in lateral instability all of the moments are redistributed to the brace. This detrimental behavior should definitely be avoided because the amount of increase in the brace end moments is intolerable. On the other hand, for cases that showed laterally stable behavior, the increase in brace end moments are on average 30 percent and 8 percent for positive and negative, loadings, respectively. As explained before, this increase is attributable to the yielding in the beam. The under-prediction of beam end moments in positive loading results in an over-prediction of the brace end moment. The discrepancies between the estimated and actual brace end moments are more pronounced for positive loading simply because the discrepancy in beam end moment predictions are more pronounced for this type of loading.

4.9 PM Ratios

Throughout this study PM ratio was used as a measure to assess the stability of the EBF systems. Both the beam and the brace are subjected to high bending moments and axial forces and these members should be designed as beam columns. PM ratio was extensively used in the design of these members. In this section the actual PM ratios exhibited by these members are investigated. The primary aim is to explore whether the calculations for the PM ratios are reasonable. As mentioned in earlier chapters, various assumptions are utilized in calculating PM ratio. In addition, the calculation of PM ratios as recommended in the specifications has inherent simplifications. It is worthwhile to reiterate that the PM ratio combines a capacity check with a stability check. During the loading history, if the member shows stable behavior, it eventually fails by reaching to its capacity. In Chapter 2 two measures namely, PM_b and PM_y, were utilized to separate these failure modes. Results presented in this chapter showed that instability is the governing factor when the member's slenderness is high and formation of a plastic hinge is the governing factor when the member's slenderness is low.

In assessing the PM ratios, the data set is divided into two according to the failure mode of the system. Again, cases with and without lateral torsional buckling were studied separately. For a given loading history, the variation of the PM factor was calculated considering both

instability and member capacity. In other words, the history of PM_b and PM_y was calculated for each analysis case. In calculating the PM values for the beam, the actual yield strength was used by considering 10 percent increase (R_y=1.1) in the yield strength. Although the models include an increased yield strength for the brace the PM ratios for this member was calculated based on nominal yield strength. In discussion of the results the difference between the actual and nominal yield strength will be taken into account. The resistance factor of 0.9 was used in all PM calculations.

Loading direction was considered in the assessments. When a member, beam or brace, is under compression, then the governing PM factor is the PM_b. When a member is under tension the member can still experience lateral instability if the moments are high but such cases were not observed during the analyses. Therefore, for cases where the member is under tension, PM_y was used as the governing factor. In addition, for case that showed laterally stable behavior the PM_y value was considered for both loading directions.

The calculated PM ratios from all analyses are presented in Tables 4.7 and 4.8. When the cases with lateral buckling are examined, it is observed that the average PM_b ratios for the beam are 1.16 and 1.08 for positive and negative loadings, respectively. These values suggest that the calculation of the PM value to assess the instability of the systems is adequate. PM values in excess of unity are due to the use of a resistance factor in calculating this factor. Some cases have PM values in excess of 1.1 and this is attributable to the assumptions adopted in calculating this ratio. In addition, there is considerable scatter in the actual test data which the column strength curve presented in the AISC Specification (2005) was derived from.

When the cases without lateral torsional buckling are examined, it is observed that the average PM_y ratios for the beam are 1.03 and 1.12 for positive and negative loadings, respectively. These values also suggest that the PM value can be safely used to assess the member capacity.

When the PM ratios for the brace are considered it is observed that the average values are close to 1.0 and 0.92 for cases with and without lateral buckling, respectively. This suggests that the brace members in general are designed properly. The PM value for the brace can

reach up to 1.22 (1.1/0.9) when the resistance factor is omitted and the actual yield strength of the brace material is considered. It should be mentioned that some cases that experienced lateral buckling have brace PM values that are beyond the 1.22 limit. Values in excess of 1.22 are an indication of possible plastification and hardening of the brace member. These observations strengthen the assertions that the beam should show a laterally stable behavior during the entire loading history. Formation of lateral instabilities can prove to be detrimental in terms of brace performance. When the capacity of the beam is exhausted the, the forces and especially the moments are redistributed to the brace leading to the failure of this member.

Table 4-5: Comparison of Estimated and Actual Response Quantities (LTB Cases)

Case #	e/(Mp/Vp)	Estimated Mlk(kNm)	Actual (+) Mlink	Actual (-) Mlink	Ratio (+)	Ratio (-)	Estimated Mbeam (kN-m)	Actual (+) Mbeam (kN-m)	Actual (-) Mbeam (kN-m)	Ratio (+)	Ratio (-)	Estimated Mbrace (kN-m)	Actual (+) Mbrace (kN-m)	Actual (-) Mbrace (kN-m)	Ratio (+)	Ratio (-)
1	1.691	349	388	509	1.10	1.16	201	188	229	0.92	0.91	203	267	299	1.79	1.62
2	1.03	425	505	658	1.01	0.92	257	249	325	0.82	0.75	230	303	333	1.53	1.18
3	3.269	539	529	664	0.97	1.02	464	413	525	0.88	0.94	103	350	161	4.63	1.79
4	1.517	308	457	465	1.01	1.03	153	173	263	0.77	1.17	213	348	242	1.53	1.07
5	1.798	680	706	877	1.01	1.05	523	469	519	0.87	0.81	216	431	411	2.67	2.13
6	2.023	406	505	504	0.94	1.00	186	185	236	0.76	1.02	303	321	268	1.10	0.98
7	2.471	813	928	980	0.99	0.99	613	611	695	0.87	0.93	275	714	342	3.10	1.40
11	2.278	864	926	1033	0.99	1.02	691	655	703	0.88	0.87	238	666	435	3.56	2.15
14	2.133	571	690	696	0.99	1.05	479	518	564	0.88	1.01	126	449	267	4.01	2.51
28	1.477	327	441	465	1.07	1.09	180	186	249	0.82	1.06	202	318	216	1.72	1.12
29	2.417	289	350	393	1.01	1.03	190	187	240	0.82	0.96	136	267	197	2.25	1.51
30	1.924	473	594	587	0.97	1.01	255	250	323	0.76	1.03	301	427	277	1.51	1.03
31	1.779	309	377	440	1.00	1.15	202	204	257	0.82	1.03	147	281	440	2.15	3.35
32	1.523	337	439	503	1.03	1.02	280	324	352	0.91	0.86	79	243	189	3.33	2.25
33	1.483	603	768	917	0.90	1.05	455	498	561	0.78	0.86	204	446	417	2.13	1.95
35	1.909	863	1073	1055	0.96	0.96	589	648	702	0.85	0.94	377	859	671	2.41	1.93
37	1.878	912	1126	1109	0.94	0.97	638	694	735	0.83	0.92	378	890	607	2.48	1.77
39	1.909	863	1084	1055	0.95	0.97	684	780	808	0.86	0.94	246	377	247	1.59	1.09
40	1.961	528	466	495	0.97	1.01	276	187	254	0.75	0.99	348	291	241	1.27	1.03
41	2.065	305	312	391	1.07	1.07	149	115	168	0.81	0.94	215	209	223	1.39	1.19
42	1.798	680	599	712	0.92	1.00	363	253	370	0.73	0.97	437	417	342	1.37	1.03
43	2.052	376	410	418	0.99	1.02	215	188	242	0.79	1.03	221	237	178	1.34	1.01
44	1.961	528	544	562	0.98	1.01	280	232	295	0.79	1.00	341	356	272	1.36	1.04
45	1.961	528	604	602	0.97	1.00	349	328	377	0.79	0.95	247	409	235	1.92	1.15
				Av	**0.99**	**1.03**			Av	**0.82**	**0.95**			Av	**2.17**	**1.55**
				StD	**0.05**	**0.06**			StD	**0.05**	**0.09**			StD	**0.94**	**0.61**
				Max	**1.10**	**1.16**			Max	**0.92**	**1.17**			Max	**4.63**	**3.35**
				Min	**0.90**	**0.92**			Min	**0.73**	**0.75**			Min	**1.10**	**0.98**

Table 4-6: Comparison of Estimated and Actual Response Quantities (Non LTB Cases)

Case #	e/(Mp/Vp)	Estimated Mlk(kNm)	Actual (+) Mlink	Actual (-) Mlink	Ratio (+)	Ratio (-)	Estimated Mbeam	Actual (+) Mbeam	Actual (-) Mbeam	Ratio (+)	Ratio (-)	Estimated Mbrace	Actual (+) Mbrace	Actual (-) Mbrace	Ratio (+)	Ratio (-)
8	2.461	443	553	547	0.98	1.00	248	259	301	0.82	0.98	268	294	247	1.19	1.02
9	2.529	406	532	521	0.97	1.00	206	232	274	0.84	1.04	275	299	250	1.11	0.97
10	1.517	308	475	474	0.99	1.03	156	198	252	0.82	1.08	209	277	222	1.18	0.98
12	1.813	262	360	349	1.00	1.02	172	215	237	0.91	1.05	124	145	113	1.17	0.96
13	1.247	490	853	798	1.07	1.03	261	376	488	0.88	1.19	315	477	371	1.28	1.03
15	2.417	289	386	379	1.00	1.03	213	263	283	0.93	1.04	105	123	96	1.20	0.99
16	2.079	785	1016	1006	0.96	1.00	342	412	471	0.89	1.07	609	604	535	1.01	0.94
17	1.247	490	855	857	1.07	1.11	323	483	585	0.92	1.15	230	372	272	1.37	1.03
18	2.231	1130	1323	1297	0.95	0.97	858	903	931	0.85	0.92	373	509	366	1.52	1.14
19	2.405	492	629	619	0.98	1.01	364	421	451	0.88	0.99	175	209	169	1.25	1.06
20	2.189	338	474	465	0.96	0.99	196	226	268	0.80	0.98	196	247	197	1.20	0.99
21	1.969	436	530	531	0.98	1.02	359	383	418	0.86	0.98	105	148	112	1.56	1.23
22	1.924	473	615	611	0.94	1.02	355	416	452	0.85	1.00	163	198	159	1.22	1.06
23	1.624	578	838	823	1.04	1.06	378	488	525	0.93	1.04	275	349	298	1.26	1.11
24	1.546	1332	1914	1841	0.94	0.94	1051	1353	1361	0.84	0.88	387	561	483	1.31	1.17
25	1.958	1029	1271	1268	0.99	1.02	717	824	871	0.92	1.00	428	455	399	1.17	1.06
26	1.624	578	841	828	1.05	1.06	411	568	592	0.99	1.06	230	273	236	1.18	1.04
27	1.539	917	1315	1294	0.96	0.98	751	986	1022	0.87	0.94	229	329	272	1.32	1.14
34	1.779	309	417	404	0.96	0.97	229	265	297	0.83	0.96	111	195	113	1.72	1.04
36	1.969	436	532	530	0.99	1.03	325	331	373	0.82	0.97	153	201	157	1.46	1.19
38	1.866	1033	1329	1299	0.93	0.97	767	905	931	0.85	0.93	366	428	368	1.16	1.06
46	2.397	757	877	885	0.95	0.99	577	570	627	0.81	0.92	247	312	259	1.43	1.22
47	1.798	680	838	818	0.95	0.98	523	543	582	0.80	0.91	216	295	236	1.45	1.23
48	2.278	864	1011	1030	0.94	0.97	691	707	768	0.82	0.91	238	451	263	2.10	1.24
49	2.052	376	435	444	1.00	1.07	303	311	341	0.88	1.02	100	125	103	1.47	1.28
50	2.133	571	685	706	0.98	1.05	479	514	566	0.88	1.00	126	171	139	1.53	1.29
51	1.969	436	532	531	0.99	1.03	359	378	413	0.85	0.97	105	153	117	1.62	1.30

Table 4-6 (continued)

Case #	e/(Mp/Vp)	Estimated Mlk(kNm)	Actual (+) Mlink	Actual (-) Mlink	Ratio (+)	Ratio (-)	Estimated Mbeam	Actual (+) Mbeam	Actual (-) Mbeam	Ratio (+)	Ratio (-)	Estimated Mbrace	Actual (+) Mbrace	Actual (-) Mbrace	Ratio (+)	Ratio (-)
101	1.961	528	616	605	0.98	1.03	276	242	305	0.74	1.00	348	374	300	1.24	1.07
102	2.052	376	435	437	0.99	1.06	195	167	218	0.73	1.02	248	268	219	1.27	1.11
103	1.977	804	936	897	0.96	0.96	623	660	665	0.87	0.92	249	283	231	1.28	1.10
104	1.909	863	1049	1011	0.95	0.97	684	749	762	0.86	0.92	246	300	249	1.31	1.15
105	2.042	695	857	832	0.95	0.97	487	515	551	0.82	0.92	286	342	280	1.27	1.10
106	2.058	751	945	929	0.93	0.98	360	382	446	0.79	0.98	538	566	483	1.07	0.97
107	2.065	305	380	371	1.05	1.07	224	242	267	0.91	1.04	111	138	108	1.44	1.17
108	2.045	847	1051	1025	0.95	0.98	517	584	622	0.87	0.97	455	468	403	1.08	0.98
109	1.958	1029	1271	1267	0.97	1.03	602	700	751	0.91	1.04	587	571	516	1.05	1.01
110	1.924	1146	1475	1447	0.96	0.98	726	903	938	0.93	1.01	578	573	516	1.02	0.96
111	2.032	989	1252	1244	0.94	0.98	539	650	708	0.89	1.02	619	603	540	0.99	0.93
112	1.998	1118	1447	1436	0.94	0.97	665	854	898	0.93	1.02	622	594	539	0.95	0.90
113	2.997	757	928	921	0.97	1.01	566	599	664	0.84	0.98	263	329	262	1.36	1.14
114	3.269	539	642	646	0.98	1.01	448	459	506	0.84	0.95	125	184	147	1.66	1.36
115	2.848	864	1058	1069	0.97	1.03	675	716	781	0.84	0.97	260	342	299	1.43	1.32
116	3.067	621	741	785	0.99	1.01	521	555	625	0.89	0.96	138	186	169	1.55	1.35
117	2.797	729	882	916	0.95	1.02	524	543	638	0.82	0.99	281	345	290	1.33	1.16
118	2.965	347	456	440	1.01	1.03	224	252	285	0.86	1.04	170	204	154	1.27	1.01
119	2.552	695	907	914	0.96	1.01	395	459	529	0.85	1.03	412	461	385	1.13	0.99
120	2.639	633	805	816	0.96	1.00	458	533	580	0.88	0.98	240	271	241	1.18	1.07
121	2.615	539	634	625	0.97	1.00	352	351	387	0.82	0.94	256	283	251	1.25	1.16
122	2.667	571	716	733	0.99	1.05	461	525	577	0.90	1.02	150	191	167	1.37	1.25
123	1.634	440	584	591	0.96	1.02	285	283	356	0.72	0.95	214	302	235	1.40	1.15
124	1.634	440	587	587	0.96	1.00	289	308	365	0.76	0.95	208	279	222	1.32	1.11
125	1.543	280	426	424	1.01	1.06	197	252	304	0.85	1.08	113	174	120	1.41	1.03

Table 4-6 (continued)

Case #	e/(Mp/Vp)	Estimated Mlk(kNm)	Actual (+) Mlink	Actual (-) Mlink	Ratio (+)	Ratio (-)	Estimated Mbeam	Actual (+) Mbeam	Actual (-) Mbeam	Ratio (+)	Ratio (-)	Estimated Mbrace	Actual (+) Mbrace	Actual (-) Mbrace	Ratio (+)	Ratio (-)
126	1.6	456	649	654	0.95	1.01	287	322	416	0.75	1.02	233	326	238	1.28	0.98
127	1.691	349	505	485	1.04	1.06	201	244	285	0.88	1.08	203	261	200	1.28	1.03
128	1.632	530	775	770	0.97	1.00	322	386	475	0.80	1.02	285	389	294	1.25	0.98
129	1.534	476	668	660	0.94	0.97	266	267	348	0.67	0.92	289	416	314	1.33	1.04
130	1.694	394	555	542	0.97	0.99	239	281	338	0.80	1.02	213	274	203	1.21	0.95
131	1.539	917	1300	1276	0.95	0.98	560	713	769	0.85	0.96	491	587	507	1.10	1.00
132	1.677	436	630	609	0.98	0.98	380	492	516	0.88	0.95	77	138	93	1.66	1.15
133	1.583	501	730	716	0.97	0.99	337	417	466	0.82	0.96	226	313	250	1.27	1.05
134	1.663	653	977	954	1.00	1.01	442	602	649	0.91	1.01	290	375	305	1.18	0.99
135	1.678	612	847	810	0.95	0.97	373	423	482	0.77	0.95	327	425	328	1.22	1.01
136	1.56	282	411	403	0.98	1.01	216	276	310	0.86	1.02	91	134	93	1.35	0.99
137	1.588	565	795	772	0.95	1.00	337	372	458	0.75	0.99	314	422	314	1.25	1.01
138	1.426	713	1030	1033	0.95	0.99	506	620	707	0.80	0.95	284	410	326	1.30	1.08
139	1.528	191	269	277	0.96	1.05	111	111	162	0.68	1.06	110	158	115	1.34	1.04
140	1.588	565	796	765	0.96	0.99	409	492	535	0.82	0.96	214	304	230	1.33	1.08
				Av	**0.97**	**1.01**			Av	**0.84**	**0.99**			Av	**1.30**	**1.08**
				StD	**0.03**	**0.03**			StD	**0.06**	**0.06**			StD	**0.19**	**0.11**
				Max	**1.07**	**1.11**			Max	**0.99**	**1.19**			Max	**2.10**	**1.36**
				Min	**0.93**	**0.94**			Min	**0.67**	**0.88**			Min	**0.95**	**0.90**

Table 4-7: PM Ratios for the Beam and the Brace (LTB Cases)

	Beam		Brace	
	Positive Loading	Negative Loading	Negative Loading	Positive Loading
Case	PM_b	PM_v	PM_b	PM_v
1	1.27	0.97	1.02	0.77
2	1.18	1.04	1.14	0.73
3	1.17	1.18	1.10	1.53
4	1.14	1.02	1.01	1.03
5	1.23	1.03	1.19	1.01
6	1.00	0.90	0.78	0.77
7	1.21	1.13	1.02	1.45
11	1.19	1.08	1.19	1.37
14	1.23	1.22	1.25	1.65
28	1.13	0.94	0.93	0.95
29	1.16	1.06	1.18	1.22
30	1.12	1.00	0.85	0.98
31	1.15	1.39	1.15	1.09
32	1.19	1.07	1.35	1.25
33	1.23	1.12	1.31	1.16
35	1.23	1.14	1.20	1.34
37	1.22	1.10	1.16	1.38
39	1.23	1.20	0.93	1.04
40	1.06	0.94	0.65	0.60
41	1.07	1.06	0.86	0.64
42	1.05	1.04	0.74	0.69
43	1.12	1.08	0.77	0.77
44	1.05	1.01	0.69	0.70
45	1.17	1.13	0.81	0.95
Av	**1.16**	**1.08**	**1.01**	**1.04**
StD	**0.07**	**0.11**	**0.21**	**0.30**
Max	**1.27**	**1.39**	**1.35**	**1.65**
Min	**1.00**	**0.90**	**0.65**	**0.60**

Table 4-8: PM Ratios for the Beam and the Brace (Non LTB Cases)

	Beam		Brace	
	Positive Loading	Negative Loading	Negative Loading	Positive Loading
Case	PM_y	PM_y	PM_b	PM_y
8	0.83	0.93	0.84	0.85
9	0.79	0.93	0.83	0.85
10	0.82	0.97	0.91	0.91
12	0.98	1.07	0.90	0.91
13	0.88	1.03	1.02	1.01
15	1.06	1.14	0.88	0.90
16	0.79	0.91	0.82	0.83
17	0.95	1.09	1.11	1.09
18	1.07	1.12	0.89	0.98
19	1.00	1.09	0.91	0.92
20	0.80	0.95	1.01	1.02
21	1.02	1.11	0.93	0.89
22	1.01	1.12	0.93	0.95
23	0.89	0.96	0.90	0.90
24	1.10	1.17	1.07	1.08
25	0.99	1.10	0.89	0.88
26	0.95	1.00	0.94	0.93
27	1.03	1.09	1.07	1.05
34	1.02	1.14	0.94	1.08
36	0.96	1.06	0.92	0.91
38	1.09	1.14	0.96	0.96
46	1.10	1.17	0.91	0.88
47	1.13	1.19	0.93	0.93
48	1.10	1.22	0.94	1.05
49	1.06	1.16	0.84	0.80
50	1.12	1.24	0.94	0.88
51	1.01	1.10	0.94	0.91
101	1.06	1.15	0.79	0.79
102	0.98	1.08	0.75	0.72
103	1.07	1.08	0.82	0.83
104	1.09	1.05	0.70	0.90
105	1.04	1.10	0.91	0.92
106	0.96	1.05	0.85	0.86
107	1.06	1.16	0.83	0.81
108	0.93	1.02	0.87	0.87
109	0.93	1.06	0.84	0.84
110	0.98	1.10	0.88	0.88
111	0.91	1.03	0.88	0.88
112	0.96	1.06	0.90	0.90
113	1.16	1.22	0.90	0.90
114	1.11	1.19	0.93	0.87
115	1.15	1.20	0.94	0.94

Table 4-8: (continued)

	Beam		Brace	
	Positive Loading	Negative Loading	Negative Loading	Positive Loading
Case	PM_y	PM_y	PM_b	PM_y
116	1.10	1.22	0.99	0.91
117	1.09	1.20	0.92	0.91
118	0.96	1.04	0.83	0.85
119	1.00	1.10	0.83	0.85
120	1.05	1.15	0.88	0.88
121	1.03	1.08	0.77	0.75
122	1.12	1.21	0.93	0.91
123	1.16	1.29	0.98	0.94
124	1.12	1.22	0.89	0.86
125	0.95	1.11	1.04	1.06
126	1.13	1.29	1.02	0.98
127	1.00	1.11	0.85	0.87
128	0.91	1.07	1.01	1.02
129	1.16	1.30	0.99	0.97
130	1.06	1.18	0.97	0.97
131	0.93	0.99	0.96	0.96
132	1.17	1.24	1.08	1.00
133	1.07	1.16	0.95	0.93
134	0.99	1.08	1.01	1.01
135	1.16	1.22	0.94	0.96
136	1.12	1.22	0.97	0.89
137	1.15	1.26	0.95	0.93
138	1.19	1.29	1.09	1.01
139	1.09	1.26	0.92	0.93
140	1.15	1.21	0.95	0.93
Av	**1.03**	**1.12**	**0.92**	**0.92**
StD	**0.10**	**0.10**	**0.08**	**0.08**
Max	**1.19**	**1.30**	**1.11**	**1.09**
Min	**0.79**	**0.91**	**0.70**	**0.72**

CHAPTER 5

CONCLUSIONS

The overstrength problem associated with EBF systems were studied numerically. A total of 91 cases were analyzed to understand the important parameters that influence the system response. These analysis cases include beams outside of the link with no lateral supports, a single intermediate lateral support and full supports. Both lateral instability of the beam outside of the link and local flange buckling of the brace connection panel were studied in detail. Throughout the study the PM factor was extensively used to classify the system performance together with slenderness measures. The followings can be concluded from this study.

The overstrength factor recommended by the AISC Specification (2005) provides a stringent requirement and can safely be neglected so long as the PM factor of the beam outside of the link is kept below unity. There are several reasons that contribute to the possible omission of the link overstrength at the design stage.

- Investigations of typical designs showed that the overstrength issue is particularly important for long and intermediate links. These links produce high shear and bending moments on the beam outside of the link and make the design of this member difficult. Shear yielding links are less problematic when compared to the long and intermediate links. The analysis results of this thesis and previous experimental studies reveal that the single most important factor influencing the overstrength is the normalized link length. The amount of overstrength possessed by the links reduces as the normalized link length increases. AISC Specification (2005) recommends a single value for overstrength which is overly conservative for long and intermediate links. The counterbalancing effect of link length and overstrength is neglected in the provisions. While long and intermediate length links are problematic the overstrength possessed by these links are generally much lower than

the code specified level. On the contrary, the level of overstrength possessed by shear yielding links matches with the one specified by the code. However, these links are in general not problematic because of the lesser amount of moments developed at the link ends.

- The resistance factor of 0.9 used in the calculation of the PM factor provides some level of safety against overstrength of the link.

- An important factor that should be considered is the yielding of the beam outside of the link. When the increased forces due to the overstrength of the link cannot be resisted by the beam outside of the link, then a plastic hinge forms at the beam end. Formation of a plastic hinge modifies the force balance and additional moments applied at the braced link end are transferred entirely to the brace rather than the beam. This force redistribution contributes significantly to the stability of the system.

- The second order effects contribute to the stability of the beam outside of the link. The second order moments due to translation between the beam ends is usually ignored at the design stage. When the beam is under compression, the axial force helps reduce the moment acting on the beam end. The reduced amount of moment provides a level of safety against the overstrength of the link.

In cases where the PM factor cannot be kept below unity certain measures have to be taken to ensure the stability of the system. When the PM_b factor is above unity the unbraced length of the beam should be kept below $0.13r_yE/F_y$. When the PM_y factor is above unity the flange slenderness of the beam should be kept below $0.27(E/F_y)^{1/2}$.

The overstrength provisions for the brace were found to be adequate. The margin of safety incorporated into the design of braces is adequate to account for additional moments transferred to the brace due to redistribution of forces. The capacity of the brace member can be exhausted if the beam outside of the link experienced lateral instability.

This study was limited to the design space developed by the methods explained in Chapter 2. The results of this stduy are valid for EBFs with one end of the link connected to a column. Future research should consider other design spaces that can include different EBF geometries and brace designs.

REFERENCES

AISC, 2005. Seismic Provisions for Structural Steel Buildings, ANSI/AISC 341-05, American Institute of Steel Construction, Chicago, Ill.

AISC, 2005. Specification for Structural Steel Buildings, ANSI/AISC 360-05, American Institute of Steel Construction, Chicago, Ill.

AISC Design Manual, 2006, American Institute of Steel Construction and The Structural Steel Educational Council, Chicago, Ill.

ANSYS. Version 8.1 on-line user's manual; 2006.

Arce G., Engelhardt M. D., Okazaki T. and Ryu H. (2005). Experiment study of local buckling , overstrength ,and fracture of links in eccentrically braced frames. *Journal of Structural Engineering*; **131**(10): 1526-1535

Becker R. and Ishler M. (1996). Seismic design practice for eccentrically braced frames based on the 1994 UBC. Steel Tips, Structural Steel Educational Council.

Bruneau M., Uang C. M., and Whittaker A. S. (1997). Ductile design of steel structures.Chapter 7, McGrawHill , New York, NY.

Engelhardt M. D., Kasai K. and Popov E. P. (1987). Advances in design of eccentrically braced frames. *Earthquake Spectra*; **3**(1): 43-55

Engelhardt M. D. and Okazaki T. (2007). Cyclic loading behavior of EBF links constructed of ASTM A992 steel. *Journal of Constructional Steel Research* ; **63**(6): 751-765

Engelhardt M. D., and Popov E. P. (1988). Seismic eccentrically braced frames. *Journal of Constructional Steel Research*; **10:** 321-354

Engelhardt M. D., and Popov E. P. (1989a). On design of eccentrically braced frames. *Earthquake Spectra*; **5**(3): 495-511

Engelhardt M. D., and Popov E. P. (1989b). Behavior of long links in eccentrically braced frames. *Report No. UCB/EERC-89/01,* Earthquake Engineering Research Center, University of California, Berkley ,California, CA.

Engelhardt M. D., and Popov E. P. (1992). Experimental performance of long links in eccentrically braced frames. *Journal of Structural Engineering*; **118**(11): 3067-3088

Engelhardt M. D., Popov E. P., and Tsai K. (1992). Stability of beams in eccentrically braced frames. *Chapter in Stability and Ductility of Steel Structures Under Cyclic Loading, Y. Fukumoto and G. C. Lee, Editors*: 99-112

Kasai K., and Popov E. P (1986a). General behavior of WF steel shear link beams. *Journal of Structural Engineering*; **112**(2): 362-382

Kasai K., and Popov E. P (1986b). Cyclic web buckling control for shear link beams. *Journal of Structural Engineering*; **112**(3): 505-523

Richards P. and Uang, C.M. (2002). Evaluation of rotation capacity and overstrength of links in eccentrically braced frames. *Report No. SSRP-2002/108*, Department of Structural Engineering, University of California, San Diego, CA.

Richards P., and Uang C. M. (2003). Development of testing protocol for short links in eccentrically braced frames. *Report No. SSRP-2003/08,* Structural Department of Structural Engineering, University of California, San Diego, CA

Richards P. and Uang, C.M. (2004). Recommended EBF link loading protocol for the AISC Seismic Provisions. *Technical Note*.

Richards P. and Uang, C.M. (2005). Effect of flange width-thickness ratio on eccentrically braced frames link cyclic rotation capacity. .*Journal of Structural Engineering*; **131**(10): 1546-1552

Richards P. and Uang, C.M. (2006). Testing protocol for short links in eccentrically braced frames. *Journal of Structural Engineering*; **132**(8): 1183-1191